IJOER
RESEARCH JOURNAL

International Journal of Engineering Research & Science

ISSN
2395-6992

www.ijoer.com
www.adpublications.org

Preface

We would like to present, with great pleasure, the inaugural volume-3, Issue-5, May 2017, of a scholarly journal, *International Journal of Engineering Research & Science*. This journal is part of the AD Publications series *in the field of Engineering, Mathematics, Physics, Chemistry and science Research Development*, and is devoted to the gamut of Engineering and Science issues, from theoretical aspects to application-dependent studies and the validation of emerging technologies.

This journal was envisioned and founded to represent the growing needs of Engineering and Science as an emerging and increasingly vital field, now widely recognized as an integral part of scientific and technical investigations. Its mission is to become a voice of the Engineering and Science community, addressing researchers and practitioners in below areas

Chemical Engineering	
Biomolecular Engineering	Materials Engineering
Molecular Engineering	Process Engineering
Corrosion Engineering	
Civil Engineering	
Environmental Engineering	Geotechnical Engineering
Structural Engineering	Mining Engineering
Transport Engineering	Water resources Engineering
Electrical Engineering	
Power System Engineering	Optical Engineering
Mechanical Engineering	
Acoustical Engineering	Manufacturing Engineering
Optomechanical Engineering	Thermal Engineering
Power plant Engineering	Energy Engineering
Sports Engineering	Vehicle Engineering
Software Engineering	
Computer-aided Engineering	Cryptographic Engineering
Teletraffic Engineering	Web Engineering
System Engineering	
Mathematics	
Arithmetic	Algebra
Number theory	Field theory and polynomials
Analysis	Combinatorics
Geometry and topology	Topology
Probability and Statistics	Computational Science
Physical Science	Operational Research
Physics	
Nuclear and particle physics	Atomic, molecular, and optical physics
Condensed matter physics	Astrophysics
Applied Physics	Modern physics
Philosophy	Core theories

Chemistry	
Analytical chemistry	Biochemistry
Inorganic chemistry	Materials chemistry
Neurochemistry	Nuclear chemistry
Organic chemistry	Physical chemistry
Other Engineering Areas	
Aerospace Engineering	Agricultural Engineering
Applied Engineering	Biomedical Engineering
Biological Engineering	Building services Engineering
Energy Engineering	Railway Engineering
Industrial Engineering	Mechatronics Engineering
Management Engineering	Military Engineering
Petroleum Engineering	Nuclear Engineering
Textile Engineering	Nano Engineering
Algorithm and Computational Complexity	Artificial Intelligence
Electronics & Communication Engineering	Image Processing
Information Retrieval	Low Power VLSI Design
Neural Networks	Plastic Engineering

Each article in this issue provides an example of a concrete industrial application or a case study of the presented methodology to amplify the impact of the contribution. We are very thankful to everybody within that community who supported the idea of creating a new Research with IJOER. We are certain that this issue will be followed by many others, reporting new developments in the Engineering and Science field. This issue would not have been possible without the great support of the Reviewer, Editorial Board members and also with our Advisory Board Members, and we would like to express our sincere thanks to all of them. We would also like to express our gratitude to the editorial staff of AD Publications, who supported us at every stage of the project. It is our hope that this fine collection of articles will be a valuable resource for *IJOER* readers and will stimulate further research into the vibrant area of Engineering and Science Research.

Mukesh Arora

(Chief Editor)

Board Members

Dr. S.R.Boselin Prabhu

Ph.D, Wireless Sensor Networks, M.E. Network Engineering, Excellent Professional Achievement Award Winner from Society of Professional Engineers Biography Included in Marquis Who's Who in the World (Academic Year 2015 and 2016). Currently Serving as Assistant Professor in the department of ECE in SVS College of Engineering, Coimbatore.

Dr. Maheshwar Shrestha

Postdoctoral Research Fellow in DEPT. OF ELE ENGG & COMP SCI, SDSU, Brookings, SD Ph.D, M.Sc. in Electrical Engineering from SOUTH DAKOTA STATE UNIVERSITY, Brookings, SD.

Zairi Ismael Rizman

Senior Lecturer, Faculty of Electrical Engineering, Universiti Teknologi MARA (UiTM) (Terengganu) Malaysia Master (Science) in Microelectronics (2005), Universiti Kebangsaan Malaysia (UKM), Malaysia. Bachelor (Hons.) and Diploma in Electrical Engineering (Communication) (2002), UiTM Shah Alam, Malaysia

Dr. D. Amaranatha Reddy

Ph.D.(Postdocteral Fellow,Pusan National University, South Korea), M.Sc., B.Sc. : Physics.

Dr. Dibya Prakash Rai

Post Doctoral Fellow (PDF), M.Sc.,B.Sc., Working as Assistant Professor in Department of Physics in Pachhuncga University College, Mizoram, India.

Dr. Pankaj Kumar Pal

Ph.D R/S, ECE Deptt., IIT-Roorkee.

Dr. P. Thangam

BE(Computer Hardware & Software), ME(CSE), PhD in Information & Communication Engineering, currently serving as Associate Professor in the Department of Computer Science and Engineering of Coimbatore Institute of Engineering and Technology.

Dr. Pradeep K. Sharma

PhD., M.Phil, M.Sc, B.Sc, in Physics, MBA in System Management, Presently working as Provost and Associate Professor & Head of Department for Physics in University of Engineering & Management, Jaipur.

Dr. R. Devi Priya

Ph.D (CSE),Anna University Chennai in 2013, M.E, B.E (CSE) from Kongu Engineering College, currently working in the Department of Computer Science and Engineering in Kongu Engineering College, Tamil Nadu, India.

Dr. Sandeep

Post-doctoral fellow, Principal Investigator, Young Scientist Scheme Project (DST-SERB), Department of Physics, Mizoram University, Aizawl Mizoram, India- 796001.

Mr. Abilash

MTech in VLSI, BTech in Electronics & Telecommunication engineering through A.M.I.E.T.E from Central Electronics Engineering Research Institute (C.E.E.R.I) Pilani, Industrial Electronics from ATI-EPI Hyderabad, IEEE course in Mechatronics, CSHAM from Birla Institute Of Professional Studies.

Mr. Varun Shukla

M.Tech in ECE from RGPV (Awarded with silver Medal By President of India), Assistant Professor, Dept. of ECE, PSIT, Kanpur.

Mr. Shrikant Harle

Presently working as a Assistant Professor in Civil Engineering field of Prof. Ram Meghe College of Engineering and Management, Amravati. He was Senior Design Engineer (Larsen & Toubro Limited, India).

Design, Construction and Testing of a Hybrid Photovoltaic (PV) Solar Dryer

JB Hussein[1], MA Hassan[2], SA Kareem[3], KB Filli[4]

[1,4]Department of Food Science and Technology, Modibbo Adama University of Technology Yola, Nigeria
[2]Department of Mechanical Engineering, Modibbo Adama University of Technology Yola, Nigeria
[3]Department of Chemical Engineering, Modibbo Adama University of Technology Yola, Nigeria
[4]Product Design and Perception, Agrifood and Bioscience - Research Institutes of Sweden (RISE) Gothenburg, Sweden

Abstract— *A hybrid photovoltaic solar dryer was designed, constructed and tested in the Department of Food Science and Technology, Modibbo Adama University of Technology Yola, Nigeria. The thin layer drying behaviour of tomato slices using a hybrid drying method compared to solar and open sun drying was investigated. The dryer consists of solar collector, photovoltaic solar panel, battery and drying chamber. The dryer was operated as both a solar-energy dryer and as a hybrid solar dryer. The drying performance of the dryer was evaluated with fresh tomato slice and compared with open sun drying under the same climatic conditions. The dryer recorded a raised temperature of 62 ℃ attainable in the drying chamber of hybrid dryer and 54^{o}C attainable in the drying chamber of solar dryer. The moisture content of tomato slices was reduced from 94.22 % wet basis to 10 % in 6 hours for hybrid drying method while it took 9 hours to achieve the same moisture content reduction in the solar dryer. The average drying rate and the efficiency was computed as 0.0800kg/h and 71% for hybrid dryer and 0.0578kg/h and 65% for solar-energy dryer respectively. The quality of the tomato samples dried using the hybrid dryer was superior to those of solar and sun drying methods. From the result of this study it shows that a hybrid solar-energy dryer using photovoltaic (PV) solar panel suggested a promising process for adoption to preserve tomato which can prevent it from spoilage and post-harvest losses. The good quality and shelf stable dried tomato slices is indicative for a sustainable productivity that will create a sound avenue for economic growth in tomato producing regions of the world*.

***Keywords— design, hybrid dryer, photovoltaic solar panel, solar dryer and tomatoes*.**

I. INTRODUCTION

Drying traditionally using the sun is the oldest preservation technique of agricultural products worldwide which dates back to human civilization. To date, open sun drying is still widely used for preservation of agricultural products in the tropics and subtropical regions of the world. The traditional practice of open sun drying however has inherent limitations which includes; high crop losses due to inadequate drying to safe water activity, microbial/enzymic attacks as a result of longer drying time, insects, birds and rodents encroachment, unexpected weather changes without control and other effects environmental elements [1]. With such drawbacks of open sun drying, the adoption of solar-energy based dryers demonstrates increasingly more attractive and promising for applications as commercial propositions. Solar drying can simply be considered as an elaboration of sun drying, and it is an efficient system of utilizing solar energy [2]. As an alternative to open sun drying, solar energy dryers avail farmers with possibility of improved post-harvest management system that is sustainable for increased economic growth that will overcome most drawbacks of the traditional open sun drying systems by yielding products which is acceptable to both national and international standards[3,4]. In addition the solar drying systems have added advantages of savings in energy, time and space requirements during drying operations which add up to making the method not only more efficient but also more environmentally friendly without constituting any danger to the environment [5, 6]. Solar energy for crop drying is environmentally friendly and economically viable in the developing countries of the world. It's also form a sustainable energy utilization that has a great potential for wide variety of applications because it is abundant and accessible, especially for countries located in the tropical region of the world like Nigeria. Solar-energy drying systems overcomes the drawbacks of traditional open sun drying such as, contamination from dust, insects, birds and animals, lack of control over drying conditions, possibility of chemical, enzymic, and microbial spoilage due to longer drying times [2, 4]. Solar-energy drying offers an alternative which can be exploited to preserve vegetables and fruits in clean, hygienic and sanitary conditions that can be acceptable by the consumer. The process saves energy, time, occupies less drying area, improves product quality, makes the process more efficient and protects the environment [1, 5, 6].

However, one significant disadvantage of solar-energy dryer is that it can only be used during the daytime when there is adequate solar radiation for conversion to heat. Solar dryers are constructed normally with no any form of back-up heating

systems [7] and makes it difficult to use them for drying at nights or when there is no adequate sunshine. For commercial processors, this factor limits their ability to process a crop when there is no adequate sunshine; this limitation usually results in extended drying periods because drying can only occur during the day time when there is adequate solar radiation. This gap does not only limit productivity but results in an inferior product quality which does not encourage Agricultural productivity increase. For commercial processors, the ability to process continuously with reliability is important and crucial in order to satisfy and meet their markets demand. Most existing solar dryers are actually designed to operate only during the daytime and thus are constructed without any form of back up heating system [7]. A possibility of extending the process efficiency, in order to reduce the drying time and controlling the dependence of production cycle period on the weather would definitely be a welcome development, as this could lead to the improvement in both quality and quantity of processed products which can be more sustainable.

It then becomes expedient to consider innovative solutions for solar dryers that would have added advantage over the longer period of residence during drying, increase productivity and reliability through its ability to augment available heat during days with limited radiation as well as ability to operate during the night or during low sun radiation periods. Some hybrid dryers were developed to control the drying air conditions throughout the drying time independent of sun-shine especially at night or poor weather when it is not possible to use the solar energy, using alternative heating sources such as sawdust burner [8]; kerosene stove [9] or by using a biomass stove [10,11]; electric heater [12,13].

Grid-connected electricity and supplies of other non-renewable sources of energy are unavailable, unreliable, scarce or too expensive for many farmers and processors generally in most developing countries; this results in reduced expected profit as a result of inappropriate post-harvest processing [1]. It is therefore necessary to provide a solar-energy drying system with additional source of energy such as in the case of hybrid dryer (solar-energy dryer with energy storage system) to close the gap of continuous drying even when there is no solar radiation.

Based on the aforementioned fact, considerable studies on photovoltaic (PV) module to power dryers for forced convection air circulation have been reported among which are; [14] that developed a PV operated forced convection solar energy dryer; Barnwal and Tiwari (2008) [15] reported a hybrid solar grain dryer with a PV – driven DC fan which was used to dry maize [16] and also designed, analysed and evaluated a forced convection photovoltaic solar dryer which was used to dry plantain chips.

There is little information to our knowledge regarding the design of a hybrid photovoltaic solar dryer meant for the drying of fruits and vegetables such as tomato slice. The objective of this study was to develop a hybrid photovoltaic solar dryer with an energy storage system so as to improve the drying efficiency by reducing the drying time of tomato slices.

II. MATERIALS AND METHODS

2.1 Components of the hybrid dryer and materials used

The main components of the hybrid dryer are; drying chamber, rack and trays, heater, fan/blower, solar panel, solar battery and control panel. The materials used for the construction were; mild steel, galvanized steel and wire, plywood, solar panel, solar battery, on and off switch and thermostat (thermocouple). The drying chamber had a volume of 0.300 m^3 constructed with galvanized steel. It was painted in silver colour inorder to reduce heat loss by radiation. The chamber was also enclosed by an outer chamber of 0.432 m^3 volume made from the same material with the space between the two volumes filled with insulation material so as to reduce conductive heat loss. The insulation materials used was packed wool fiber of 0.050m thick was used as the insulating material to achieve a minimal heat loss of 5% from the drying chamber. The rack was constructed with mild steel and positioned in such a way that it allows easy insertion of individual trays at a distance of 0.1m apart. The trays were constructed with plywood and its base was made of fine wire gauze which allows for heated air circulation and to pass through the tomatoes being dried.

2.2 Design Consideration and Specifications

The following determinant factors and assumptions were taken into consideration when constructing the hybrid dryer based on the procedures described by [16, 4];

- Geographical and meteorological data of location.
- The solar radiation of the location (Yola, Nigeria) as a case study was used as starting points in solar equipment design.
- Sanitary design factors: the construction materials must be noncorrosive and nontoxic.

- Ease of assembly and disassembly: the hybrid dryer was constructed in such a way that all the surfaces contacting the drying samples can be exposed, clean and inspect. Easy to adjust, dismantle and couple.
- Time constraint.
- The initial and expected final moisture content of the vegetables and fruits to be processed.
- The ambient temperature and operating in-chamber temperature.

Having considered and analysed the above listed factors with specific reference to the case study location Yola, the following design specifications were arrived at;

- Use tomatoes as a case study vegetable so as to cover a large range of fruits and vegetables. Also, tomatoes are vegetables of high interest in the study area as being widely grown and having a very high percentage of post-harvest loss due to inadequate post-harvest processing in the study area.
- The required thermal performance was identified.
- Based on the expected capacity of the dryer, economic considerations and engineering and ergonomic factors considerations, the shape and size of the dryer and its components were analysed and a cabinet-type dryer was chosen as the most optional.
- Initial moisture content: 95% wet basis.
- Expected moisture content: 10 % wet basis.
- Operating temperatures: ambient was 30^{o}C and in-chamber was 60^{o}C.
- Residency period per batch: 8 Hours.
- Heat loss from drying chamber ≤ 5 %.

2.3 Design calculations

2.3.1 The heater design

A. Amount of moisture removed

The amount of moisture removed from a given quantity of wet tomatoes slices to bring the moisture content to a safe storage level in a specified time was calculated using the following equation described by [17].

$$M_w = M_p\left(M_i - M_f\right)/\left(100 - M_f\right) \quad (1)$$

Where; M_p = Initial mass of the tomatoes (kg)

M_i = Initial moisture content (% wet basis)

M_f = Final moisture content (% wet basis)

B. Quantity of heat required to remove the moisture (Ea) in KJ

The quantity of heat required to evaporate the moisture was calculated as follow;

Quantity of heat required to evaporate the moisture = heat energy to raise the temperature to 60^{o}C + latent heat to remove moisture

$$E_a = M_p x\, C_T\, x\, \Delta T + M_w L_v \quad (2)$$

Where; C_T = Specific heat capacity of tomatoes (3.676KJ/kgK)

ΔT = Change in temperature of the drying chamber 30^{o}C to 60^{o}C

L_v = Latent heat of vapourization of water at s.t.p 2257KJ/kg

C. Power = Quantity of heat/ time (sec)

$$Power = E_a/t_d \quad (3)$$

Where; t_d = time of drying 8 hours

Based on the above calculations, a heating coil element of 0.5KW power was chosen for use.

2.3.2 The fan/blower design

A. Mass flow rate of air (kg/s)

The mass flow rate Ma (in kg/sec) of the air was given as

$$M_a = E_a / C_{pa} \, x \, \Delta T \, x \, t_d \quad (4)$$

Where; E_a = the quantity of heat required to evaporate the H_2O

C_{pa} = Specific heat capacity of air (1.005KJ/kgK)

t_d = Theoretical time taken for drying (8 hours)

B. Volumetric flow rate Va (m^3/s)

$$V_a = M_a/\rho_a \quad (5)$$

Where; ρ_a = density of air at 60°C = 1.2754 kg / m^3

Converting the value of the discharge obtained to cubic foot per min (cfm) for standard fan selection, we have [18];

$$1cfm = 4.91747x10^{-4}m^3/s$$

$$0.00808m^3/s = 16.4229cfm$$

$$\text{Fan horse power} = (Air\ flow\ x\ static\ presure)/(6320\ x\ fan\ efficiency) \quad (6)$$

From literature, most industrial fans have efficiency ranging from 70-85% as described by [19].

Using an efficiency of 85%

Based on the above calculations and to ensure proper distribution of air to the drying chamber and for effective heat distribution, an axial flow fan with 0.02 Hp and 110mm of water static pressure was used.

2.3.3 Total energy required

The total energy required for drying is given as [20];

$$E = M_a(H_2 - H_1) \quad (7)$$

Where; M_a = mass flow rate of air, kg / sec
H_2 = Enthalpy of warm air, KJ / kg dry air
H_1 = Enthalpy of ambient air, KJ / kg dry air

Enthalpy of the air can be calculated using [20];

$$H = 1006.9T + H_r(2512131.0 + 1552.4T)$$

Where; Hr = Humidity ratio, Kg H_20 / Kg dry air (from psychometric chart)
T = air temperature, °C

2.3.4 The solar thermal collector design

A. The solar collect area (Ac) in m^2

The solar collect area (Ac) was calculated from the following equation as given by [21].

$$A_c = \frac{V_a \times \rho_a \times \Delta T \times C_{pa}}{I\eta} \quad (8)$$

Where;

I = Total global solar radiation on the horizontal surface during the drying period. The mean value of global radiation of Yola is given as 0.725 W/m^2 [22].

η = the collector efficiency, 30 – 50 % [20].

Therefore, the collector area was 1.0345 m^2. However, by making the collector width equal to 0.60m to match the width of the dryer, the required collector length used was 1.7856m ≈ 1.80m.

B. Absorber of the solar collector

The solar absorber of the collector was constructed using 0.55 mm thick corrugated iron sheet, painted black and it was mounted in a box constructed of the same area. The absorber was implicit to be a perfect black body and so as to absorb greatest heat. Corrugated iron sheet was used because of its low cost, high melting point, inflammable and easily available in the local market.

C. Covering material of the solar collector

To create a greenhouse effect, a single layer transparent glass sheet of 5 mm thickness was placed on top of the absorber at a distance of 0.11m apart. Glass was selected as glazing because it is easily available, has low cost, high value of transmittance for long and short wave radiations (80%), not flammable and have high melting point. It also shelters the absorber from wind and allows solar radiation to reach the absorber.

D. Solar thermal collector orientation and tilt angle

The solar collector was tilted and oriented in such a way that it receives maximum solar radiation during operation. The best stationary orientation is due South in the northern hemisphere and due north in Southern hemisphere [23, 4]. The angle of tilt (β) of the solar collector is given by the formula below [24, 25];

$$\beta = 10^o + Lat\emptyset \tag{9}$$

Where; LatΦ = the latitude of the collector location = 7^o for Yola Adamawa state.

Therefore, solar collector in this work was oriented facing south and tilted at 17^o which is the best recommended orientation for stationary absorbers. This inclination also allow easy run off of water and enhance air circulation.

2.3.5 Design of the drying chamber insulation

Different materials are available for insulation but considering the availability and cost of insulating materials, wool fibers was used since it has thermal conductivity of 0.04W/m^oC and can be favourably compared with other effective insulating materials such as glass wool [9]. Assumption of a loss of 5% of the quantity of heat produced and the temperature of external part of drying chamber 30^oC was made (Normal atmosphere temperature).

Heat transfer through the wall was by conduction hence Fourier's equation was relevant [18].

Quantity of heat lost per unit area $= (T_1 - T_2)\, K_1 / X_1$

$$= (T_2 - T_3)\, K_2 / X_2$$

$$= (T_3 - T_4)\, K_3 / X_3$$

$$= U\,(T_1 - T_4) \tag{10}$$

Where; K_1 and K_3 = Heat transfer coefficient for mild steel i.e. 46 W / m^oC

K_2 = Heat transfer coefficient for wool fiber i.e. 0.04 W / m^oC

X_1, X_2 and X_3 = the respective thickness of mild steel and wool fiber

U = Overall heat transfer coefficient

T_1 = Temperature of internal part of cabinet i.e. 60^oC

T_4 = Temperature of external part of cabinet i.e. 30^oC

$X_1 = X_3 = 0.0015$m

2.3.6 The solar panels with storage battery

A PV system has to generate enough energy to cover the energy consumption of the loads and energy used by the system itself. The size and configuration of solar panel was then optimized in order to match the energy yield of the system with the energy consumption of the system. An estimate of the sizing of the panel and battery was made using the following design processes.

A. Determination of the total power consumption

Prior to determination of power consumption, 12V was used as the nominal operational voltage of the PV system, the total power rating of the dryer was around 600W and the average daily operational time was 3 hours.

The daily energy requirement (Wh) = $600W \times 3h = 1800Wh$ (11)

B. Addition of system losses

Some components of the PV system, such as charge regulator and battery use energy to perform their functions. Thus, we denote the energy used by the system as system energy losses. Therefore, the total energy requirement by loads, which was determined above was increase by a factor of 20% in order to compensate for the system losses.

Add system losses = $1800Wh \times 1.2 = 2160Wh/day$ (12)

C. Sizing of the PV modules

Different size of PV modules produce different amount of power. To find out the correct size of a PV module, the total peak watt produced needs was determined. The peak watt (Wp) produced depends on size of the PV module and climate of site location. Also we have to consider "panel generation factor" which is different in each site location and for Yola (Nigeria), the panel generation factor is 6.20.

$$Total\ peak\ watt\ (Wp)\ of\ PV\ panel\ capcity\ needed = \frac{\text{total daily energy requirement}}{panel\ generation\ factor} \quad (13)$$

$$= \frac{2160}{6.20} = 348.3871Wh/day$$

Therefore, number of PV panels needed $= \frac{348.3871}{180} = 1.94\ modules$

So this dryer was powered by at least 2 modules of 180 Wp PV modules.

D. Determination of the battery size for recommended reserve time

Batteries are a major component in the stand-alone PV systems. The batteries provide load operation at night or in combination with the PV modules during periods of limited sunlight. For a safe operation of the PV system one has to anticipate periods with cloudy weather and plan a reserve energy capacity stored in the batteries. This reserve capacity is referred to as PV system autonomy, which means a period of time that the system is not dependent on energy generated by PV modules, and is rated in days. For this design the autonomy of the system was taken as 24 hours (one day).

The Battery capacity required by the system = the total DC energy required by loads × the number of days of recommended reserve time.

Therefore, the minimal capacity of the battery was determined by dividing the required capacity by a factor of 0.9. So for this hybrid dryer the battery used was rated 12 V 200 Ah.

2.3.7 The control panel

The control panel is simply the unit that controls the system and maintains constant temperature in the drying chamber. It contains the following;

- On and off switch.
- Signal light.
- Thermostat (thermocouple)

2.4 Performance Evaluation of the Hybrid Dryer

The following materials were used for the testing of the hybrid dryer; tomatoes, tomatoes slicer, wet and dry mercury-in-bulb thermometer, weighing balance and digital multimeter (model; DT-830B).

2.4.1 Operation of the hybrid dryer

The dryer was placed in the open space free from shade throughout the day and night of operation. There are two heating sources that can be used independently or complimentarily, solar collector and heating coil element. When there is abundance of sun radiation with high intensity, sun radiation falling on the glass is being absorbed by the collector plate

painted black and transmitted into the drying chamber through the inlet window by forced convection system. This removes the moisture given out in the drying process. On the other hand, when there is drop in temperature set or there is need to continue drying in the night to dry the products to its safe level for storage or when weather condition is bad, the thermostat switch on the heater to compliment the drying process. The photovoltaic solar panels convert solar energy to electricity. The electricity generated is used to power the heater, fans and the control system and at the same time charge the battery. The battery serves as a storage bank to store charge which is used in the night or in case of bad weather.

2.4.2 Testing of the hybrid dryer

Two type of testing was conducted in evaluating the dryer. They are;

A. Test without loading

This is a preliminary evaluation which involves the test for determining the maximum temperatures obtainable in the dryer when it is not loaded. The parameters that were monitored in this evaluation include temperatures of the ambient air and drying chamber and the relative humidity of the ambient air and the drying chamber. The ambient temperature was taken as initial temperature and measurement was taken at 30 minutes interval.

B. Test with product loaded in the dryer

This is the test that was carried out by loading the dryer with a product in order to determine the minimum drying time obtainable to reach a desirable final moisture content of the dried product. The parameters that were monitored here include the temperature of the drying chamber and weight of loaded samples at interval of drying time (30 minutes) in order to determine the moisture loss.

2.4.3 Determination of the power generated by the photovoltaic (PV) solar panel

The solar panels were mounted on a horizontal stand of about 250cm height in an open space very close to the dryer. They were oriented facing south and tilted at an angle of 17^{o}. The panels were connected in parallel so as to get maximum output power of the panels. The output terminals of the panels were connected to the input terminals of the digital multimeter (Model: DT-830B). The knobs of the digital multimeter were set to the appropriate range, while the current and voltage readings are taken directly from the screen display at every 30 munities interval. The power generated was calculated as:

$$P = IV \tag{15}$$

Where;

P = Power output (W)

I = Current (A)

V = Voltage (V)

2.4.4 Drying procedure

The tomatoes used for this study were obtained from the Jimeta main Modern Market Yola, Adamawa State. Samples of tomatoes were sorted and selected from the lot based on firmness, colour and size uniformity. They were cleaned by washing thoroughly with tap water, rinsed with distilled water and then wiped with an absorbent paper [26]. The cleaned tomatoes were pretreated in boiling water for 2 minutes, and the water drained. The samples were then divided into three portions. Then, each portion was slice with Tomato Slicer to a thickness of 6 mm. The first portion of the sliced tomato (4kg) was spread in a single layer on a four different wire meshes (1kg on each wire mesh) and sun dried until equilibrium moisture content was achieved. The second portion (4kg) was dried in the constructed hybrid dryer by using solar collector as the heating source alone and the third portion (4kg) was dried by using both heating source together. One (1kg) on each wire mesh tray and it was left until constant weight was achieved. The the average weight of each dry weight was taken and recorded. The thermostat in the control panel monitored and controls the temperature of the drying chamber.

2.4.5 Determination of the efficiency of the dryer

The efficiency of the dryer indicates the overall thermal performance of a dryer including the efficiency of a solar collector, the drying chamber and any other supplement added to the system. The efficiency of the constructed hybrid dryer was calculated by using the formula below as described by [27, 28];

For forced convection solar dryers that use a fan or a bowler;

$$\eta = \frac{WL}{IA+P_f} \quad (16a)$$

For hybrid solar dryers that use a second source of energy the efficiency is calculated as;

$$\eta = \frac{WL}{IA+P_f+P_h} \quad (16b)$$

Where;

η = efficiency of the dryer

W = weight of water evaporated from the tomatoes (kg)

I = solar radiation (W/m^2)

A = area of collector (m^2)

L = latent heat of vaporization of water (J/kg)

P_f = energy consumption of fan (J)

P_h = energy consumption of hater (J)

The drying rate which was the quantity of moisture removed from the tomatoes slices in a given time was computed as described by [29].

$$Drying\ rate = \frac{amount\ of\ moisture\ removed\ (kg)}{total\ drying\ time\ (h)} \quad (16c)$$

III. RESULTS AND DISCUSSION

3.1 Design and Construction of a Hybrid Solar-Energy Dryer

A hybrid solar-energy dryer was designed and constructed using readily available local materials. Figure 1 and Plate 1 showed the essential features of the hybrid dryer, consisting of the solar collector, the drying cabinet, solar panels and solar battery.

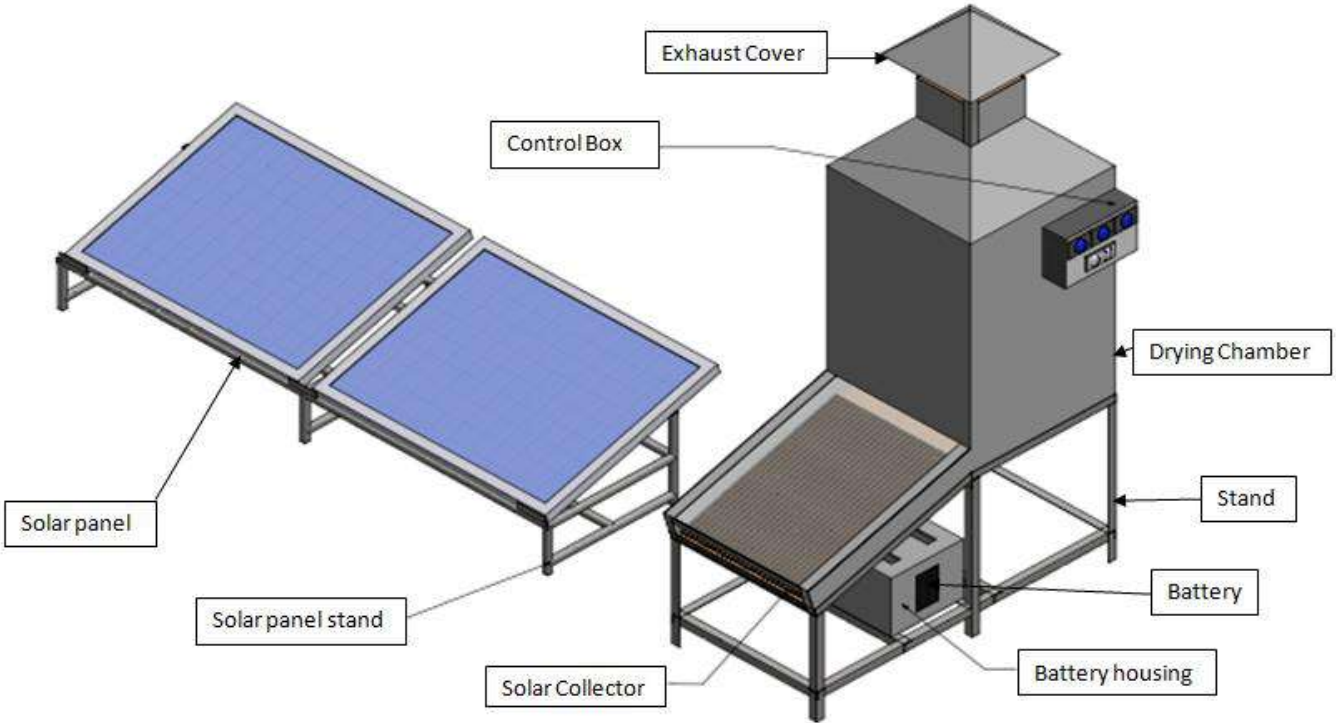

FIGURE 1: ISOMETRIC VIEW OF THE HYBRID DRYER

PLATE 1: FABRICATED HYBRID DRYER

3.2 Description of the Fabricated Hybrid Dryer

Figure 2 showed the general features of the constructed hybrid dryer.

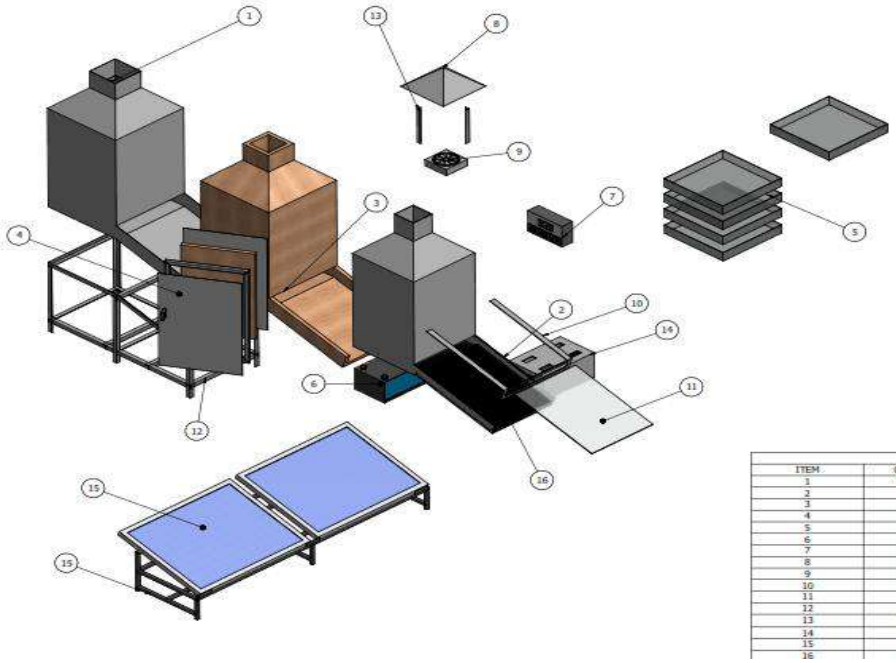

PARTS LIST		
ITEM	QTY	PART NUMBER
1	1	External case
2	1	Internal case
3	1	plywood insulation
4	1	Door Assembly
5	5	Tray
6	1	Battery
7	1	Control Panel
8	1	Head cover
9	1	Fan
10	1	Cover Strip
11	1	Glass
12	1	Stand
13	4	Head cover support
14	1	Battery Cover
15	1	Solar Dryer Assembly
16	1	Collector

FIGURE 2: EXPLODED VIEW OF THE HYBRID DRYER

The dryer consists of an external case (1) of 600 mm in diameter and 1200 mm in height and an internal case (2) of 500 mm diameter and 1100 mm in height both are made with mild steel. The wall of the drying chamber where the drying trays (5) were located was made of plywood of 50 mm in thickness and build up to form a box which served as plywood insulation (3) between internal and external casing. The dryer consists of a chimney of 220 mm in diameter and 225 mm in height located on the top of the dryer chamber. Inside it was located a DC extractor fan (9) to discharge heated air and moisture from the products into the atmosphere. The top head is cover with a head cover (8) to protect the extractor fan and protect the chamber. The wall of the drying box is connected to the solar collector (16) and tilted at an angle of 17^{o}C to the horizontal to give an inclination equal to the latitude of Yola (7^{o}C). The collector consists of an absorber plate made of aluminum sheet painted black and a transparent glass (11) of 5mm tick which permit in only sun radiation. The absorber plate is insulated from the bottom to prevent heat losses. Air vent is provided on the lower front side of the collector for easy passage of air into the dryer it is covered with mosquito net to prevent insects into the dryer. The legs of the stand (12) are made of angle iron and tilted at an angle 17 to the horizontal at the top of the stand. The dryer also have a DC blower fan and a 500W power heater located at the bottom of the drying chamber. Two solar panel (15) with 180W power each and a battery (6) with

200Ah power rating is use to power the system. A temperature sensor is located at the center of the chamber to sense the chamber temperature. The control box which contain on and off switch, solar regulator, and signal light.

3.3 Performance Evaluation

3.3.1 Testing under unloaded condition

This testing was carried out to determine the maximum temperature attainable in an unloaded condition of the dryer using the heating sources separately and combined. The test was carried out in five days and the results averaged. The solar collector alone was first evaluated. The test started at 7.00am on the 6th day of March 2015 when the ambient temperature was 27^{o}C. Figure 3 showed the changes in the temperature levels. It was observed that at 1.30pm the maximum average ambient temperature for the day was 45^{o}C, the temperature of the solar collector was 64^{o}C and the drying chamber temperature was 54.9^{o}C. Thereafter, the chamber temperature was stable for $1^{1}/_{2}$ hour before it started to decrease. Then it was observed that the ambient and the solar collector temperatures had fall to 44^{o}C and 56^{o}C respectively. This result shows that the dryer is hottest about mid-day when the sun is usually overhead, similar results were reported by [30] for a batch solar dryer under Ibadan climate, [31] for a Mixed-Mode Solar Dryer, [25] for a Small Scale Solar Dryer and [29] for a village-level solar dryer for tomato under Savanna Climate.

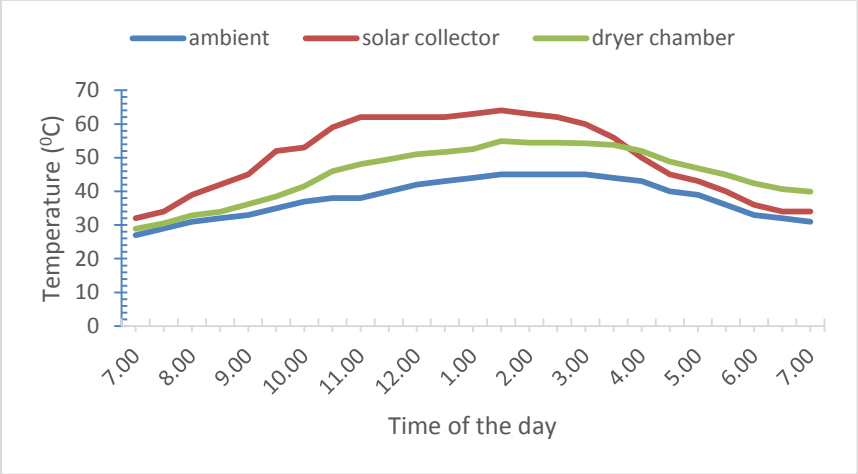

FIGURE 3: AMBIENT, SOLAR COLLECTOR AND CHAMBER TEMPERATURE DURING SOLAR HEATING ONLY

Heating with the heating element coil was also examined for 6 hours at a period when the ambient temperature has reduced. The test was carried out for three days and the results averaged. The test started at 6.00pm on the 10th day of March 2015 when the ambient temperature was 34^{o}C and reduces gradually to 27^{o}C. The graphical trend results obtained was showed in Figure 4. This shows that the chamber temperature increases irrespective of the ambient air temperature and it would require controlling the thermostat in order to control the drying chamber's temperature.

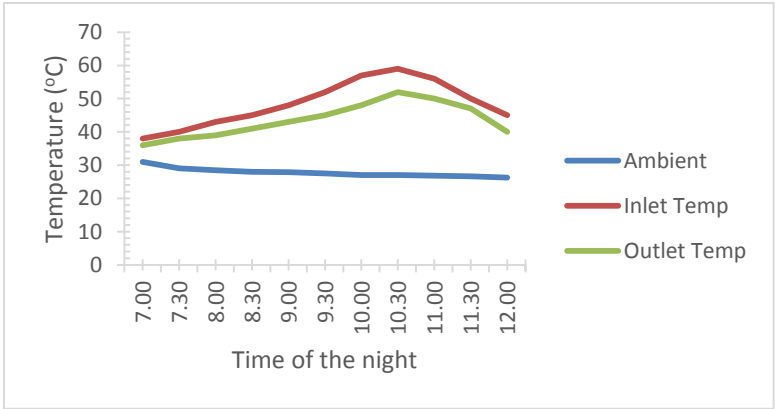

FIGURE 4: AMBIENT, DRYING CHAMBER'S INLET AND OUTLET TEMPERATURES DURING HEATING WITH HEATING ELEMENT COIL ONLY

On the 11th of March, 2015 the two heating sources were combined. The test was carried out for five days and the results averaged. The test started at 6.00am when the ambient temperature was 28.5^{o}C. The evaluation started with using solar

collector only and at the peak of the chamber temperature, the heater was introduced in order to increase the temperature. It was observed that at 1.00pm the maximum average ambient temperature for the day was 44°C, the temperature of the solar collector was 72°C and the drying chamber temperature was 60°C. Thereafter, the chamber temperature increased to 62.2°C for 1 hour before it started to decrease. Then it was observed that the ambient and the solar collector temperatures were 45°C and 70°C respectively. Figure 5 showed the temperature various level. This result was slightly higher than 56.7°C maximum chamber temperature reported by [15] for hybrid photovoltaic integrated greenhouse dryer and 55°C by [16] for forced convention photovoltaic solar dryer for the tropics. The temperatures range inside the hybrid dryer chamber was much higher than that inside the solar dryer chamber and ambient temperature during most hours of the daylight. This indicates prospect for better performance of hybrid drying method than solar and open-air sun drying methods.

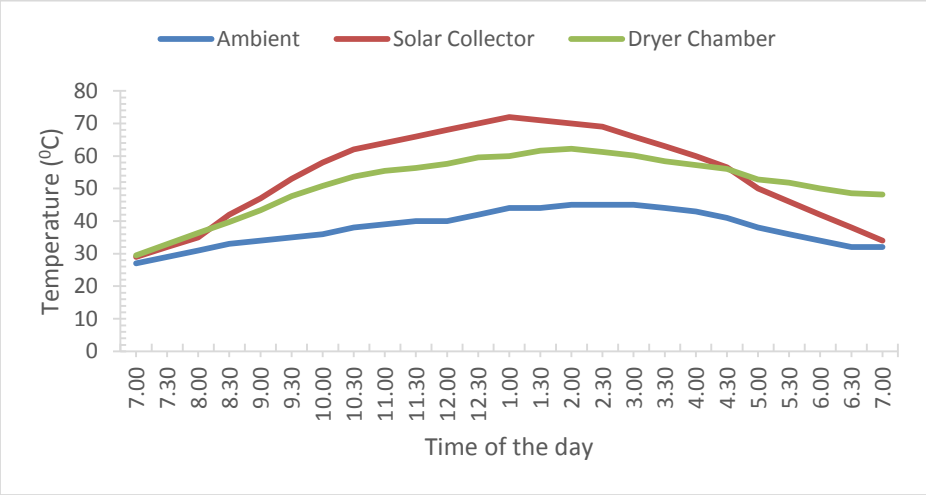

FIGURE 5: AMBIENT, SOLAR COLLECTOR AND CHAMBER TEMPERATURES DURING HYBRID HEATING

Figure 6 showed the results obtained for the diurnal variation of the relative humidity of the ambient air, solar drying chamber and hybrid drying chamber. The test was carried out in five days and the results averaged. The relative humidity of the ambient air during the testing of the dryer ranges form 51.95 – 92.45% while that of solar and hybrid drying method ranges from 8.22 – 79.03% and 5.20 – 79.03% respectively. This result was slightly higher than the relative humidity range (80 – 87%) for ambient air and lower than the relative humidity range (11.5 – 45%) for solar drying method obtained by [29]. This variation was observed to be due to variation in the months in which the experiment was carried out. This experiment was carried out in March/April (dry season) while their own was carried out in September/October (wet season). The power output of the panel was also determined to see if the panel can power the whole system and to test the efficiency of the panel. Figure 7 showed the graphical trend of the average results obtained for the power output of the panels. It was observed that the output power of the panel can power the hybrid drying system.

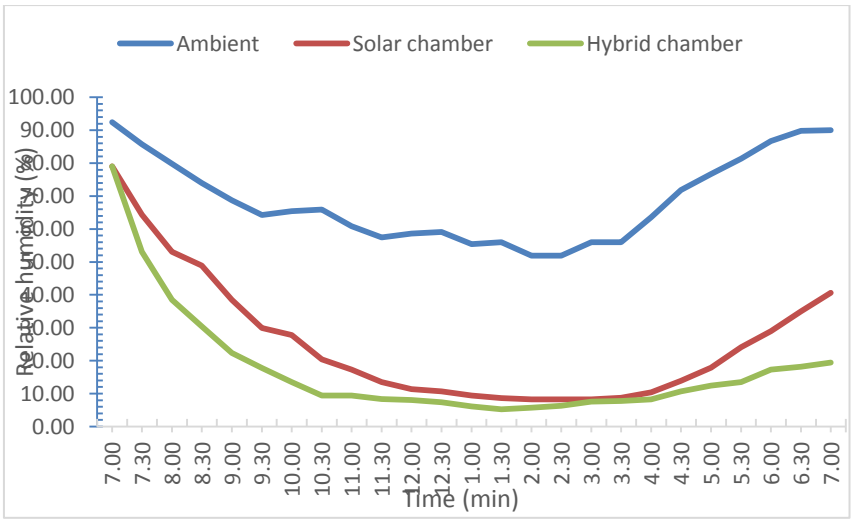

FIGURE 6: A TYPICAL DAY RESULTS OF THE DIURNAL VARIATION OF RELATIVE HUMIDITY IN THE DRYER

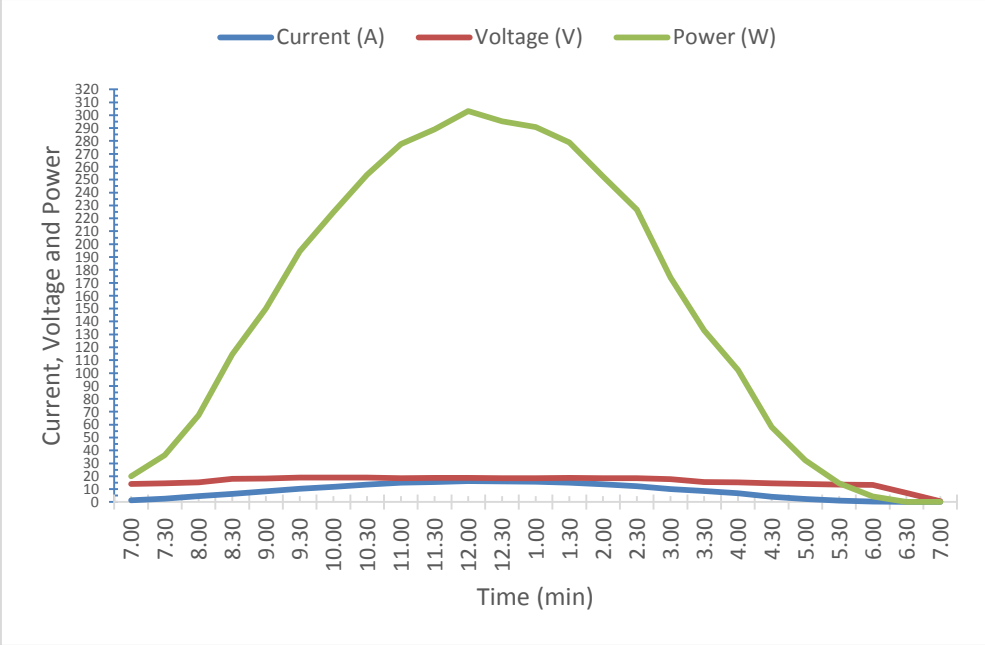

FIGURE 7: AVERAGE RESULT FOR CURRENT, VOLTAGE AND POWER OUTPUT

3.3.2 Testing under loaded condition

This test was carried out to determine the technical viability of the dryer. The test started at 7.00am on the 16th day of March 2015 when the ambient temperature was 27°C. The initial moisture content of the tomato was determined in the laboratory using [32] AOAC (2000) air oven method and 94.22% (wet basis) moisture content was obtained. The comparison of tomato's drying curves in the hybrid and solar method of drying with the natural open sun drying was shown in Figure 8.

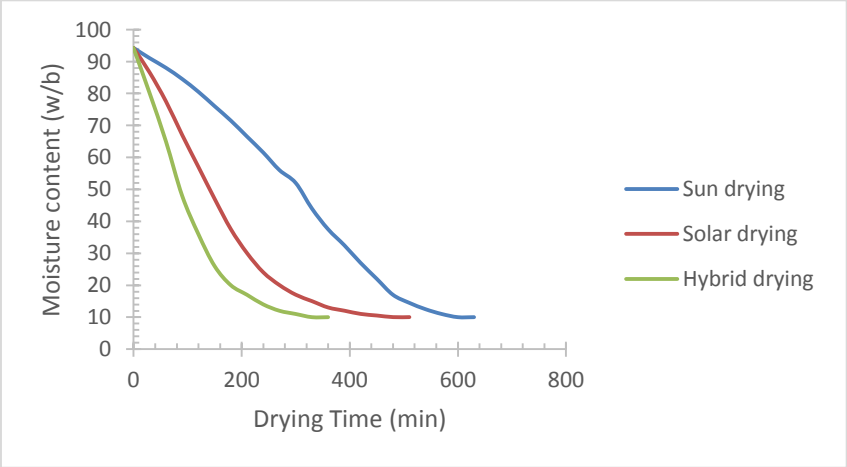

FIGURE 8: COMPARISON OF TOMATO'S DRYING CURVES IN THE HYBRID, SOLAR AND OPEN SUN DRYING METHODS

Plate 2 showed the dried tomatoes in the hybrid, solar and open sun drying methods. The natural open sun drying took about $10^1/_2$ hours to dried to equilibrium moisture content of 10% (w/b) while the drying inside the solar dryer took $8^1/_2$ hours (20% of the time spent for the natural sun drying) and hybrid took about 6 hours (43% of the time spent for the natural sun drying) respectively. The average drying rate and the efficiency of forced convection solar dryer was computed as 0.0578kg/h and 65% respectively. While hybrid was computed as 0.0800kg/h and 71% respectively. This result was higher than 39.6% and 0.0169kg/h reported by [16] for forced convention photovoltaic solar dryer for the tropics. Barnwal and Tiwari (2008) [15] reported that for a hybrid photovoltaic integrated greenhouse dryer, an overall thermal efficiency for summer and winter conditions was about 65 and 77% respectively. It was observed that the drying rate increased due to increase in temperatures thereby reducing the drying time. Similar results were reported by [25] for a Small Scale Solar Dryer and [29] for a village-level solar dryer for tomato under Savanna Climate.

IV. CONCLUSION

A hybrid solar-energy dryer using photovoltaic (PV) solar panel to power the heating element coil and charging the battery which had a storage energy system was developed, which was used to study the drying behaviour of tomato slices (result not shown). The hybrid solar-energy dryer was compared to solar and open sun drying was systems. The performance showed that the hybrid solar-energy dryer was able to generate temperatures inside the hybrid chamber to (62.20^{o}C) and the solar chamber (54.90^{o}C) and the maximum open sun drying ambient temperature was (45.00^{o}C) during most hours of the daylight. The average drying rate and the efficiency was computed to be 0.0800kg/h and 71% for hybrid dryer and 0.0578kg/h and 65% for solar-energy dryer. Good quality shelf stable dried tomato slices were produced using the hybrid drying method and which performance was influenced by effective drying time by reducing the period of the drying cycle and relatively higher drying temperature of about 62.20^{o}C. The temperature attained was 62.20^{o}C which was suitable for drying of fruits and vegetables with vital components that are heat sensitive when dried at higher temperatures. The study has therefore provided useful information in drying process design for commodities like tomatoes which can assist in reducing post-harvest losses often incurred during harvest period of these type crops in developing economies like Nigeria. It also proved that the efficiency of agricultural dryers could be increased through the use of a combination of solar and heating element coil powered by photovoltaic (PV) solar panel, compared to conventional dryers with only solar or only biomass heating sources.

REFERENCES

[1] Ekechukwu OV and Norton B (1999). Review of solar-energy drying systems II: an overview of solar drying technology. *Energy Conversion & Management*, 40: 615 – 655.

[2] Janjai S and Bala BK (2012). Solar Drying Technology, *Food Engineering Review* 4:16 – 54.

[3] Ajayi C, Orsunil KS and Deepak DP (2009). Design of Solar Dryer with Turbo ventilator and Fireplace. *International Solar Food Processing Conference: 1*-5 www.solarfood.org/solarfood/.

[4] Gutti B, Kiman, S and Mustafa BG (2012). Design and Construction of Forced/Natural Convection Solar Vegetable Dryer with Heat Storage. *ARPN Journal of Engineering and Applied Sciences*, 7(10): 1213 – 1217.

[5] Zhang M, Tang J, Mujumdar AS and Wang S (2006). Trends in Microwave Related Drying of Fruits and Vegetables, *Trends in Food Science and Technology*, 17: 524 – 534.

[6] Aware R and Thorat BN (2012). Solar Drying of Fruits and Vegetables. In solar drying: *Fundamentals, Applications and Innovations.* (Hii CL, Ong SP, Jangam SV and Mujumdar AS Eds.), ISBN - 978-981-07-3336-0, published in Singapore, pp. 51-72.

[7] Geramitcioski, T. and Mitrevski, V. (2011). Design and construction of a new mobile solar dryer, Second International Conference on Sustainable Postharvest and Food Technologies INOPTEP 2011, Velika Plana. Pp 24 – 26.

[8] Bassey MW (1985). Design and performance of hybrid crop dryer using solar-energy and sawdust. In: Proceedings of the ISES congress INTERSOL 85, Montreal, Canada, Oxford: Pergamon Press, 1038–1042.

[9] Babarinsa FA, Williams JO and Ngoddy PN (2006). Development of a Hybrid Dryer with Kerosene and Solar Heat Source. *Nigeria Drying Symposium series*, 2: 27 – 34.

[10] Prasad J and Vijay VK (2005). Experimental studies on drying of Zingiber officinale, Curcuma longa L. and Tinospora cordifolia in solar-biomass hybrid dryer. *Renew Energy* 30:2097–109.

[11] Amer BM., Hossai, MA and Gottschalk K (2010). Design and performance evaluation of a new hybrid solar dryer for banana, *Energy Conversion and management* 51: 813–820.

[12] Boughali S, Benmoussa H, Bouchekima B, Mennouche D and Bouguettaia H (2009) Crop drying by indirect active hybrid-solar-electrical dryer in the eastern Algerian Septentrional Sahrta. Solar Energy 83: 2223-2232.

[13] Reyes A, Mahn A, Huenulaf P and González T (2014) Tomato Dehydration in a Hybrid-Solar Dryer. *Journal Chemical Engineering Process Technology* 5 (4): 1 – 8.

[14] Saleh T and Sarkar MAR (2002). Performance Study of A PV Operated. Forced convection solar energy dryer. A paper accepted for presentation at the technical session of the 8th International Symposium for Renewable Energy Education (ISREE-8), August 4-8, to be held at Orlando. University of Florida, USA (http://www.doce-conferences.ufl.edulisree8/papers.asp and *http: //www.* fsec. ucf eduledliasee/isreel sarkar -dryer. pdf).

[15] Barnwal P and Tiwari A (2008). Design, Construction and Testing of Hybrid Photovoltaic Integrated Greenhouse Dryer, *International Journal of Agricultural Research* 3 (2): 110-120.

[16] Adelaja AO and Ojolo SJ (2010). Design, Analysis and Experimental Evaluation of Photovoltaic Forced Convection Solar Dryer for the Tropics. *International Journal of Engineering Research in Africa*, 3: 49 – 61.

[17] Ehiem JC, Irtwange SV and Obetta SE (2009). Design and Development of Industrial Fruits and Vegetable Dryer. *Journal of Applied Science, Engineering and Technology*, 1(2): 44 – 53.

[18] Adzimah KS and Seckley E (2009). Improvement on the design of a cabinet grain dryer. *American Journal of Engineering and Applied Science*, 2(1): 217 – 228.

[19] Holman JP (1998). Heat Transfer. 9th Edn., McGraw Hill, New York.

[20] EL- Amin OMA, Mohamed AI, El-Fadil AA and Luecke W (2005). Design and Construction of a Solar Dryer for Mango Slices. *Department of Agricultural Engineering,* University of Zalinga, Sudan.

[21] Brenndorfer B, Kennedy L, Bateman COO, Mrema GC and Wereko-Brobby C (1985). *Solar dryers their role in postharvest processing.* London: Commonwealth Science Council (Commonwealth Secretariat Publications), 1985.

[22] Medugu DW and Yakubu D (2011). Estimation of mean monthly global solar radiation in Yola – Nigeria using angstrom model. *Advances in Applied Science Research, 2011,* 2 (2): 414 – 421.

[23] Bukola OB (2008). Design and Performance Evaluation of a Solar Poultry Egg Incubator. *Thammasat International Journal of Science and Technology*, 13(1): 47 – 54.

[24] Adegoke CO and Bolaji BO (2000). Performance evaluation of solar-operated thermo siphon hot water system in Akure. *International Journal of Technology*, 2(1): 35 – 40.

[25] Onigbogi IO, Sobowale SS and Ezekoma OS (2012). Design, Construction and Evaluation of a Small Scale Solar Dryer. *Journal of Engineering and Applied Science,* 4: 8 – 21.

[26] Owusu J, Haile M, Zhenbin W and Agnes A (2012). Effect of Drying Methods on Physicochemical Properties of Pre-treated Tomato (*lycopersicon esculentum mill.*) Slices. *Croatian Journal of Food Technology, Biotechnology and Nutrition* 7 (1-2): 106 – 111.

[27] Augustus LM, Kumar S and Bhattacharya SC (2002). A comprehensive procedure for performance evaluation of solar food dryers, *Renewable and Sustainable Energy Reviews,* 6 (4), 367-393.

[28] Bennamoun L (2012). An Overview on Application of Exergy and Energy for Determination of Solar Drying Efficiency, *International Journal of Energy Engineering* 2(5): 184 – 194.

[29] Aliyu B, Kabri HU and Pembi PD (2013). Performance evaluation of a village-level solar dryer for tomato under Savanna Climate: Yola, Northeastern Nigeria, *Agric Eng Int: CIGR Journal* 15(1): 181 – 186.

[30] Adejumo AOD and Bamgboye AI (2004). Development and evaluation of a batch solar dryer under Ibadan climate. *Proceeding Nigerian Institution of Agricultural Engineers*, 26: 412-423.

[31] Olalusi AP and Bolaji BO (2008). Performance Evaluation of a Mixed-Mode Solar Dryer, *AU J.T.* 11(4): 225-231.

[32] AOAC (2000). Official Methods of Analysis of the Association of Official Analytical Chemists. 17 editions. AOAC International, Maryland.

Design and Development of Arduino based Automatic Soil Moisture Monitoring System for Optimum use of Water in Agricultural Fields

Sudip Das[1], Biswamoy Pal[2], Partha Das[3], Milan Sasmal[4], Prabuddhamoy Ghosh[5]

Assistant Professor, Department of Electrical Engineering, JIS College of Engineering, Kalyani, W.B.,India

Abstract— *The research aim was to the study the intelligent soil moisture control system in agricultural green house based on Adriano Uno microcontroller automation control. This kind of intelligent soil moisture control system helps to control the moisture level of the field and supply the water if required. In this research embedding a control system into an automatic water pump controller depend upon the moisture of the soil. This system also ability to detect the level of methane gas in the green house. The intelligent soil moisture control system in agricultural green house designed in the research had wonderful effort of man-machine interface, it is very simple, cheep and convenient high degree of automation system. Not only that this system helps to prevent wastage of water. This system is a prototype, which makes this self-sufficient, watering itself from a reservoir. Solar energy is used in this system makes it more environment friendly.*

Keywords— ATmega328p microcontroller, temperature sensor, methane sensor, soil moisture sensor , solar cell, DC Motor. L293D Motor Driver.

I. INTRODUCTION

India is a country where majority of our population are dependable on the agriculture to live their daily life. In this modern technological era poor farmers of india cannot get enough assistance from others to help them with technology and make their work easier. This project made automatic field monitoring & controlling system that can be utilize to improve the condition of green houses. Arduino Uno microcontroller is the main controlling unit of whole system. This system performed the following task:

1. Supply water according to moisture level of soil.

2. Automatic alarming system to avoid the burning of plants by excessive temperature of atmosphere.

3. Automatic methane gas detecting system in green house.

4. Reusing process of excessive water in the field.

II. HARDWARE REQUIREMENTS

The basic components of our projects are ATmega328p microcontroller, solar panel, dc motor, L293D motor driver module, LM35 temperature sensor, MQ22 methane sensor.

2.1 LM35 Temperature Sensor

The temperature sensor is used to sense the temperature in the field and its output voltage is proportional to the centigrade. The LM35 sensors have low output impedance, linear output and precise inherent calibration makes interfacing to the control circuitry easy. It is shown in figure 1.

FIG.1 TEMPERATURE SENSOR

2.2 MQ2 Methane Sensor

It is used for gas leakage detecting (in home and industry).It can detect LPG, methane, i-butane, smoke and so on. Based on its fast response time, measurements can be taken as soon as possible and necessary actions are taken. This type of sensor is shown in figure 2.

FIG.2 METHANE SENSOR

2.3 Soil Moisture Sensor:

The soil moisture senses the moisture content in the soil and based on the value that is showed on the display, according to the control circuit motor will be start ant it will pump the water with the help of a pump and the pumping actions will continue till it fulfills the conditions. With the help of this sensor which is shown in figure 3 we can find whether the soil is dry or wet. A local circuit connection is shown in figure 4.

FIG.3 SOIL MOISTURE SENSOR

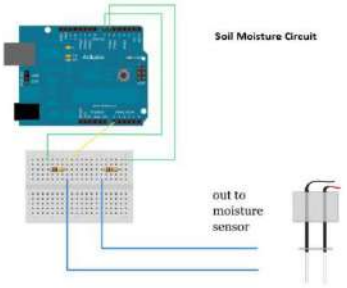

FIG.4 SOIL MOISTURE CIRCUIT

2.4 DC Motor & Drive Circuit:

There are two dc motors used in this project. The 1st dc motor works only to help the pump to pump water into the soil when the moisture level of the soil shown in the monitor is below the rated level that has been set in microcontroller program. And the 2nd dc motor works only in case when rain fall and execs water was suction by that motor. Stored in a supply tank for reusing the store water. The fig.5 shows the dc motor which used in this system. In this project L293D used for conversion binary data to mechanical data. The driver circuit as shown in figure 6.

FIG.5 DC MOTOR

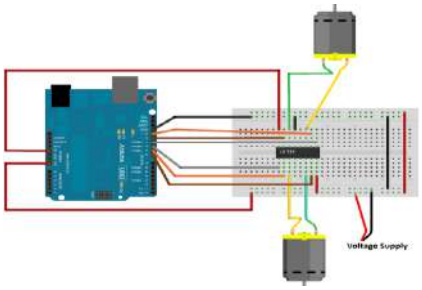

FIG.6 MOTOR DRIVER CIRCUIT

2.5 Arduino Uno

The Arduino Uno is a microcontroller is shown in figure 7 that has 14 digital input-output pins.6 analog inputs,16 MHz ceramic resonator. It is connected with a computer with the help of a USB cable or powers it with ac to dc adapter or a battery for power supply.

FIG.7 ARDUINO UNO MICROCONTROLLER

III. OBJECTIVES

In non conventional energy era, solar energy is one of the most effective energy sources , so solar cells are used to power our circuit .The main objective of this project was to design a greenhouse monitoring system that is be highly reliable and is useful for harvesting crops. Our project mainly focuses on the control of parameters such as-temperature, methane quantity, soil moisture .The block diagram of the greenhouse monitoring system has been shown in Figure 8.

IV. BLOCK DIAGRAM

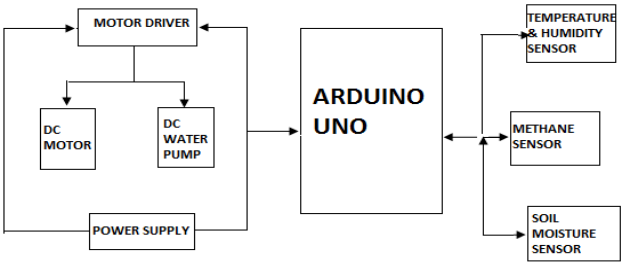

FIG. 8 BLOCK DIAGRAM

V. FLOW CHART

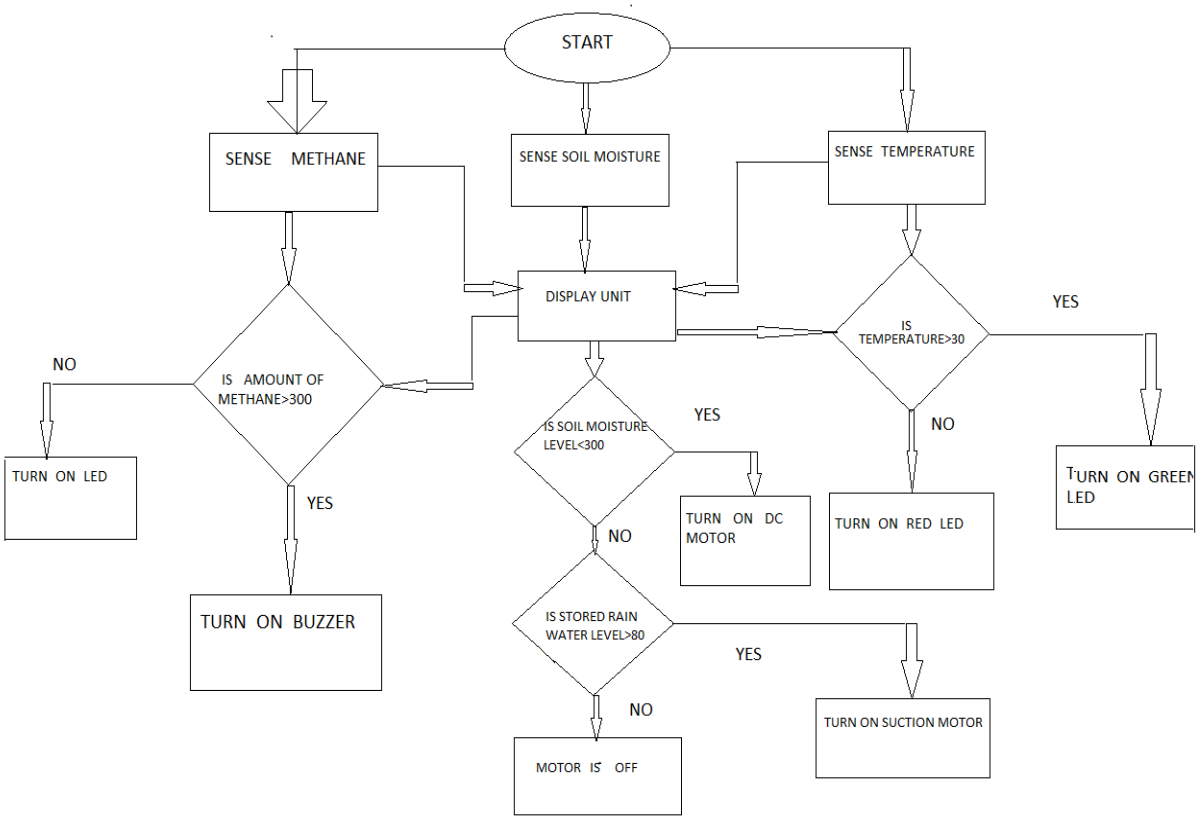

FIG. 9 FLOW CHART

VI. METHODOLOGY

In case of hardware implementation the sensors –temperature sensor, soil moisture sensor, methane sensor were connected with the ATmega328p microcontroller and was connected with the microcontroller with the motor driver module and the power was supplied with the help of a solar panel. Flow chart of this entire project has been shown in Figure 9. The sensors sensed the parameters such as temperature, methane quantity, soil moisture and the microcontroller sensed the values from them and was displayed onto the LCD screen and accordingly the control actions were done that were needed. In case of temperature sensor, if temperature is increased then the greenhouse door was closed manually and if the moisture

quantity of the sand is less than the desired value then accordingly motor was on and vice-versa. Schematic diagram of this project is shown in figure 10.

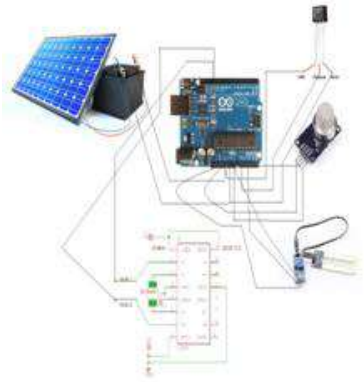

FIG.10 SCHEMATIC DIAGRAM

VII. RESULT

All Sensors determined the soil moisture level, Humidity, Temperature, Methane gas at the root zone. Arduino Micro controller should get sensor data in per minute. Micro controller should record & analyze all the data and take correct action. Soil moisture sensor takes an important role in an agricultural system controller. Soil moisture level set as per based on plant specification, soil type, seasonal rainfall. Arduino microcontroller should upload that observed data in every hour and supply water flow as per requirements.

Efficient results have been obtained from the following project. Table 1 shows the recorded data at field in several days. The hardware implementations have been successful and they are reliable and the sensors that we are using are giving good results and performing to the expectations.

TABLE 1
RECORDED DATA

Date & Time (11.30am)	Atmospheric Temperature	Atmosphere Humidity(%)	Soil Temperature	Soil Moisture (%)
20/04/2017	29	55	28	32
21/04/2017	28	52	27	30
22/04/2017	30	67	29	28
23/04/2017	32	75	31	26
24/04/2017	33	81	32	21

VIII. APPLICATION AND FUTURE SCHOPE

The application of greenhouse monitoring system in agricultural aspect is immense. The automated greenhouse monitoring system will help to reduce the efforts and workloads of human and will be helping to produce plants at the absolute parameters they want them to plant and it will reduce the error. Its ability to control appliances through internet may be integrated for further case. In near future the system can be made 100% autonomous so that it can take all the necessary actions and will result in a effective plant growth. And if we use the bi-directional motor pump, but the rest of the project set up will be same, in that case the system will be cost effective.

IX. CONCLUSION

This project of greenhouse monitoring system has been developed based on the arduino Uno. The microcontroller circuit has been developed with less number of components and is highly reliable. After verifying the data that was shown in got in monitor, assured about the success of the project. Presence of each module has been systematic out and placed carefully, thus contributing to the best working of the every unit. Thus, the Arduino Based Automatic soil moisture monitoring system has been designed and tested successfully. Project snapshots are shown in figure 11.

FIG 11. SNAPSHOTS OF AUTOMATIC SOIL MOISTURE MONITORING SYSTEM

REFERENCES

[1] K.S.S. Prasad, Nitesh Kumar, Nitish Kumar Sinha and Palash Kumar Saha "Water-Saving Irrigation System Based on Automatic Control by Using GSM Technology" Middle-East Journal of Scientific Research 12 (12): 1824-1827, 2012.

[2] N.R. Mohantyandc.Ypatil, "Wireless Sensor And Network Design For Greenhouse Automation", International Journal Of Engineering Technology,Volume3,Issue2,August 2013

[3] "Irrigation System Controllers", SSAGE22, Agricultural and Biological Engineering Department, Florida Cooperative Extension Service, Institute of Food and Agricultural Sciences, University of Florida. Available: http://edis.ifas.ufl.edu

[4] Sanjukumar, R.V.Krishnaiah " Advance Technique for Soil Moisture Content Based Automatic Motor Pumping for Agriculture Land Purpose" Volume 04, Article 09149; September 2013.

[5] Khaled Reza, S.M., Shah Ahsanuzzaman Md. Tariq, S.M. Mohsin Reza (2010), 'Microcontroller Based Automated Water Level Sensing and Controlling: Design and Implementation Issue'. Proceedings of the World Congress on Engineering and Computer Science, pp 220-224.

[6] WWW.PROJECTSOF8051.COM

[7] WWW.ARDUINO.CC

[8] WWW.CIRCUITSTODAY.COM

Assessing Workers Safety Management Knowledge on Construction Site

Y.D. Mohammed[1], B.M.T. Shamsul[2], M.I. Bakri[3]

[1]Department of Quantity Surveying, Federal University of Technology Minna
[2]Department of Environment and Occupational Health, University Putra Malaysia
[3]Department of Environmental Management, University Putra Malaysia

Abstract— *Safety management is associated with the policies, objectives, procedures, methods, roles and functions that aim at controlling hazard and risk in socio-technical systems. Companies that have implemented effective OSH Management system have reported benefit from increase operational efficiency, reduction in insurance cost and improve in workers retention and satisfaction. Many accidents that occur at construction site are due inadequate adherence of workers to work procedures. The awareness and perception of workers toward safety, health and their working environment are important aspect to enhance the building construction to the better condition to the workers. Workers play an important role in accomplishment of the building construction. All these supporting evidence reflects on the needs to study building construction workers knowledge of safety management system. The study is a criteria – based study, in which 24 construction companies were selected for the study The respondent samples used in the study were drawn from the total population of permanent construction workers in the 24 construction companies selected. The total numbers of permanent construction workers in the 24 construction companies are 750 while 254 were selected for the study. The research questionnaires were administered on 254 permanent construction workers within the 24 construction companies in Abuja. The analysis of the questionnaires survey data was undertaken using the statistical package for social science (SPSS) version 20. A reliability test was conducted on the data in order to control error within the data. The Cronbach's Alpha of the two variable data are .853 and .863 respectively and make the data reliable. Correlation analysis was conducted in order to determine the relationship between worker's general knowledge and worker's safety management knowledge and the result was found to be significant (P<0.005). This relationship was modelled using simple linear regression and from the model the result shows that improvement on the worker's safety management system knowledge practice on sites will improves general knowledge among construction workers. Therefore, workers' knowledge of safety management systems significantly influences the overall benefits of safety management system on the construction sites. As such there is need for potential improvement on the knowledge or awareness of the workers to safety management system as perceived from the analysis in order to bring about the expected high performance standard on construction sites.*

Keywords— Safety Management, Knowledge, Workers, Construction Sites, Improvement.

I. INTRODUCTION

Construction industry is vital to the development of any nation, as it strongly contributes to the economic growth of the nation. As such there is need for the industry stakeholders to comply with necessary law and regulations as regard to safety and health of workers. The poor performances record of safety and health in construction industry is because the Occupational Safety and Health (OSH) management system is a neglected area and a function that has not been pursued systematically in the construction industry (Bakri *et al*. 2006). High rate of injury are primarily due to inadequate or non-existence of an OSH management. Therefore Davies & Tomasin (1996) were of the opinion that effective application of OSH Management system can lead to safe construction work and reduce the rate of accidents at construction site.

Occupational safety and health (OSH) is aim at preventing accidents at workplace. Despite the achievement in accidents prevention at most construction sites it has been identified that accidents still exists in construction sites (Levitt & Samelson, 1993). Safety management relates to the actual practices, roles and functions associated with remaining safe Kirwan, (1998), while Reiman & Rollenhagen, (2011) safety management is associated with the policies, objectives, procedures, methods, roles and functions that aim at controlling hazards and risk in socio-technical systems.

Researchers like, Shannon, *et al*., (1996), DePasquale & Geller, (1999) , revealed that organizations with lower accidents rates were characterized by a few of the following factors: safety officers held high rank; management showed personal

involvement in safety activities; superior training for new employees; frequent training for existing employees; display of safety posters for identifying hazards; well defined procedures for promotion and job placements; daily communication between workers and supervisors about health and safety; frequent safety inspections; higher priority for safety in meetings and decisions concerning work practice; thorough investigation of accidents; more frequent attendance of senior managers at health and safety meetings and empowerment of the workforce.

According to Vredenburgh, (2002), the commitment of the management toward safety management system can manifest itself through job training program, management participation in safety committee, consideration of safety in job design, and review of the pace of work, for example, people working for a supervisor that never mentions safety will make people perceive that safety is not an important issues and they will not place more emphasis on safety at the workplace. Companies that have implemented effective OSH Management system have reported benefit from increase operational efficiency, reduction in insurance cost and improve in workers retention and satisfaction (Bakri, *et al.*, 2006).

The construction workers occupation has been recognized as the most dangerous in term of accidents and fatality rates. Leung, *et al.* (2010) stated that Construction workers are obliged to work in a poor physical environment, tolerating extreme outdoor temperatures, poor air quality, excessive noise from bulky equipment, various hazards from working at height, poor housekeeping, and exposure to chemicals, and additional factors. Prolonged work under such adverse physical conditions induces stress in construction workers, such as emotional and physical fatigues. Sawacha, *et al*. (1999); Choudhry and Fang. (2008) working under poor physical environment, which causes discomfort to construction workers, subsequently reduces their attention on safety behaviors.

The concepts of safety culture and safety climate are important contributions from the behavioural and social sciences to workers understanding of occupational safety. Zohar, (1980) defined Organizational Climate, as a summary of molar perceptions that employees share about their work environments. And Neal and Griffin, (2006) defined perceived safety climate as individual perceptions of policies, procedures and practices relating to safety in the workplace". In most construction sites, poor safety awareness, lack of skills, unclear safety responsibilities, boring and simple safety activities or education etc., are major factors affecting workers performances at construction sites.

For example in Malaysia the government have realised the importance of safety management system awareness among the construction workers and through the Construction Industry Development Board (CIDB) together with the National Institute of Occupational Safety and Health (NIOSH) are conducting a safety and health induction program for construction workers or popularly known as Green Card program. This program according to CIDB is an integrated safety and health training program for all construction workers and personnel, which involves the registration and accreditation of construction personnel to enhance safety level at construction site. Similarly the objectives of the program include ensuring that the construction worker is aware of the importance a safe and healthy working place, to provide a basic knowledge on safety and health at construction work site and to inform construction worker of the legal requirement in relation to safety and health (CIDB, 2011).

In a study conducted in Kuala Lumpur and Selangor by Norfairuz, (2003), she among others discovered that awareness on the importance of safety management compliance among many construction workers was low. Safety is reflected in good behaviors. Also according to Hassan, (2007), that many accidents that occur at construction site are due inadequate adherence of workers to work procedures. The awareness and perception of workers toward safety, health and their working environment are important aspect to enhance the building construction to the better condition to the workers themselves (Hassan, 2007). Workers play an important role in accomplishment of the building construction. All these supporting evidence reflects on the needs to study building construction workers knowledge of safety management system.

II. MATERIALS AND METHODS

According to Creswell, (2003) that the factor to be consider in selecting the best research methodology should be the influence that such method have on the research problem and objectives. The study largely derives qualitative measure in order to understand the perception of building construction workers towards safety management system. Therefore, qualitative research is used to gain insight into people's attitudes, behaviors, value systems, concerns, motivation, aspiration, culture or lifestyles (safety management system). Also, Denzin & Lincoln, (2000), claim that qualitative research involves an interpretive and naturalistic approach: "this means that qualitative researcher study things in their

natural settings, attempting to make sense of or to interpret, and phenomena in terms of the meanings people bring to them". Therefore, qualitative research can be used to inform business decisions policy formation, communication and research focus groups etc. about the extent situation of things (sites condition to the management).

The study is a criteria – based study, in which certain criteria were outline for the selection of the construction companies and their construction workers. Those criteria are:

1. The construction company must be built/civil engineering, construction.
2. The construction firm or company must be more than twenty (20) years in civil/building construction work.
3. The construction workers must at least be with the construction company for not less than fifteen (15) years.
4. His qualification must at least not less than secondary school certificates.
5. The location of the study is Abuja, the Nigeria federal capital.

The target construction companies for this study are large size (with more than 100 workforces) with both permanent and temporary construction workers. The reason was that large construction companies tend to have a high degree of safety awareness of the concepts and notions of management system. This will provide a clear image about safety environment in Abuja, Nigeria

Twenty- five (25) construction companies were identified that meet the study criteria and as such twenty – four (24) of the construction companies were selected for the study. The selection is based on sample selection rules of Krejcie and Morgan, (1970). The respondent samples used in the study were drawn from the total population of permanent construction workers in the 24 construction companies selected for the study. The total numbers of permanent construction workers that meet the study criteria in the 24 construction companies are 750 while 254 were selected for the study following the rules of Krejcie and Morgan, (1970). The research questionnaires were administered on 254 permanent construction workers within the 24 construction companies in Abuja. The analysis of the questionnaires survey data was undertaken using the statistical package for social science (SPSS) version 20. Which is a software package used for statistical analysis. It is now named "IBM SPSS Statistics". It is manufacture in Chicago USA, by SPSS Inc. The SPSS Inc is a leading global manufacturer of software used in data analysis, reporting and modelling.

III. RESULT AND DISCUSSION

In social science study, there is need to ascertain the reliability of the data prior to data analysis. As such quality control mechanism is established in order to control error within an existing data in order to make it reliable.

3.1 Result of Reliability Test

The table 3.1 below shows the numbers of test conducted on each items and the final number of items that qualified for the analysis.

TABLE 3.1
RESULTS OF RELIABILITY TESTS

S/no	Components	1st Test		2nd Test		3rd Test		No. of Items	
		α	No of items	α	No of items	α	No of items	Initial	Final
1	Workers General Knowledge (WGK)	.712	7	.853	6	-	-	7	6
2	Workers Safety Management Knowledge (WSMK)	.840	11	.846	10	.863	9	11	9

Source: Researcher analysis

Testing the reliability of the items under workers general knowledge show that one item is deleted as its Cronbach's Alpha if item deleted is greater than initial Cronbach's Alpha (.712). The finial Cronbach's Alpha is .853, and all the six items

have their Cronbach's Alpha if item deleted less than .853. The reliability test of workers safety management knowledge show that three test were carried out and three items are deleted as their Cronbach's Alpha if deleted is greater than initial Cronbach's Alpha of .840 and .846 respectively. The finial Cronbach's Alpha is, .863 and all the nine items that qualified for the analysis have their Cronbach's Alpha if item deleted less than .863.

Correlation analysis was conducted in order to determine the relationship between workers general knowledge and workers safety management knowledge. Table 3.2 shows the result of the correlation analysis.

TABLE 3.2
AVERAGE WORKERS GENERAL KNOWLEDGE (AVGWGK)

Component	r	P
AVGWSMK	0.599	0.001

listwise N=254

Where,

AVGWGK = Average Workers Knowledge

AVGWSMK= Average Workers Safety Management Knowledge

Table 3.2 above reveal the correlation of average workers general knowledge and its correlation is significant at the 0.01 level (2- tailed). N = 254. The Pearson's correlation reveals a positive, strong and highly significant relationship between average workers general knowledge and average workers safety management knowledge, The Pearson's correlation (*r*) from table 3.2 is 0.599 while its P< 0.001. This means that as the level of general knowledge among construction workers improves there is corresponding improvement on the safety management system knowledge practice on sites or high level of general knowledge among the construction workers improve safety management standard knowledge on site.

Following the existing of positive relationship between the variables, there is a need to predict the outcome of the variables. Therefore, simple linear regression is adopt, the simple linear regression seek to examine the effectiveness of workers safety management standard knowledge on site.

In the simple linear regression model develop, workers general knowledge is the dependent variable while workers safety management knowledge is the independent variable. The result of simple linear regression analysis are presented in Table 3.3.

TABLE 3.3
MODEL SUMMARY

Model	R	R Square	Adjusted R Square	Std. Error of the Estimate
1	.695[a]	.483	.479	1.54873

a. Predictors: (Constant): WSMK
b. Dependent Variable:WGK

Table 3.3 shows that 48% (R^2 = 48) of the proportion of variation in workers general knowledge is explained by the variation of level of safety management knowledge of the workers. The R^2 adjusted is 0.479 implying that the model explains 47% of the variation in the workers general knowledge within the population leaving 53% unexplained. The level of awareness or knowledge of workers on safety management standard on site fails to explain all possible variation in the workers general knowledge. Lack of individual competency understanding of workers and supervisors, ineffectiveness or lack of training and certification of competency, lack of ownership, engagement and empowerment of, communication with responsibility for workers and supervisor are responsible for such knowledge failure.

However, the relationship between workers general knowledge and level of awareness among construction workers of safety management system may not necessarily be entirely linear and therefore, there is need to explore other regression techniques so as to see the amount of variance explained increases. The relationships between the two variables of the model described below. Workers general knowledge, the equation abstracted from Table 3.4 below:

TABLE 3.4
COEFFICIENT ANALYSIS

Coefficients[a]								
Model		Unstandardized Coefficients		Standardized Coefficients	t	Sig.	95.0% Confidence Interval for B	
		B	Std. Error	Beta			Lower Bound	Upper Bound
1	(Constant)	2.661	.244		10.888	.000	2.180	3.142
	AVGWSMK	.427	.060	.360	7.135	.000	.309	.544

a. Dependent Variable: AVGWGK

TABLE 3.5
ANALYSIS OF VARIANCE (ANOVA)

ANOVA[a]						
Model		**Sum of Squares**	**df**	**Mean Square**	**F**	**Sig.**
1	Regression	8.496	1	8.496	50.902	.000[b]
	Residual	57.080	342	.167		
	Total	65.575	343			

a. Dependent Variable: AVGWGK
b. Predictors: (Constant), AVGWSMK

AVGWGK = 2.661 + 0.427AVGWSMK

Shows the contribution that workers safety management system knowledge or awareness makes to the workers general knowledge, the result reveals that workers safety management system knowledge contributes additional benefits of unstandardized coefficient = 0.427, t = 7.135 and P<0.005. In the model the system (t=7.135, P<0.005) is a predictor of workers general knowledge and clearly make a great significant contribution to this model. Based on the fact that the t-statistic is greater than 2(rule of thumb) is a confirmation of the reliability of the proposed model. The t-test determine whether each β differ significantly. The β – value has an associated standard error which is used to determine whether or not the β – value differ significantly from zero. The t – test associated with β – value is significant at P < 0.005. This means that the predictor is making a significant contribution to the proposed model. According to Field, (2005) the smaller the significant value the greater the contribution of the predictor. From the magnitude of the t – statistic, the level of workers knowledge or awareness of safety management system has a great impact on workers general knowledge. As the P<0.005 for F-statistic indicate that the model has a high statistical significance level as shown in table 3.5.

The Table 3.4 indicates further that the independent variable accounts well for the variation in the level of workers safety management knowledge. The positive β of 0.427 confirms the positive relationship between workers safety management knowledge and workers general knowledge. This result implies that further implementation of workers safety management knowledge will provide more understanding on workers general knowledge.

Table 3,5 i.e the ANOVA table test shows the importance of the model as a useful predictor of effective workers general knowledge with results of F = 50.902 and P< 0.005 indicating that the model is making a great significant contribution in predicting the benefit of workers knowledge of safety management system. The existence of large residual sum of squares compare to regression sum of squares indicate that the model do not explain certain variation in the dependent variables. May be other variables that are not in the model are accounting for such variation in the independent variables.

IV. CONCLUSION AND RECOMMENDATION

The effectiveness of workers general knowledge on site through construction workers' knowledge of safety management system was determined. It was revealed that a reasonable correlation exists between workers' knowledge of safety management system and workers' general knowledge (r = 0.360, P < 0.001). This means that workers' general knowledge and workers' knowledge of safety management systems are significantly related. This indicates that as the level of workers' knowledge of safety management system increases, the benefit of the safety management system also increase, i.e improve workers general knowledge.

The regression models finding indicate that additional improvement on the level of knowledge of safety management system among the workers' will spring up enormous benefit of workers general knowledge on the construction sites. Those are the evidence that improving workers' awareness of safety management system would improve safety and health measures on construction sites. As such workers' knowledge of safety management systems significantly influence the overall benefits of safety management system on the construction sites. The implication of the finding is that while it might be important for contractors to put in place all necessary training relating to safety management system, the training program identified may not bring about the expected high performance standard of safety and health on construction sites. There is need for potential improvement on the knowledge or awareness of the workers to safety management system as perceived from the analysis in order to bring about the expected high performance standard on construction sites. Knowledge or awareness to safety management system is an important consideration to effective safety management system on site as high safety and health performance could improve the organization image through less accident, less absentees of workers from work, less medical bills, etc. The importance of knowledge of safety management system among construction workers is that it will encourage the management to develop and implement an effective safety management system in construction industry. The models could be of help to the stakeholders in the construction industry in developing an effective safety management.

Adequate training of workers is important in order to increase their knowledge or awareness most especially as regard to identifying and minimizing risks/hazards on the sites. Many safety professionals were of the opinion that training and educating construction workers help in reducing cost and save lives. Toole, (2002), had found out that if workers lack proper training on safety and health, the workers' may not be able to recognized potential hazard at the construction sites. This shows that safety and health training plays a significant role in the enhancement of safety in construction. For those contractors that have been beneficiaries of improved safety and health management system in their organization/or construction sites, it is recommended that they should pay more emphasis on meeting the safety requirement standard at construction sites by organizing induction training for new workers, training and educating the old workers, promoting safety measures at the workplace through poster, video and audio media.

REFERENCES

[1] Bakri, A., Misnan, M. S., Yusof, Z. M., & Wan, W. Y. (2006). *Safety Training For Construction Workers: Malaysian Experience*.

[2] Choudhry, R.M. and Fong, D. (2008). Why operatives engage in unsafe work behaviour investigating factors on construction sites. *Journal of Safety Science*(46), 556 – 584.

[3] CIDB. (2011). *Newsletter of Construction Industry Development Board Malaysia. Issue 1/2010* .

[4] Creswell, J. (2003). J. 2003. Research Design Qualitative, Quantitative, and Mixed Methods Approaches. *Handbook of mixed methods in social & behavioral research*, 209-240.

[5] Davies, V. J., & Tomasin, K. (1996). Construction Safety Handbook. london: Thomas Telford

[6] Denzin, N. K., & Lincoln, Y. S. (2000). Handbook of Qualitative Research. London: Sage Publications.

[7] DePasquale, J. P., & Geller, E. S. (1999). Critical Success Factors for Behavior-Based Safety:: A Study of Twenty Industry-wide Applications. *Journal of safety Research*, *30*(4), 237-249.

[8] Field, A. (2005). Discovering Statistics: Using SPSS for Window

[9] Hassan, Kamal Halil., (2007). Udang-undang Keselamatan Industri di Malaysia. Kuala Lumpur. Dewan Bahasa dan Pustaka.

[10] Kirwan, B. (1998). Safety Management Assessment and Task Analysis: a Missing Link? *Safety Management: The Challenge of Change. Elsevier, Oxford, 67*, 92.

[11] Krejcie & Morgan (1970). Determining Sample Size for Research activities, *Journal of education and psychological measurement* 30, P. 607 – 610.

[12] Leung, MY. Chan, YS. & Yue, KW. (2010). Impacts of Stressors and Stress on the Injury Incidents of Construction Workers in Hong Kong. *Journal of Construction Engineering and Management* 136 (10): 1093 – 1103.

[13] Levitt, R. E., & Samelson, N. M. (1993). *Construction safety management*: London, Wiley.

[14] Neal, A. & Griffin, M.A. (2006). A study of the lagged Relationships among Safety Climate Safety, Motivation, Safety Behavior and Accidents at the Individual and Group Levels. *Journal of Applied Psychology*. 91 (4), 946 – 953.

[15] Norfairuz, F. (2003). *Amalan Keselamatan di tapak bina: Kajian kes Projek perumahan di sekitar Kuala Lumpur dan Selangor.* Fakulti Kejuruteraan Awan, Universiti Teknologi Malaysia. Unpublished thesis.

[16] Reiman., T., & Rollenhagen, C., (2011). Human and Organizational biases affecting the Management of Safety. *Reliability Engineering and System Safety*, *96*(10), 1263 - 1274.

[17] Sawacha, E. Naoum, S. and Fong, D. (1999). Factors Affecting Safety Performance on Construction sites. *International Journal of Project Management*. 17,(5). 309 – 315.

[18] Shannon, H. S., Walters, V., Lewchuk, W., Richardson, J., Moran, L. A., Haines, T., & D. Verma. (1996). Workplace organizational correlates of lost-time accident rates in manufacturing. *American Journal of Industrial Medicine.*, *29*, 258-268.

[19] Toole, T. M. (2002). Construction site safety roles. *Journal of Construction Engineering and Management*, *128*(3), 203-210.

[20] Vredenburgh, A. G. (2002). Organizational safety: which management practices are most effective in reducing employee injury rates? *Journal of safety Research*, *33*(2), 259-276.

[21] Zohar D. (1980). Safety Climate in Industrial Organizations: Theoretical and Applied, Implications. *Journal of Applied Psychology*. 65(1):96−102.

Correlation between Destructive Compressive Testing (DT) and Non Destructive Testing (NDT) for Concrete Strength

Oke, D. A.[1], Oladiran, G. F.[2], Raheem, S. B.[3]

The Department of Civil Engineering, The polytechnic, Ibadan, Oyo State, Nigeria

Abstract— *Concrete is the most widely used construction material worldwide. Strength of a concrete structure may have to be assessed without causing physical damage to it, due to various reasons like its monumental importance or the legal dispute on whether the strength of the concrete in the structure is satisfactory enough or not. In an attempt to meet the above demand, correlation and comparison between Destructive Test (DT) and Non Destructive Test (NDT) were carried out.*

A total of 24 concrete cubes (150 mm x 150 mm x 150 mm) were cast with concrete mix ratio of 1:2:4. 12 cubes were tested destructively for compressive strength with compression machine and 12 cubes were also tested non-destructively with Schmidt Rebound Hammer. Compressive strength test results at curing ages (7, 14, 21 and 28days.) were collated and analysed.

The results obtained from the non-destructive testing method were correlated with the results obtained from destructive testing method. The coefficient of correlation between the two set of compressive strength was 0.988 which indicates a perfect relationship between compressive strength results from both methods.

Keywords— Compressive Strength, Non Destructive test, Destructive Compression test, Schmidt Rebound Hammer.

I. INTRODUCTION

The standard method of determining strength of hardened concrete consists of testing concrete cubes in compression. It is very important to ascertain the compressive strength of concrete before subjecting to its anticipated loads. Compressive strength of hardened the concrete can be determined using the destructive (DT) and non-destructive testing (NDT) method. The destructive testing (DT) method is carried out by crushing the cast specimen to failure while non-destructive testing (NDT) is carried out without destroying the concrete specimen. The rebound (Schmitz) hammer is one of the most popular non-destructive testing (NDT) method used to test the strength of the concrete.

This is due to it relatively low and simplicity in use. Although the non-destructive testing (NDT) result are much quicker compare to the destructive methods. They are more of an approximation than exact compressive value. In as much as the rebound hammer result are quicker and do not destroy the surface of concrete tested, there is no established relationship between compressive strength obtained using NDT and DT.

Various non-destructive methods of testing concrete have been developed, which include, Firing method, Skramtayev's method, Polakov's method, Magnitostroy method, Fizdel ball hammer, Einbeck pendulum hammer, Ball indentation hammer, Rebound hammer, Pull out techniques, Windsor probe, Ultrasonic pulse velocity methods, Radioactive and nuclear methods, Magnetic and electrical methods. In all these methods of tests, due to simplicity, rebound hammer test based on surface hardness becomes most popular in the world for non-destructive testing of in-situ concrete.(Kaushal Kishore 2000).

The rebound (Schmitz) hammer is one of the most popular non-destructive testing (NDT) method used to test the strength of the concrete. This is due to it relatively low and simplicity in use. Although the non-destructive testing (NDT) result are much quicker compare to the destructive methods. They are more of an approximation than exact compressive value. In as much as the rebound hammer result are quicker and do not destroy the surface of concrete tested, there is no established relationship between compressive strength obtained using NDT and DT.

Pratt D.U. and Lawrence J. (1990) claims non-destructive test (NDT) methods are used to obtain information about a structure in an indirect way.

The research aimed at comparing the strength of concrete obtained by Schmidt rebound hammer (NDT) and compressive testing machine (DT).

II. MATERIALS AND METHODS

The various types of materials used in this study to cast the concrete include: Fine aggregate (sand), Coarse aggregate (granite), Cement and Water.

A total of 24 concrete cubes (150 mm x 150 mm x 150 mm) were cast with concrete mix ratio of 1:2:4. 12 cubes were tested destructively for compressive strength with compression machine and 12 cubes were also tested non-destructively with Schmidt Rebound Hammer. Compressive strength test results at curing ages (7, 14, 21 and 28days.) were collated and analysed.

TABLE 1
TABLE SHOWING NUMBER OF CUBES TESTED

Test Methods	Age 7	Age 14	Day 21	Day 28
Schmidt Hammer Test (N.D.T)	3	3	3	3
Compression Machine Test (D.T)	3	3	3	3
Total				24

III. RESULTS AND DISCUSSION

3.1 Slump Test

The result of slump test carried out to assess the workability of fresh concrete is shown in table 2.

TABLE 2
SLUMP TEST RESULT

Percentage (%)	Slump (mm)	Kind of slump
1:2:4	20	True

3.2 Compressive Strength Tests Results

The compressive test results achieved by crushing cured cubes under the compressive test machine at different crushing ages are shown in table 3 From the results obtained a gradual general increase was recorded in strength of concrete, with the concrete cubes attaining the highest strength at 28th day curing age.

3.3 Schmidt Hammer Test Results

The Schmidt hammer is used to get the surface hardness of concrete which is a function of the concrete strength. The rebound numbers gotten were converted to compressive strength using the standard conversion graph. Three cubes were subjected to testing with the Schmidt hammer on each of the different curing ages.

TABLE 3
AVERAGE COMPRESSIVE STRENGTHS FOR BOTH N.D.T AND D.T

Test Methods	Age 7	Age 14	Day 21	Day 28
Schmidt Hammer Test (N.D.T)	15.68	18.80	23.06	34.61
Compression Machine Test (D.T)	14.03	17.60	20.6	27.50

3.4 Correlation and Regression Analysis

The strength of relationship and governing equation between the NDT and DT compressive strength test results were determined statistical tool.

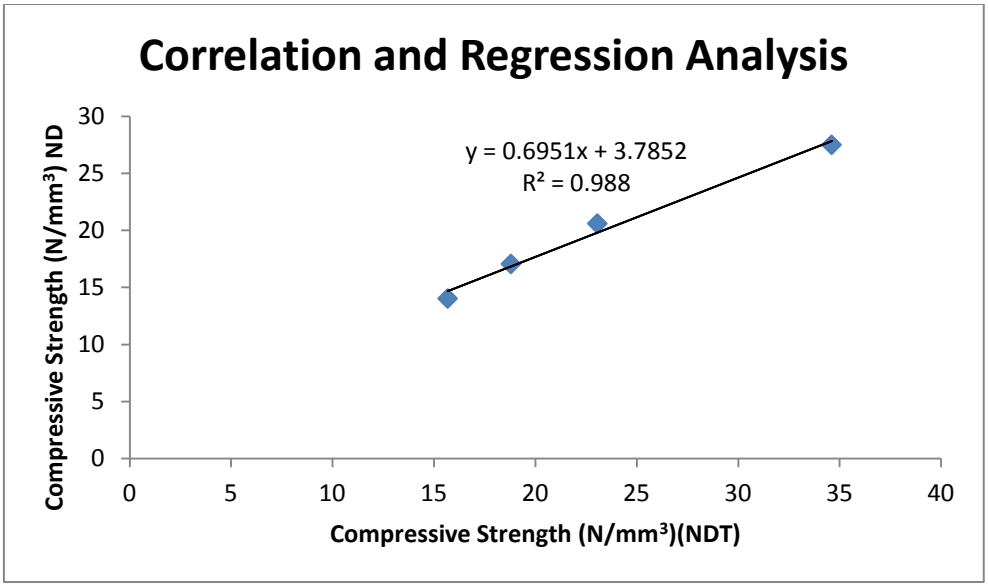

FIGURE 1: CORRELATION AND REGRESSION ANALYSIS

Conversion equation:

$$y = 0.6951x + 3.7852$$

Where "x" is the rebound hammer compressive strength of the concrete cube

Where "y" is the compressive strength of the concrete cube

Where R^2 is the correlation coefficient

3.4.1 Regression Validation

TABLE 4
REGRESSION VALIDATION

Curing Age	Schmidt Hammer Test (N.D.T)	Compression Machine Test (D.T) Experimental Values	Predictive or Correlated Values y = 0.6951x + 3.7852
7	15.68	**14.03**	**14.68**
14	18.80	**17.60**	**16.85**
21	23.06	**20.6**	**19.81**
28	34.61	**27.50**	**27.84**

IV. CONCLUSION AND RECOMMENDATIONS

The correlation among the strength values obtained by DT and NDT test methods on concrete cubes has been established. Schmidt Hammer test method has been used as a non-destructive test. The following conclusions have been drawn:

- There exist a strong relationship between the compressive strength results from both methods with Correlation coefficient of $R^2 = 0.988$.
- The predictive equation $y = 0.6951x + 3.7852$

The following recommendations were made based on result and observation recorded in this study.

- Increased number of test sample cubes is suggested to for better correlation of both rebound hammer test and compressive strength test values.

- The Schmidt rebound hammer is recommended for the assessment of compressive strength of hardened concrete to rule out difficulties (delayed feedbacks on laboratory analysis, epileptic power supply for running tests on concrete cubes.) in testing cubes for their strength using compression testing machine.

REFERENCES

[1] Aksahi t, Amasaki s (1984). Non destructive testing in concrete, ACI SP- 82 Detroit pp 19 – 34

[2] Amasaki S (1991) Estimation of strength of concrete structure by the rebound number CSJ Proc conc 45 pp 345 - 351

[3] Blezard (1998) "Durable concrete structure" Thomas Telford publishing company limited

[4] Bungey.J.H and S.G. Millard (1996). Testing of concrete in structure Blackie Academy and professional, London, newyork, 3rd ed, pp 286

[5] British Standard Institution, (1980). Method for determination of compressive strength of concrete cubes, BS 1881: Part 116, London, British Standard Institution.

[6] Duna Samson Omoniyi, Tope Moses. Correlation between Non-destruction testing (NDT) and destructive testing (DT) of compressive strength of concrete. September 2014, pp 12-17.

[7] Ferhat Asphin and Mehmet Saribiyik. '' Correlation between Schmidt hammer and destructive compressive testing for concretes in existing buildings, June 2010, pp 1664 - 1648.

[8] Greene G.W. Test hammer provides new method of evaluating hardened concrete, ACIJ.

[9] Hassan R.Hajjeh correlation between destructive and non destructive strength of concrete cubes vol.5, 2012, no. 10, 493-509

[10] Hassan R. Hajjeh, (2012) Correlation between destructive and Non-destructive strength of concrete cubes using regression analysis. Pp 493-509

[11] Kaushal Kishore, (2000) '' Non destructive testing of concrete by rebound hammer.

Income Structure, Profitability and Stability in the Tunisian Banking Sector

Houda Belguith[1], Meryem Bellouma[2]

GEF2A lab, ISG Tunisia, University of TUNIS, TUNISIA
GEF2A lab, Faculty of Economic and Management of Nabeul, TUNISIA

Abstract— *This study examines the effect of revenue diversification across and within interest and non-interest income on bank stability and performance in Tunisian banks over the period 2001-2014. Using panel estimations and instrumental variables approach to handle the endogeneity problem of diversification variables. We find that revenue diversifications among and within interest and non-interest revenue generating operations boost bank profitability and stability. Our findings suggest also that the benefits from diversification are largest for banks with more shifts to nontraditional banking business lines (investment banking) while, absent for banks which follow cross-selling strategies of financial services.*

Keywords— bank performance, bank stability, interest income, non-interest income, Tunisian Banks.

I. INTRODUCTION

The banking industry in both developed and developing countries has experienced important shifts that have been related to its increasing deregulation and competition. This has led banking institutions to diversify their income generating activities toward non-interest income operations. Unsurprisingly, the share of the classical financial intermediation operations has decline in both developed and developing banking industries. While the major source of income for banks is interest revenue from credits to customer, new banking business lines which generate non-interest revenue, have emerged such as fee generating activities, trading securities, investment banking and other operations.

The effects of shifts toward non-traditional banking activities on bank performance and stability have been widely examined in developed economies while rarely addressed in developing economies. There has been no large consensus in the empirical literature regarding the impact of the shift toward non-interest income generating operations on bank performance and risk in developed countries. For instance, Stiroh (2004a, 2004b, 2006), Stiroh and Rumble (2006) and Lepetit and al. (2008) find that non-interest activities positively affect bank performance but negatively impact bank stability. This is because non-interest income generating operations are highly volatile. However, diverging results have been found in the context of developing countries (Sanya and Wolfe, 2011; Nguyen and al., 2012; Pennathur and al., 2012). Thus, one of the aims of this study is to contribute to the limited literature that analyzes the impact of bank's income diversification on performance and stability in the context of developing economies. As this group of countries presents different features compared to developed countries mainly in terms of banking regulatory framework and maturity and structure of the banking sector, we would expect to find different effect of income diversification on bank performance and risk.

The recent financial crisis has shown that banking supervisors should be concerned with banks' business models in addition to the classical prudential norms such that bank capitalization, liquidity and risk management. The analysis of banks' business models which signals the way in which banks generate profits and serve customers can provide banking supervision authorities with a deeper understanding of the sustainability of bank performance and stability (Köhler, 2015).

The recent financial crisis has showed that not all banks were impacted equally. The effect of the crisis has been related to the business model chosen by each bank. Banks with traditional banking model, mainly those relying on the classical financial intermediation function, faced huge losses (ECB, 2010). In fact, banks with high rates of loan growth have reported a significant decrease in their performance during the recent financial crisis. For instance, in Europe, the return-on-equity (ROE) of EU banks with the highest average rate of loan growth within the period 2003-2006 dropped, on average, from 13.34% in 2006 to 6.77% in 2008. However, the ROE of banks with the lowest loan growth rates decreased less importantly from 10.46% to 5.65%. Interestingly, in 2009, while the performance of the first group of EU banks declined further, the ROE of the second group of banks (with the lowest rates of loan growth) increased (Köhler, 2015). Thus, if we consider the decline in banks' profitability as an indicator of risk-taking, we would argue that banks with high growth rate in terms of lending activity have incurred greater risks than those with low growth rate of their lending activities.

While large banks with high share of non-interest income have also faced large losses during the recent financial crisis, small banks relying on non-interest banking activities have benefited from diversification of their income sources as it has allowed them to be less dependent on overall business condition and therefore to be more stable (Liikanen, 2012).

In this study, we use detailed information on interest and non-interest income categories as well as on their components for a sample of 11 banks over the period 2001-2014. We try to answer the question regarding which business models allow for high profitability gains for banks and which ones expose banks to higher return volatility and instability. To do so, we examine the effect of business models on bank stability and performance. We test whether banks become more stable in case they increase their non-interest banking activities due to the effect of the diversification of revenue sources. We also examine whether this positive effect of the diversification of banking activities depends on the type of both interest and non-interest incomes and on their correlation. In addition, we try to answer the question of which banks are taking much more benefits from revenue diversification through controlling for bank funding and ownership structures.

Our findings indicate that revenue diversification through a shift toward non-interest income generating activities leads to higher performance and risk-adjusted profitability of Tunisian banks. This result confirms the findings of Sanya and Wolfe (2011), Pennathur and al. (2012) and Meslier and al. (2014) who find a positive association between income diversification and bank performance in emerging countries. Furthermore, our results show that diversification gains are more pronounced in banks where non-interest income are generated from nontraditional banking business lines while absent in those following cross-selling strategy of their financial products to a core business customers.

This work has two main motivations. The first motivation comes from the diverging findings with regard to the relationship between revenue diversification and bank performance and stability in emerging economies. Indeed, this study explores this gap in the literature in an emerging country. The second motivation of this study stems from the fact that it has been shown that some types of banks with different kinds of business models proved to be vulnerable during the recent financial crisis (Mergaerts and Vennet, 2016). Thus, this work aims at reconsidering banks' business models in the direction of strengthening the resilience of banks.

This work contributes to the existing literature in two important ways. First, contribute to the related empirical literature by using the instrumental variables approach to handle the problem of endogeneity of the diversification variables. This is because we believe that the income diversification decision of banks can be thought as being itself impacted by bank performance. This might be the case when, for instance, poorly performing banking institutions decide, under the pressure of their shareholders, to diversify their income structure to reduce their overall risk. Second, we complement the existing literature on banks' business models by analyzing the effect of the subcategories of interest income and non-interest income on bank stability and performance. This is because previous studies have shown that not every type of the interest and non-interest income is equally volatile or has the same impact on bank performance and stability (DeYoung and Torna, 2013; Stiroh, 2007).

The remainder of this paper is organized as follow. Section 2 discusses the related literature and formulates the hypotheses to be tested. Section 3 presents the data and the econometric methodology. Section 4 shows the descriptive analysis. Section 5 presents our findings. Finally, section 6 concludes.

II. LITERATURE REVIEW AND HYPOTHESIS

The empirical literature on banking stability argues that excessive growth rates of lending activity lead to higher risk taking by banks (Foos and al., 2010; Jimenez and Saurina, 2006). However, the effect of bank's business mix on bank stability has not been demonstrated clearly. For instance, while many authors argue that an increase in non-interest banking activities, like for instance investment banking, allows banks to benefit from additional sources of income and to diversify their overall revenue which would make them more stable, others argue that bank instability may arise when banks diversify their income sources by relying on non-interest activities due to the higher volatility of these activities. Busch and Kick (2009) suggest that the volatility of banks' profitability significantly increases when they become involved in fee business.

However, Chiorazzo and al. (2008) finds that an increase of the share of non-interest income by Italian banks will lead to higher risk-adjusted returns. For the case of Germany, Busch and Kick (2009), show that savings and cooperative banks will have their performance improved if they increase their share of non-interest income, while the authors find no impact of non-interest income on the profitability of commercial banks. For developing countries, there are also findings which suggest that banks benefit from a better revenue diversification (Sanya and Wolfe, 2011).

Mergaerts and Vennet (2016) argue that the diversification of income structure should lead to better trade-off between the expected level and variance of banks' performance. Of course, for this positive effect of income source diversification to hold, banks' income-generating operations should not be perfectly correlated. A bank's business model that relies on income diversification allows banks to generate more non-interest income from the average asset, which more than compensates the lower level of net interest income and higher expenses. However, Stiroh and Rumble (2006) and Demirgüc-Kunt and Huizinga (2010) show that income diversification has a positive impact on profitability, but a negative one on bank stability.

Altunbas and al. (2011) and Köhler (2015) find that more diversified banks are generally less likely to be under stress. Lepetit and al. (2008) argue that revenue diversification toward non-interest income generating activities can lower the cyclical variations in profits if incomes across bank activities are not perfectly correlated. Further, income diversification leads to increased competitive pressures between banks across a large number of banking business lines which can increase innovation and efficiency in the provision of banking services.

2.1 H1: Revenue diversifications across and within interest and non-interest revenue generating operations enhance bank performance and stability.

DeYoung and Torna (2013) find that banks which diversify into non-interest income are less likely to encounter financial distress. Further, the authors argue that the effect of non-interest income on bank stability significantly depends on the type of non-interest income. While a larger share of revenue from asset-based non-traditional banking operations, such as investment banking and asset securitization, is found to make financially distressed banks significantly more likely to fail, a larger share of fee-based non-traditional banking activities, such as insurance sales, significantly decreases the probability of a failure.

The authors examine, in the context of the recent financial crisis, whether banks with a larger share of non-interest income were more likely to fail. They find that it is not non-interest revenue per se that made banks more likely to fail, but rather the type of non-interest income. More specifically, the authors show that a larger share of income from asset-based non-traditional activities, such as investment banking and asset securitization, has led to higher banks failures. However, the authors argue that a larger share of fee-based non-traditional activities such as insurance sales has reduced the probability of failure during the financial crisis.

It is important to note that a shift toward non-interest revenue that stems from traditional banking activities may not lead to diversification benefits. Instead, it may, lead to a reduction of diversification benefits. This is because this type of income is subject to the same variations as interest-generating activities which might lead to further volatility of banks' benefits. This is the case when banks follow cross-selling strategy through providing financial products to a core customer base. However, diversification benefits are higher when a bank shifts toward non-interest revenue generated from nontraditional banking operations.

In addition, it may be the case that both categories of income coming from traditional and nontraditional baking activities are uncorrelated but both highly volatile. The standard portfolio theory argues that the overall variance of operating income increases when the variations of revenues stemming from both traditional and nontraditional banking operations increase (Meslier el al., 2014).

2.2 H2: An increase in non-interest income generated from nontraditional banking activities enhance bank stability, while those generated from traditional banking activities worsen bank stability.

Many papers have examined the impact of the diversification of income and funding sources on bank risk and return. Demirgüc-Kunt and Huizinga (2010) find some risk diversification benefits at very low shares of non-interest income and non-deposit funding. However, for the most banks, they find that increases in the shares of both non-interest revenue and non-deposit funding are associated with higher instability. Altunbas and al. (2011) find that banks with a more diversified income structure are more stable.

Köhler (2015) argues that the way in which banks diversify their income and funding sources impacts their risk and profitability. The author suggests that this impact depends on the business model chosen by each bank. For instance, for retail-oriented banks, while a shift towards non-interest revenue leads to higher stability and performance, an increase in the share of non-deposit funding is associated with bank instability. This is because such business strategy will make them less dependent on interest banking activities which improves their risk diversification and, therefore, leads to more stability and profitability. However, for investment-oriented banks, while a shift towards non-interest revenue leads to higher instability, an increase in the share of non-deposit funding leads to more significant stability. This is because these banks, with such business model, already have higher share of non-interest income and a further increase in it will limit the benefits of diversification of income sources as it leads to over diversification.

Lepetit and al. (2008) and Mercieca and al. (2007) show that European banks that have increased their non-interest income operations are more risky than banks that mainly supply loans.

However, the related literature argues that the opposite sign of the relationship between revenue diversification and bank performance may also occur. Mercieca and al. (2007) argue that when banks over expand their operations toward new market segments where they face higher competition or lack of expertise, revenue diversification may worsen bank performance.

The authors indicate that there is a threshold or a risk optimal level that diversifying beyond it may lead to an increased idiosyncratic risk for banks.

2.3 H3: Revenue diversification positively impact bank performance but up to a given threshold.

Altunbas and al. (2011) show also that larger banks and those with higher growth rates of loans are more risky, while stable banks are those characterized by a strong deposit base. Demirgüc-Kunt and Huizinga (2010) obtain similar findings. They show that banks which are mostly relying on fee and trading income are less stable. The authors indicate also that banks which are heavily relying on wholesale funding are more risky. However, Demirgüc-Kunt and Huizinga (2010) find no evidence that high growth rate of loans leads to higher risk-taking by banks.

Recent studies have argued that a higher reliance on customer deposits decreases bank distress (Altunbas and al., 2011; Betz and al., 2013) and inspires market confidence (Beltratti and Stulz, 2012). Mergaerts and Vennet (2016) find that banks characterized by a traditional funding structure are both more profitable and stable. The authors show that a higher deposit ratio is associated with lower interest expenses, which leads to higher net interest income and greater returns. Further, banks with business model characterized by a higher share of customer deposits are also better able to generate non-interest income due to the greater scope of cross-selling products to an expanded group of retail clients, which can raise fee income.

The literature on the bank capital argues that the use of equity as a funding source of banks decreases the ability of banks' creditors to exert market discipline (Diamond and Rajan, 2001). However, equity financing may induce banks to monitor borrowers more intensively (Mehran and Thakor, 2010). Beltratti and Stulz (2012) find that during the recent financial crisis, banks with business models that rely on higher capital ratios performed better and were less likely to encounter severe distress. These banks had higher levels of net interest margins and return on assets, but this did not suffice to offset the mechanical negative impact on return on assets. The positive impact of such business model on ROA and NIM can mainly be attributed to lower interest expenses. This can be explained by the fact that the use of a higher capital ratio decreases banks' reliance on interest-bearing funding sources.

Mergaerts and Vennet (2016) find that banks which rely on high capital ratios have significantly higher Z-scores and therefore are more stable. However, the authors also confirm the results of Delis and al. (2014), who find that a higher capital ratio increases ROA volatility which leads to bank risk. Nevertheless, their results show that the positive impact of a higher capital ratio on ROA more than offset the positive effect on ROA volatility. These findings support the strengthening of the capital rules by Basel III and the continuous pressure of supervisory authorities on banks to increase capital ratios.

2.4 H4: The impact of revenue diversification on stability in more pronounced in under capitalized banks.

The literature that analyzes the influence of different types of ownership on the profitability of banks also draws divergent conclusions. While some empirical studies show that foreign banks are more efficient (Ahmad 2017, Meselier 2014), others find evidence that public banks are more efficient (Das and Ghosh, 2010). Microco et al. (2007), for industrialized countries, found no evidence to support the idea that private banks are more profitable than public banks. However, they have found support for developing countries. In addition, Iannotta et al. (2007) argue that public banks are less profitable than their counterparts because of the increased risk associated with project financing. On the other hand, Dietrich and al, (2011) argue that Swiss public banks are more profitable than private banks during the financial crisis. Chen and Liu (2013) show that the performance of banks varies by ownership structure, with public and foreign banks playing a more unfavorable role than private banks.

2.5 H5: Revenue diversification gains are more pronounced in private banks.

The empirical literature on bank stability argues that, in addition to banks' income and funding structure, there are many other variables that affect bank stability. For instance, Köhler (2015) argues bank stability is positively associated with capitalization but negatively correlated with bank scale. Also, the author finds that a higher rate of asset growth makes banks significantly more risky, while a higher net interest margin and a larger loan portfolio is found to reduce bank risk.

Regarding the impact of bank size on the relationship between banks' business models and bank stability, Köhler (2015) finds that smaller banks will be significantly more stable if they generate a larger share of their income from non-traditional activities, but will be instable if they increase their share of non-deposit funding. The author also finds that larger banks will have significantly less volatile returns if they increase their share of non-interest income.

III. DATA AND ECONOMETRIC METHODOLOGY

3.1 Data and variables définition

The bank-specific data used in this study stem from the Thomson Reuters Eikon database. The sample contains the eleven largest banks operating in Tunisia which represent together a market share of more than 88% of the total assets of the Tunisian banking sector. The period of study is 2001-2014. We have, therefore, a dataset which contains 154 bank-year observations for each variable.

There has been a huge discussion in the empirical literature regarding how to measure bank risk-taking as one proxy for banking stability. In this study, we follow the empirical related literature (Altunbas and al., 2011; Demirgüc-Kunt and Huizinga, 2010; Köhler, 2015) and use as a proxy for bank stability the variable Z-Score which is defined as follows:

$$Z - score_{it} = (\frac{ROA_{it} + CAR_{it}}{\sigma_{ROAi}})$$

Where:

ROAit : is the return on assets of bank i in year t,
CARit : Is measured as total equity divided by total assets of bank i in year t, and
σ_{ROA} : is the standard deviation of the return on assets.

The variable Z-Score is computed as the sum of the ROA and the ratio of total equity to total assets divided by the standard deviation of ROA. This measure indicates how many standard deviations that a bank's return on assets has to fall for the bank to become insolvent. Z-Score indicates the distance to insolvency. It can be used as a good indicator of bank risk (Delis and al., 2014). A higher level of Z-score means a lower bank risk. However, a lower value indicates higher riskiness.

Mergaerts and Vennet (2016) interpret Z-score as a measure of the distance-to-default as it represents the number of standard deviations ROA can diverge from its mean before the bank defaults. The authors argue that Z-score should be used as a distress indicator, rather than as a direct measure of bank risk-taking. This is because we have seen a decrease in the observed evolution of Z-score for European banks during the recent financial crisis instead of before it.

There has been a huge debate in the empirical literature regarding how to identify banks' business models. For instance, Mergaerts and Vennet (2016) argue that there are two approaches of business model identification. The first approach allocates banks to specific groups using direct or indirect classification. While the direct classification uses qualitative variables (e.g. the bank type according to regulation) that are assimilated to the business model, the indirect classification combines the information regarding a set of continuous variables to construct distinct groups of observations that are as homogeneous as possible (Ayadi and al., 2011, 2012; Martín-Oliver and al., 2015; Roengpitya and al., 2014). However, this approach based on classification can be criticized for the validity of its hypothesis that there exist clearly separable business models which means the non-existence of intermediate strategies. The Tunisian banking sector has been characterized since 2001, by very limited regulations in what concerns the scope of bank activities. The enactment of the banking law n° 2001-65 of 10 July 2001 has introduced the concept of universal bank which can operate as commercial and investment bank at the same time.

The second approach suggested by the related literature (Altunbas and al., 2011; Demirgüc-Kunt and Huizinga, 2010) directly relates individual business model features to bank performance. This approach allows us to identify the specific characteristics of a business model that improve bank performance and stability. One drawback of this strategy is that it is unable to directly identify the effect of the business model, because it does not clearly define how the individual features are interrelated to compose a business model. In this research, we choose the second approach by using a set of indicators that capture a bank's strategic choices related to the income and liability structure. These specific variables are presented below.

In this study, we define banks' business models by taking into account the level of diversification of both income sources and funding sources. This is done through examining the share of non-interest revenue in total operating revenue and the share of non-deposit funding in total bank's liabilities. The related empirical literature has identified many banks' business models. For instance, banks which mostly provide lending and deposit-taking services for households and SMEs have a more retail-oriented business model. These banks are typically smaller. On the other hand, investment-oriented banks are those which

have a large share of their revenue generated through non-traditional banking activities such that investment banking and trading. These banks are typically larger and fund most of their activities on wholesale markets (Köhler, 2015).

Köhler (2015) indicates that business models show how banks generate profits, what customers they serve and which distribution channels they use. Therefore, examining business models goes beyond looking at classical indicators of bank risk and performance and should give banking supervisors a deeper understanding of the sustainability of bank profits and stability. In this study, we describe a bank's business model by the structure of its income and funding. We proxy the income structure using the ratio of non-interest income over total operating income (NII) and the funding structure using the ratio of non-deposit funding over total liabilities (NDF).

The previous studies have shown that banks' income structure as it is measured using the share of both non-interest income and interest income to total operating income, has a significant impact on bank performance and stability. Also, banks' funding structure measured by the share of both non-deposit funding and customer deposits to total liabilities, has been shown to affect bank performance and stability. Nevertheless, as we argue that not every type of non-interest income and interest income is equally volatile or has the same impact on bank performance and stability (DeYoung and Torna, 2013; Stiroh, 2007), we opt in this study, for analyzing the subcategories of the aforementioned variables instead of taking into consideration their aggregate values. We are able to implement such subdivisions in our analysis since the data are available in the Thomson Reuters Eikon database.

For the analysis of income structure, we take into consideration four subcategories of interest income and six subcategories of non-interest income. We subdivide interest income into (1) interest on loans, (2) interest on investment securities, (3) interest on deposits and (4) other interest income. For non-interest income, we take into consideration the following subcategories: (1) fees and commissions from operations, (2) dealer trading account profit, (3) investment securities gains, (4) insurance commissions, fees and premiums, (5) foreign currencies gains and other non-interest income. Then we measure the importance of each subcategory of interest and non-interest income with respect to total operating income.

In what concerns the analysis of the funding structure, we take into consideration three items, namely, (1) equity, (2) customer deposits and non-deposit funding. Then we measure the importance of each subcategory with respect to total assets.

In addition to the diversification variables, we use a set of control variables related to bank-specific factors (bank size, capitalization, loan growth, and deposit growth and bank efficiency) and macro-economic condition (GDP growth and inflation rate).

We use efficiency indicator as we believe that the way a bank manage its expenses does impact its performance. EFFICIENCY is computed as the ratio of non-interest expenses to total revenue less interest expenses and it measures the cost to the bank of each unit of revenue. Belaid and Bellouma (2016) use the ratio of operating expenses divided by operating incomes as one control variable that is not directly related to business model but is important to determine bank performance and stability. This ratio measures banks' cost inefficiency and reflects bank managers' skills in terms of controlling and monitoring their operating expenses where a high value of this ratio indicates high cost inefficiency.

3.2 Econometric methodology

A detailed dataset is used in this study on eleven Tunisian banks over 14 years (from 2001 to 2014) for a total 154 bank-year observations. We start our empirical analysis by panel data estimation. We regress our dependent variables which measure bank risk-adjusted performance, namely, risk-adjusted ROA (RAROA) and risk-adjusted ROE (RAROE) and bank's insolvency risk (Z-score) on a set of variables related to revenue diversification across and within interest and non-interest income. We use also a set of bank specific variables including bank size, capitalization, loan and deposit growth rates and bank efficiency. In addition, we control for macroeconomic factors by taking into consideration GDP growth and inflation rate.

Thus, we estimate the following model:

$$Y_{it} = \alpha + X_{it} + Z_{it} + \theta_t + \varepsilon_{it} \quad (1)$$

Where:

Y represents:

RAROAit : risk-adjusted return on assets computed as ROA divided by its standard diviation.
RAROEit : risk-adjusted return on equity computed as ROE divided by its standard diviation.
Z-Scoreit : defined as the sum of ROA and the ratio of total equity to total assets divided by the standard deviation of ROA.

X represents a set of our variables of interest that indicate the bank's revenue diversification through shifts across interest and non-interest generating operations and within these two types of income:

HHI_REVit: measures the revenue diversification between interest and non-interest income.
NIIit: measures the share on non-interest income in total operating income..
HHI_NIIit: measures the diversification within non-interest income generating activities.
HHI_IINit: measures the diversification within interest income generating activities.

Z represents a set of bank specific control variables:

EQUITYit: measures bank capitalization using the ratio of equity to total assets.
DEPOSITSit: is computed as deposits from customers divided by total assets.
NDF it: is calculated as the ratio of non-deposit funding over total assets.
SIZEit: measures bank size using the logarithm of total assets.
EFFICIENCYit: is the ratio of non-interest expenses to total revenue less interest expenses and it measures the cost to the bank of each unit of revenue.
LOAN_G it: measures the annual growth in total loans.
DEPOSIT_G it: measures the annual growth in total deposits.
θ Represents macroeconomic variables:

GDPt: annual GDP growth rate.
INFt: inflation rate.

As we are using panel data, both fixed and random effects models can be used. While random effects model considers that the variation across individuals is assumed to be random and uncorrelated with the regresses included in the model, fixed effects does not. We run Husman test in order to determine our appropriate method of estimation.
The result of the test of Hausman shows a p-value which is greater than the 5%. Thus, we use random effects method as we cannot reject the null hypothesis.

In a second stage of our empirical analysis, and for robustness checks, we use an instrumental variables (Two-Stage least squares, 2SLS) regression. This econometric choice is motivated by the fact that our revenue diversification variables may be endogenous which leads to an inconsistency of the estimators. Indeed, a problem of reverse causality between bank performance and revenue diversification may exist which can cause an endogeneity problem in our explanatory variables of interest. This is because we believe that the revenue diversification decision can be thought as being itself affected by bank performance. This might be the case when, for instance, poorly performing banking institutions decide, under the pressure of their shareholders, to diversify their income structure. To solve this problem of endogeneity we use the instrumental variable approach. To do so, we choose new variables as instruments for our diversification indicators. These instruments have to satisfy the two important properties of being exogenous (not correlated with the error term) and largely correlated with the endogenous variables. Following Maudos and Solis (2009) and Meslier and al. (2014), we use as instruments the lagged levels of our diversification variables in order to handle the endogeneity problem.

IV. DESCRIPTIVE ANALYSIS

In this section, we present a brief overview of banks' income structure in the Tunisian banking sector. Table 1 provides the descriptive statistics for the variables used in this study and Table 2 shows the pair wise correlation matrix.

In what concerns bank profitability, Table 1 shows the low level of ROA and ROE for Tunisian banks compared to the average values in emerging countries (Sanya and Wolfe, 2011). In addition, an important feature of bank performance to be highlighted is the high within volatility of bank performance over the period 2001-2014. Surprisingly, the within variations of ROA and ROE are greater than the between variations. This bank performance feature indicates the high instability of bank performance in Tunisia. For the risk-adjusted return on assets (RAROA) and on equity (RAROE) and the insolvency risk (Z-Score), the between bank variation is higher than the within bank variation which means that there is a large heterogeneity across banks included in our sample that should be examined further. For these variables, the mean and the median values are close to each other which indicate that the data are not skewed, so we do not need to use the logarithmic scales of it.

TABLE 1
DESCRIPTIVE STATISTICS OF THE VARIABLES USED IN THIS STUDY

	Mean	Median	Standard deviation		
			Within	Between	Overall
Bank performance					
Return on Assets (ROA)	0.011	0.012	0.012	0.008	0.014
Return on Equity (ROE)	0.041	0.091	0.379	0.112	0.394
Bank Stability					
Risk adjusted ROA (RAROA)	2.444	2.281	0.967	2.105	2.234
Risk adjusted ROE (RAROE)	1.734	1.184	0.967	1.899	2.058
Insolvency Risk (Z-Score)	23.336	23.453	7.018	16.876	17.603
Income Diversification					
Interest Income/Total Op. Income (IIN)	0.719	0.709	0.063	0.071	0.092
Non-Interest Income/Total Op. Income (NII)	0.281	0.291	0.063	0.071	0.092
Diversification between IIN and NII (HHI_REV)	0.613	0.587	0.066	0.068	0.092
Diversification within Interest Income					
Diversification within Interest Income (HHI_IIN)	0.925	0.990	0.067	0.069	0.094
Interest on Loans (INT_LOANS)	0.959	0.995	0.038	0.038	0.053
Interest on Deposits (INT_DEPOSITS)	0.011	0	0.016	0.013	0.021
Interest on Investments Securities (INT_INVEST)	0.017	0	0.023	0.020	0.029
Other Interest Income (INT_OTHER)	0.013	0	0.021	0.017	0.026
Diversification within Non-Interest Income					
Diversification within Non-Interest Income (HHI_NII)	0.467	0.447	0.122	0.089	0.149
Fees from operations (FEES)	0.519	0.521	0.121	0.133	0.176
Profit from trading (TRADE)	0.109	0	0.096	0.130	0.157
Gains from investment securities (INVEST)	0.206	0.185	0.082	0.193	0.202
Insurance fees (INSUR)	0.009	0	0.036	0.024	0.043
Foreign currencies gains (FX)	0.019	0	0.039	0.036	0.052
Other Non-Interest Income (NII_OTHER)	0.137	0.068	0.114	0.107	0.153
Bank Specific Controls					
Equity (EQUITY)	0.113	0.086	0.052	0.087	0.097
Customer Deposits (DEPOSITS)	0.718	0.768	0.076	0.153	0.165
Non-Deposit Funding (NDF)	0.168	1.149	0.045	0.085	0.093
Log assets (SIZE)	7.589	7.744	1.350	0.727	0.779
Efficiency (EFFICIENCY)	0.535	1.549	0.143	0.119	0.183
Loan Growth (LOAN_G)	0.099	0.089	0.081	0.024	0.084
Deposit Growth (DEPOSIT_G)	0.132	0.099	0.199	0.141	0.240

Notes: ROA is the return on assets measured as net income before taxes over total assets. ROE is the return on equity calculated as net income over total equity. RAROA and RAROE are the measures of risk-adjusted return on assets and equity, respectively. Z-score is calculated as the sum of ROA and the ratio of total equity to total assets divided by the standard deviation of ROA. IIN is computed as interest income divided by total operating income. NII is computed as non-interest income divided by total operating income. HHI_REV measures income diversification between IIN and NII (using the Herfindahl Hirschman Index). HHI_IIN measures the diversification within interest revenue generating operations. INT_LOANS, INT_DEPOSIT, INT_INVEST and INT_OTHER measure, respectively, the share of interest on loans, interest on deposits, interest on investment securities and other interest income in total interest revenue. HHI_NII measures the diversification within non-interest revenue generating operations. FEES, TRADE, INVEST, INSUR, FX and NII_OTHER measure the share of, respectively, fees generated from banking operations, gains on trading securities, profits from the sale of investment securities, fees and premium earned from taking or brokering insurance policy subscriptions, foreign currency trading gains and other non-interest income in total non-interest revenue. EQUITY measures the ratio of total equity over total assets. Deposits measure the ratio of total deposits over total assets. NDF is the ratio of non-deposit funding over total assets. Size is the logarithm of total assets. EFFICIENCY is computed as the ratio of non-interest expenses to total revenue less interest expenses and it measures the cost to the bank of each unit of revenue. LOAN_G and DEPOSIT_G measure the annual growth in total loans and total deposits, respectively.

Table 1 shows that 72% of the total operating income of Tunisian banks stems from interest-income generating activities, while 28% are generated from non-interest income operations. This indicates that financial intermediation function remains the core banking business of Tunisian banks. The concentration on bank income towards interest generating operations is confirmed by the level of the indicator Herfindahl Hirschman Index (HHI_REV) of 0.613 which close to the one observed in emerging economies (Sanya et Wolfe, 2011) of 0.62. The between and within variations of this indicator are close to each other which indicates a similar behavior of Tunisian banks regarding their diversification strategy of revenue between interest income and non-interest income activities.

Regarding the diversification within interest income generating activities, we notice a very large concentration towards interest on loans to customers with a share of 96%. This is confirmed by the high value of the indicator HHI_IIN of 0.925. So far, we conclude that the financial performance and stability of Tunisian banks is highly dependent on their lending activities' behavior and therefore their stability is determined by the quality of their loan portfolios.

TABLE 2
PAIRWISE CORRELATION BETWEEN THE VARIABLES USED IN THIS STUDY

	RAROA	RAROE	Z-SCORE	HHI_REV	IIN	NII	HHI_IIN	HHI_NII	INT_LOANS	INT_DEPOSITS	INT_INVEST	FEES	TRADE	INVEST	INSUR	FX	EQUITY	DEPOSITS	NDF	SIZE
RAROA	1																			
RAROE	0.86***	1																		
Z-SCORE	0.65***	0.46***	1																	
HHI_REV	-0.26***	-0.12	0.25***	1																
IIN	-0.35***	-0.16**	0.07	0.96***	1															
NII	0.35***	0.16**	-0.07	-0.96***	-1	1														
HHI_IIN	-0.04	-0.09	0.07	-0.01	-0.06	0.06	1													
HHI_NII	-0.12	-0.13	0.14*	0.39***	0.36***	-0.34***	-0.11	1												
INT_LOANS	-0.04	-0.08	0.07	0.00	-0.05	0.05	0.91***	-0.11	1											
INT_DEPOSITS	0.17**	0.13	0.10	-0.17**	-0.17**	0.17	-0.73***	-0.11	-0.75***	1										
INT_INVEST	-0.07	0.04	-0.11	0.29***	0.36***	-0.32***	-0.61***	0.35***	-0.60***	0.08	1									
FEES	-0.38***	-0.20**	-0.18**	0.54***	0.62***	-0.62***	-0.33***	0.75***	-0.32***	-0.02	-0.04***	1								
TRADE	-0.21***	-0.20**	-0.12	0.19**	0.15**	-0.15**	0.34***	-0.08	0.333***	-0.31***	-0.12	0.0173	1							
INVEST	0.59***	0.39***	0.38***	-0.42***	-0.46***	0.46***	-0.04	-0.03	**-0.04**	**0.18****	**-0.12**	**-0.41*****	-0.68***	**1**						
INSUR	0.17**	0.04	0.05	-0.10	-0.07	0.07	-0.12	-0.27***	**-0.12**	**0.31*****	**-0.12**	**-0.24*****	**-0.33*****	**0.28*****	**1**					
FX	0.02	0.30***	-0.12	-0.15*	-0.15*	0.15*	-0.36***	-0.21***	**-0.34*****	**0.46*****	**-0.21*****	-0.04	-0.18**	**-0.00**	**0.18****	**1**				
EQUITY	0.03	0.05	0.64***	0.69***	0.56***	-0.56***	0.16**	0.22***	**0.16***	**-0.08**	**-0.09**	**0.16****	**0.13**	**-0.20****	**0.06**	**-0.15**	**1**			
DEPOSITS	0.11	0.03	-0.43***	-0.62***	-0.52***	0.52***	-0.30***	-0.23	-0.29***	**0.19****	**0.18****	-0.00	**-0.20****	**0.26*****	-0.12	0.18**	**-0.87*****	**1**		
NDF	-0.22***	-0.11	0.09	0.36***	0.34***	-0.34***	0.35***	-0.19**	**0.35*****	**-0.26*****	**-0.22*****	**-0.16****	**0.22*****	**-0.26*****	**0.14***	**-0.18****	**0.51*****	**-0.86*****	**1**	
SIZE	0.06	0.04	-0.46***	-0.63***	-0.57***	0.57***	-0.06	-0.39***	**-0.05**	**0.07**	-0.07	**-0.40*****	**-0.15***	**0.21*****	**0.03**	**0.21**	**-0.77*****	**0.58*****	**-0.23*****	**1**

Notes: *, ** and *** means that there is a high likelihood (90%, 95% and 99%, respectively) that there is a significant relationship between the two variables.**RAROA** and **RAROE** are the measures of risk-adjusted return on assets and on equity, respectively. **Z-score** is computed as the sum of ROA and the ratio of total equity to total assets divided by the standard deviation of ROA. **IIN** is computed as interest income divided by total operating income. **NII** is computed as non-interest income divided by total operating income. **HHI_REV** measures income diversification between IIN and NII (using the Herfindahl Hirschman Index). **HHI_IIN** measures the diversification within interest revenue generating operations. **INT_LOANS**, **INT_DEPOSIT** and **INT_INVEST** measure, respectively, the share of interest on loans, interest on deposits and interest on investment securities in total interest revenue. **HHI_NII** measures the diversification within non-interest revenue generating operations. **FEES**, **TRADE**, **INVEST**, **INSUR** and **FX** measure the share of, respectively, fees generated from banking operations, gains trading securities, profits from the sale of investment securities, fees and premium earned from taking or brokering insurance policy subscriptions and foreign currency trading gains in total non-interest revenue. **EQUITY** measures the ratio of total equity over total assets. **Deposits** measure the ratio of total deposits over total assets. **NDF** is the ratio of non-deposit funding over total assets. **Size** is the logarithm of total assets.

Non-interest income generating activities display different features. In fact, the mean value of HHI_NII of 0.467 indicates that there is a relative diversification within non-interest income activities for banks included in our sample. In terms of the composition of this type of bank revenue, fee based activities present a share of 52% in total non-interest income. This subcategory of non-interest income activities includes fees related to money transferring and check clearing, and other fees. However, and despite the observed relative diversification within non-interest income activities, we notice, at this stage of the analysis, that as long as these fees and commissions are generated from traditional banking operations through a cross-selling of financial products to a core customer base, this would not lead to diversification benefits as income generated from fees earned from commercial banking operations are positively correlated with interest income1.

Table 1 shows interesting results regarding the funding structure of the banks included in this study. Indeed, on average, total assets of banks are funded by deposits from customers (72%), non-deposit funding (17%) and equity (11%). We notice the large differences among banks regarding their capitalization as it is shown by the mean and the medina of the ratio of equity to total assets of 11.3% and 8.6%, respectively. The mean of bank size is close to the median (7.6 compared to 7.7, measured using the logarithm of total assets) which ensures that our analysis is not suffering from a sample selection bias that may arise from sampling either large or small banks which would affect the diversification decision of bank revenue.

Table 1 shows a large disparity between banks in terms of efficiency as it is shown by the mean and the median levels. We notice that on average, one unit of revenue costs 0.535 units of non-interest expenses to banks.

Table 2 shows the pairwise correlation between the variables taken into consideration in this study. We notice that the diversification between interest income and non-interest income (as it is shown by the variable HHI_REV) is negatively and significantly correlated with risk-adjusted return on assets (RAROA) but positively and significantly correlated with bank stability (Z-Score). The first result indicates that a decrease in HHI_REV2 leads to higher risk-adjusted return on assets. This confirms the finding related to the relationship between income diversification and bank performance in emerging countries (Sanya and Wolfe, 2011). However, the second result indicates that an increase in diversification toward non-interest income (in other term a decrease in HHI_REV) leads to lower stability. Sanya and Wolfe (2011) find positive link between revenue diversification and bank stability in emerging economies.

The results for IIN and NII confirm the aforementioned interpretations. Indeed, Table 2 shows that NII (IIN) is significantly and positively (negatively) correlated with risk-adjusted performance but negatively correlated with bank stability.

The positive link between NII and risk-adjusted performance (RAROA and RAROE) is mostly driven by the positive correlation of these performance variables and non-interest income generated from investment securities (INVEST). One interesting result is that interest on loans to customers (INT_LOANS) is not correlated with risk-adjusted returns on assets (RAROA) and on equity (RAROE) which means that Tunisian banks are not generating much profit from their core business line (lending activity3).

As Table 2 shows that revenue diversification toward non-interest income is positively and significantly correlated with bank instability, we go further in our analysis through asking the question about which of the components of NII is driving this result. In fact, the pairwise correlation matrix shows that non-interest income generated from both fees on operations (FEES) and gains on trading securities (TRADE) which represent together a share of 63% of total non-interest income of Tunisian banks, are positively and significantly correlated with interest income (IIN). This interesting result explains the absence of the expected diversification benefit in term of bank stability. This is obvious since, in Tunisian banks, interest income generating activities are subject to the same fluctuations of non-interest income generating operations. Interestingly, the coefficient of correlation between the volume of interest income (IIN) and non-interest income (NII) is large (0.85)4. This means that most of non-interest income is generated from traditional banking activities through cross-selling financial product to a core business customer of banks.

Bank capitalization measured by the ratio of equity over total assets is positively correlated with bank stability. This is expected because well capitalized banks, through the pressure of their shareholders, are more risk-averse than under capitalized banks. Also, higher capitalization ratios allow banks to absorb losses and, therefore, reduce the overall risk. Equity ratio, however, is not correlated with risk-adjusted performance.

[1] A significant positive correlation of 0.62.

[2] Notice that a decrease in HHI_REV means an increase in revenue diversification toward non-interest income, while an increase indicates an increase in revenue concentration on interest income.

3 Interest on loans to customers represents an average share of 66% of total operating income of Tunisian banks and a share of 96% of total interest income.

4 It is not reported in Table 2 as we only report the figures regarding correlations of IIN and NII in terms of shares in total operating income (in percentage but not in volume). We report in appendix 2 the matrix of pairwise correlation between interest and non-interest incomes and their components taken as volumes.

TABLE 3
REGRESSION ANALYSIS RESULTS USING RANDOM EFFECTS REGRESSIONS

	Diversification between interest and non-interest income						Diversification within both interest and non-interest income					
Y=Dependent variable	RAROA (1)	RAROE (2)	Z-SCORE (3)	RAROA (4)	RAROE (5)	Z-SCORE (6)	RAROA (7)	RAROE (8)	Z-SCORE (9)	RAROA (10)	RAROE (11)	Z-SCORE (12)
HHI_REV	-14.8***	-8.34***	-83.64***									
	(2.464)	(2.29)	(16.016)									
NII				14.59***	7.37***	89.13***						
				(2.084)	(2.004)	(13.377)						
HHI_IIN							-3.01	-4.48***	-9.42			
							(1.875)	(1.576)	(12.17)			
HHI_NII							-3.33**	-4.11***	-1.89			
							(1.328)	(1.117)	(8.628)			
INT_LOANS										-5.65	-5.24	50.56
										(6.712)	(7.432)	(37.440)
INT_DEPOSITS										9.52	-2.14	245.64***
										(12.88)	(14.264)	(71.857)
INT_INVEST										13.04	15.64*	133.793***
										(8.241)	(9.125)	(45.971)
FEES										-3.63***	-2.11*	-18.67***
										(1.016)	(1.203)	(6.061)
TRADE										5.16***	3.01**	24.29***
										(1.157)	(1.392)	(7.013)
INVEST										8.86***	5.11***	58.57***
										(1.016)	(1.125)	(5.669)
INSUR										-6.67**	4.22	-99.34***
										(3.279)	(3.631)	(18.294)
FX										2.60	2.91	13.279
										(3.046)	(3.373)	(16.995)
EQUITY	2.836	-1.81	148.17***	-0.43	-3.84	131.13***	-5.25	-7.37**	112.33***	-2.88	-3.95	117.083***
	(3.172)	(2.95)	(20.618)	(2.922)	(2.809)	(18.751)	(3.376)	(2.838)	(21.923)	(2.435)	(2.696)	(13.582)
SIZE	-0.359	-0.36	-1.20	-0.54	-0.42	-2.49	-0.34	-0.59*	0.89	-0.55*	-0.41	-2.38
	(0.342)	(0.318)	(2.224)	(0.335)	(0.322)	(2.149)	(0.400)	(0.336)	(2.599)	(0.842)	(0.327)	(1.650)
EFFICIENCY	-5.44***	-6.47***	-14.97**	-5.52***	-6.47***	-15.78**	-5.74***	-7.37***	-12.12	-5.55***	-6.08***	-17.80***
	(1.043)	(0.970)	(6.784)	(1.008)	(0.969)	(6.473)	(1.188)	(0.999)	(7.717)	(0.842)	(0.932)	(4.699)
GDP	0.101	0.10	0.21	0.095	0.10	0.18	0.54	0.05	0.97*	0.03	0.47	-0.12
	(0.075)	(0.070)	(0.489)	(0.072)	(0.070)	(0.467)	(0.832)	(0.069)	(0.540)	(0.057)	(0.063)	(0.322)
INF	-0.562	-0.01	-1.22	-0.06	0.00	-1.35	0.08	0.04	-0.10	0.16	0.14	0.18
	(0.146)	(0.135)	(0.949	(0.140)	(0.135)	(0.902)	(0.157)	(0.132)	(1.023)	(0.110)	(0.122)	(0.616)
Constant	16.72***	12.91***	79.06***	5.37*	6.45**	15.54	12.54***	16.76***	20.06	13.85**	12.27	-20.29
R-sq	0.294	0.2805	0.5197	0.3404	0.2817	0.5627	0.1650	0.3046	0.4329	0.6199	0.4509	0.8095

TABLE 4
REGRESSION ANALYSIS RESULTS USING INSTRUMENTAL VARIABLES (2SLS) REGRESSION

	Diversification between interest and non-interest income						**Diversification within both interest and non-interest income**		
Y=Dependent variable	**RAROA (1)**	**RAROE (2)**	**Z-SCORE (3)**	**RAROA (4)**	**RAROE (5)**	**Z-SCORE (6)**	**RAROA (7)**	**RAROE (8)**	**Z-SCORE (9)**
HHI_REV	-17.4***	-9.78***	-100.51***						
	(3.03)	(2.788)	(19.780)						
NII				17.08***	8.62***	105.72***			
				(2.475)	(2.360)	(15.926)			
HHI_IIN							-1.95	-4.30*	-2.39
							(2.511)	(2.11)	(15.84)
HHI_NII							1.13	0.31	14.57
							(2.782)	(2.342)	(17.55)
EQUITY	7.35**	0.94	165.31***	3.41	-1.54	144.53***	-0.13	-2.86	126.28***
	(3.677)	(3.338)	(23.981)	(3.300)	(3.147)	(21.237)	(4.251)	(3.579)	(3.421)
SIZE	-0.10	-0.17	-0.39	-0.32	-0.26	-1.86	0.42	0.12	3.62
	(0.363)	(0.334)	(2.370)	(0.355)	(0.338)	(2.283)	(0.542)	(0.456)	(3.421)
EFFICIENCY	-5.04***	-6.22***	-14.99**	-5.12***	-6.24***	-15.71**	-4.44***	-6.18***	-8.86
	(1.077)	(0..990)	(7.028)	(1.038)	(0.990)	(6.684)	(1.456)	(1.225)	(9.187)
GDP	0.09	0.10	0.20	0.08	0.09	0.16	0.08	0.08	0.25
	(0.073)	(0.133)	(0.480)	(0.071)	(0.067)	(0.457)	(0.086)	(0.072)	(0.545)
INF	-0.10	-0.03	-1.52	-0.11	-0.02	-1.67*	0.16	0.12	0.13
	(0.145)	(0.133)	(0.948)	(0.138)	(0.132)	(0.894)	(0.164)	(0.138)	(1.040)
Constant	15.85***	12.02***	82.23***	2.53	4.54	5.45	1.96	7.45	-19.77
R-sq	0.303	0.2929	0.4964	0.3529	0.2936	0.5446	0.1144	0.2461	0.4006

V. EMPIRICAL RESULTS

Table 3 shows our empirical results using random effects models. We have twelve specifications where we examine the relationship between bank income diversification across interest and non interest income generating activities as well within these two types of revenue on bank performance and stability. In specification 1-3, we examine the link between revenue diversification and bank performance and stability using as proxy for diversification the index HHI of both main categories of income (interest and non-interest income).

In specification 4-6, we use one direct measure of diversification which is NII (non-interest income over total operating income). In specification 7-9, we try to examine the effects of diversification within both interest and non-interest income on bank performance and stability using the index HHI. In last specification 10-12, we examine the relation between each component of interest and non-interest income and bank performance and bank stability.

In all specification, we find that revenue diversification across and within interest and non-interest income enhance bank performance and stability. Notice that the negative coefficient oh HHI _REV means that an increase in diversification towards non-interest income (in other words a decrease in HHI-REV) is associated with an increase in risk-adjusted return on assets (RAROA) and on equity (RAROE) as well as in bank stability measured by Z-Score. The same reasoning is for HHI_IIN and HHI_NII. These results confirm our hypotheses which state that when banks shift towards non-interest income generating activities, their performance and stability improve.

The positive impact of revenue diversification on bank performance can be explained by the fact that when banks diversify their income structure by exploring new business lines, their innovation and competitiveness increase which leads to higher profitability. On the other hand, the positive impact of revenue diversification on bank stability can be explained by the fact that when banks shift toward non-interest generating activities the volatility of their income decreases as their interest and non-interest incomes are not perfectly correlated.

Our results show that the impact of income diversification toward non-interest revenue generating operations does depend on the category of non-interest revenue as well as its correlation with interest revenue and its subcategories. We found the diversification gains to be more pronounced when banks shift to non-interest income generating activities that are not correlated with interest income and are stemming from nontraditional banking activities. This is explained by the fact that nontraditional banking operations are not subject to the same fluctuations as interest-generating operations. This lowers earnings volatility and improves stability. Unsurprisingly, non-interest income stemming from traditional banking activities worsens bank stability.

In all specification, we find that revenue diversification across and within interest and non-interest income enhance bank performance and stability. Notice that the negative coefficient oh HHI _REV means that an increase in diversification towards non-interest income (in other words a decrease in HHI-REV) is associated with an increase in risk-adjusted return on assets (RAROA) and on equity (RAROE) as well as in bank stability measured by Z-Score. The same reasoning is for HHI_IIN and HHI_NII. These results confirm our hypotheses which state that when banks shift towards non-interest income generating activities, their performance and stability improve.

The positive impact of revenue diversification on bank performance can be explained by the fact that when banks diversify their income structure by exploring new business lines, their innovation and competitiveness increase which leads to higher profitability. On the other hand, the positive impact of revenue diversification on bank stability can be explained by the fact that when banks shift toward non-interest generating activities the volatility of their income decreases as their interest and non-interest incomes are not perfectly correlated.

Our results show that the impact of income diversification toward non-interest revenue generating operations does depend on the category of non-interest revenue as well as its correlation with interest revenue and its subcategories. We found the diversification gains to be more pronounced when banks shift to non-interest income generating activities that are not correlated with interest income and are stemming from nontraditional banking activities. This is explained by the fact that nontraditional banking operations are not subject to the same fluctuations as interest-generating operations. This lowers earnings volatility and improves stability. Unsurprisingly, non-interest income stemming from traditional banking activities worsens bank stability.

VI. CONCLUSION

In this study we use a detailed dataset on eleven banks operating in Tunisia over the period 2001-2014 to examine the relationship between revenue diversification and bank performance and stability. Using a panel data estimation as well as instrumental variables approach (2SLS) to handle the endogeneity problem of diversification variables, we find that income diversifications between and within interest and non-interest income generating activities enhance bank performance and bank stability.

Our findings confirm those of previous studies on emerging banking sectors. For instance, over the period 2001-2014, Tunisian banks show a relative large reliance on interest income generating activities (62%) which is made mainly through interest on loans to customers with a share in total interest income of 96%. Also, like in developing countries (Sanya and Wolfe, 2011), our findings suggest that banks benefit from a better revenue diversification. In fact, the diversification of income structure leads to better trade-off between the expected level and variance of banks' performance. Of course, for this positive effect of revenue source diversification to hold, banks' income-generating operations should not be perfectly correlated. Also, the positive effect of revenue diversification toward non-interest income generating activities can be explained by its role in lowering the cyclical variations in profits if incomes between bank activities are not perfectly correlated. This in addition to the role played by income diversification in increasing competitive pressures between banks across a large number of banking business lines which can increase innovation and efficiency in the provision of banking services.

The results also indicate that diversification gains are largest for banks with more shifts to nontraditional banking business lines while, absent for banks which follow cross-selling strategies of financial services.

Furthermore, our results show that the effect of revenue diversification does depend on the category of non-interest revenue and its correlation with interest revenue and its components. In fact, we found the diversification gains to be more pronounced when banks shift to non-interest income generating activities that are not correlated with interest income and are stemming from nontraditional banking activities such as investment banking and fee-based income from nontraditional operations (like for example commissions, fees and premiums earned from insurance activity).

One explanation of this result is that nontraditional banking operations are not subject to the same fluctuations as interest-generating operations which leads to lower earnings volatility. However, non-interest income coming from traditional banking activities worsens bank stability.

This study can be extended in several directions. One way for future researches would be to explore more channels through which revenue diversification can affect bank performance and stability. One channel would be the improved banking competition and innovation in presence of income diversification.

REFERENCES

[1] Ahmad, M; M. (2017). : "Asset quality, non-interest income, and bank profitability: Evidence from Indian banks. Economic Modelling. Vol. 63, pp. 1–14.

[2] Altunbas, Y; Manganelli, S and Marques-Ibanez, D, (2011): "Bank Risk During the Financial Crisis – Do Business Models Matter?". ECB Working Paper Series, N° 1394, European Central Bank, Frankfurt.

[3] Ayadi, R ; Arbak, E and de Groen, W.P, (2011) : « Business Models in European Banking: A Pre-and Post-Crisis Screening". Centre for European Policy Studies, Brussels.

[4] Belaid, F and Bellouma, M, (2016): "Determinants of loan quality: evidence from the Tunisian banking sector". International Journal of Engineering Research & Science. Vol 2. P, 67-79.

[5] Beltratti, A and Stulz, R.M, (2012) : «The credit crisis around the globe: why did some banks perform better?". Journal of Financial Econ. Vol 105 (1).P, 1–17.

[6] Busch, R. and Kick. T, (2009): "Income Diversification in the German Banking Industry". Bundes bank Discussion Paper, N° 09/2009.

[7] Chen, Y; Liu, Jun Su (2013) ; « Greasing the wheels of bank lending: Evidence from private firms in China." Journal of Banking & Finance, Vol.37(7), P, 2533-2545.

[8] Chiorazzo, V. Milani, C and Salvini, F, (2008): "Income diversification and bank performance: evidence from Italian banks. Journal of Financial Services Research. Vol 33. P.181–203.

[9] DeYoung, R and Torna, G (2013): "Nontraditional banking activities and bank failures during the financial crisis". Journal of Financial Intermediation. Vol 22. P,397-421.

[10] Demirgüc-Kunt, A and Huizinga, H, (2010): "Bank Activity and Funding Strategies: The Impact on Risk and Returns", Journal of Financial Economics, Vol. 98, pp. 626-650.

[11] Delis, M.D., Hasan, I and Tsionas, E.G, (2014): "The risk of financial intermediaries". Journal of Banking and Finance. Vol 44. P, 1–12.

[12] Diamond, D.W and Rajan, R.G, (2001): "Liquidity risk, liquidity creation, and financial fragility: a theory of banking". Journal of Political Economie. Vol 109 (2). P, 287-327.

[13] ECB, (2010): "EU Banking Structure Report", European Central Bank, Frankfurt.

[14] Foos, D; Norden L. and Weber, M, (2010): "Loan Growth and Riskiness of Banks", Journal of Banking and Finance, Vol. 34(12). P, 2929-2940.

[15] Imbierowicz, B, and Rauch, C, (2014): "The relationship between liquidity risk and credit risk in banks. Journal of Banking and Finance, Vol. 40. P, 242-256.

[16] Jimenéz, G and Saurina, J, (2006): "Credit Cycles, Credit Risk, and Prudential Regulation". International Journal of Central Banking. Vol. 2(2).P, 65-98.

[17] Köhler, M, (2015): "Which banks are more risky? The impact of business models on bank stability". Journal of Financial Stability. Vol. 16. P, 195-212.

[18] Laeven, L. and Levine, R, (2009): "Bank governance, regulation and risk taking". Journal of Financial Economics. Vol. 9. P, 259-275.

[19] Lepetit, L ; Nys, E ; Rous, P and Tarazi, A, (2008) : « Bank income structure and risk: an empirical analysis of European banks". Journal of Banking and Finance. Vol.32. P, 1452-1467.

[20] Liikanen, E, (2012): "High-Level Expert Group on Reforming the Structure of the EU Banking Sector".

[21] Martín-Oliver, A; Ruano, Sand Salas-Fumás, V, (2015): "The Fall of Spanish Cajas: Lessons of Ownership and Governance for Banks".

[22] Mehran, H and Thakor, A.V, (2010): "Bank capital and value in the cross-section" Rev.Financ. Stud. Vol. 24 (4).P, 1019-1067.

[23] Mercieca, S; Schaeck, K and Wolfe, S, (2007): "Small European banks: benefits from diversification?". Journal of Banking and Finance. Vol. 31. P, 1975–1998.

[24] Mergaerts, Fand Vennet, R. V, (2016): "Business models and bank performance: A long-term perspective". Journal of Financial Stability. Vol. 22.P, 57–75.

[25] Meslier, C; Tacneng, R and Tarasi, A, (2014): "Is bank income diversification beneficial? Evidence from an emerging economy". Journal of International Financial Markets, Institutions & Money. Vol. 31. P, 97-126.

[26] Maudos, J and Solis, L (2009): "The determinants of net interest income in the Mexican banking system: an integrated model". Journal of Banking and Finance. Vol. 33. P, 1920–1931.

[27] Nguyen, M, Skully, M and Perera, S,(2012):"Market power, revenue diversification and bank stability: Evidence from selected South Asian countries". Journal of International Financial Markets, Institutions and Money. Vol. 22. P, 897–912.

[28] Pennathur, A.K; Subrahmanyam, V and Vishwasrao, S,(2012): "Income diversification and risk: does ownership matter? An empirical examination of Indian banks". Journal of Banking and Finance. Vol. 36. P, 2203–2215.

[29] Roengpitya, R., Tarashev, N., Tsatsaronis, K, (2014): "Bank business models". BIS Q. Rev. P, 55–65.

[30] Sanya, S and Wolfe, S, (2011): "Can banks in emerging economies benefit from revenue diversification?" Journal of Financial Services Research. Vol. 40.P, 79-101.

[31] Schaeck, K and Cihak, M, (2012): "Banking competition and capital ratios". European Financial Management. Vol. 18(5). P, 836-866.

[32] Stiroh, K.J, (2004a): "Do community banks benefit from diversification?" Journal of Financial Service Research. Vol. 25. P, 135–160.

[33] Stiroh, K.J, (2004b): "Diversification in banking: is non-interest income the answer?". Journal of Money, Credit and Banking. Vol. 36. P, 853–882.

[34] Stiroh, K. J, (2006): "New evidence on the determinants of bank risk". Journal of Financial Service Research. Vol. 30. P, 237–263.

[35] Stiroh, K. J and Rumble, A, (2006): "The dark side of diversification: the case of U.S financial holding companies". Journal of Banking and Finance. Vol. 30. P, 2131–2161.

Antibacterial peptides from thermophilic bacteria

Karel Mikulík[1], Magdalena Melčová[2], Jarmila Zídková[3]

[1]Institute of Microbiology, Academy of the Czech Republic Vídenská 1083 14220, Prague 4
[2,3]Department of Biochemistry and Microbiology, Institute of Chemical Technology Prague 6, Czech Republic

Abstract— *It is becoming interestingly apparent that innovations of the classical antibiotics are not effective, that induces need for novel drugs. Peptide antibiotics exhibit a group of secondary metabolites with hydrophobic and cyclic structures containing d-amino acidc like compounds with more resistant to proteolytic degradation. Bacterial peptides can possess bactericidal, fungicidal, metal chelating and immunomodulation activities. Several bacteriocins are active as food preservation, resulting in foods with more naturally preserved and rich in nutritional properties. Antimicrobial peptides used against infections are isolated mainly from mesophilic bacterial species. Novel antibacterial peptides from thermophilic species are more stable at higher temperatures and pH, and can be improved by variation of cultivation conditions. These cells can growth either autotrophically or heterotrophically. Under mixotrophic conditions can utilize pyruvate or hydrogen with thiosulfate. The present review provides a general overview on primary structure of selected antibiotic peptides and their potential for industrial purposes as well as environmental and biotechnological applications.*

Keywords— antibacterial peptides, novel drugs, metabolites, hydrophobic structure, immunomodulation.

I. INTRODUCTION

The genus Geobacillus contains, more than 25 species, which were detected in thermophilic areas around the world. *Geobacillus thermodenitrificans* N680-2 produces a nisin analogue termed geobacillin I (Fig.1 B). This peptide was produced by heterologous expression in *Escherichia coli*. NMR results showed that geobacillin I incorporates seven thioester cross-lings and demonstrates increased stability compared with nisin. Antimicrobial activity of geobacillin I is similar to nisin A. The genome of *G.stearothermophilus* NG80-2 contains a gene product with a ring topology distinct from any known lantibiotics. The geobacillin II exhibits antibiotic activity against Bacillus only (Garg et al., 2012). Only bacteriocins type I nisin, mutacin (Fig. 1C) and planeosporin are active against multidrug resistant Gram-positive bacteria (Severina et al., 1998; Fontana et al., 2006). Bacteriocin production is stabile even at 55 °C and is dependent on the time of incubation, pH and concentrations of nitrogen.

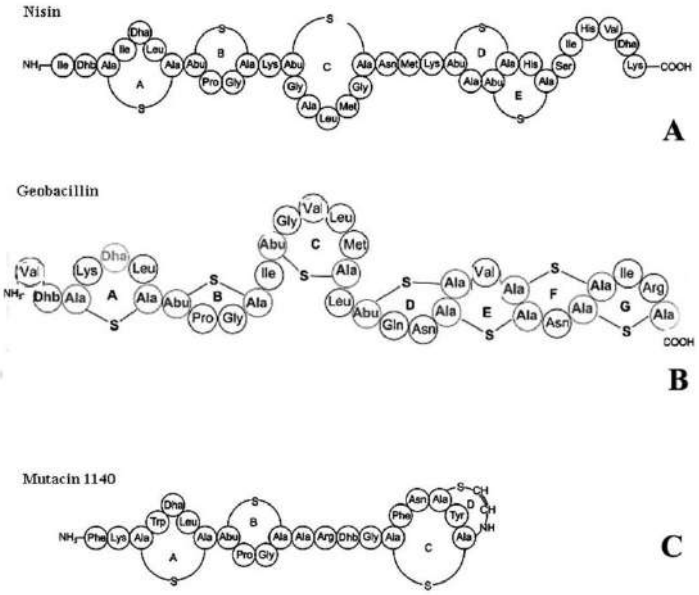

FIG.1. COMPARISON OF NISIN (A), GEOBACILLIN (B) AND MUTACIN (C). LANTIONES ARE THIOESTER-BRIDGES AMINO ACIDS. THEIR STRUCTURES ARE VERY STABLE AND ALLOW A CONFORMATIONAL CHANGES LEADING TO ENHANCED RECEPTOR SELECTIVITY AND PROTECT THE PEPTIDES AGAINST PROTEOLYTIC DIGESTION.

Dhb*- dehydrobutiline;* ***Dha****-dehydroalanine;* ***Abu****- aminobutyric acid.*

From thermal areas near to Yellowstone National Park Geobacillus M7 strain was isolated. The cells of this bacterium are globous and they are covered by a capsular layer with bacilliform structures. The bacteria generate petal shaped colonies when grown on nutrient agar at neutral pH and temperatures between 55-65 °C. 16S RNA of M-7 has a 97 % similarity with *G.stereothermophilus*. This strain produces volatile compounds (VOCs) with antibacterial activity such as benzaldehyde, acetic acid, butanol-3-methylbutanoic acid, 2- methyl-butanoic acid, propanoic acid, 2- methyl and benzeneacetaldehyde. These compounds inhibit growth of *Aspergillus fumigatus, Botrytis cinerea, Verticullium dahliae,* and *Geotrichum candidum* after 48h, and cells are killed after 72 h exposure. A mixture of synthetic volatile compounds at the same ratios as those found in the *Geobacillus* M-7 has the same inhibitory effect on activity of the test organism (Ren et al., 2010). *Aeribacillus palidus* SAT4 produses antimicrobial peptide at extreme conditions at pH 5.0, glucose concentration 2%, glutamic acis at 1.5% and under agitation at 100 rpm and 55°C. Antimicrobial compound was isolated from supernatant fluid with precipitation with ammonium sulphate to 50% saturation. Sediment was fractionationed through Sephadex G-75 permeation chromatography. Antibacterial activity was detected against *S.aureus, M. luteus* and *Ps.aeruginose*.

Thermophilic strain of *B.licheniformis* synthetised bacillosin 490. The peptide was inactivated by pronase E and proteinaseK. The peptide is good antibacterial agent, stabile to heath treatment and wide pH range (Martirant et. al, 2002).

Several Archae can synthetized a small peptides (archeocins) with potential interest to biotechnology (Charlesworth and Burns, 2015). *Sulfolobus islandicus* produce peptide sulfolobicin at pH from 2-4 and temperatures between 65 °C and 85 °C. Halocins are produced from halophilic rods (Torroblance et. al, 1994). Halocins forms two groups based on size. Microhalocins are about 3.6 kDa and higher halocins of 35 kDa. Some halocins are able to inhibit growth of *S.solfataricus*.

II. PEPTIDES STRUCTURALLY RELATED TO NISIN

Structurally similar substances to nisin were found in many bacteria. Subtilin is 32amino acids pentacyclic lantibiotic (Fig. 2A) was identified in *Lactobacillus lactis* (Ross et al., 2002). The cluster for subtilin contains specifies genes for subtilin peptide SpaS, posttranslational lantoin formation SpaBC, and translocation gene Spa T for modified species. Proteases (AprE) WprA and Vpr are involved in processing of subtilin (Corvey et al., 2003). Subtilin self-protection is mediated by ABC-translocator Spa FEG and lipoprotein Spa I (Klein and Entian 1994; Stein et al., 2003b). Biosynthesis of subtilin is regulated by sensor histidine kinase SpaK and regulatory protein SpaR that binds to spa-box of DNA, supporting expression of the genes for subtilin biosynthesis spaS, spa BTC and self protection protein Spa FEG (Stein et al., 2003b; Kleerebezem, 2004). Expressions of SpaRK are regulated by sporulation specific factor SigH, which is repressed during exponential growth by regulator AbrB (Fawcett et al., 2000). These data indicate that production of subilin is under dual control by culture density in quorum sensing mode, where subtilin response to the growth phases is directed by the Abrb/SigH (Stein et al., 2002b).

Ericin S (Fig. 2B) is closely related to the subtilin cluster. Subtilisin differs from ericin in four amino acid residues only, but their antibiotic activity is comparable. Ericin A (Fig. 2C) has different amino acid composition and ring organization with ericin S. Although ericin A is fully matured and is produced in equal quantities as ericin S, single synthetases EriC catalyses the development of two different products: ericin A and S. Requirements for single synthetase (EriBC) indicate flexibility of the lantibiotic biosynthetic route.

Mersacidin (Fig. 2D) is comprised of three melane rings along with dehydroalanine and aminovinylmethylcysteine residues. The peptide is synthesized at the beginning of the stationary phase of growth (Guder et al., 2002). Connection between cellular regulatory systems of *B. subtilis* and the mersacidin regulatory network is not known, but Mrsd the Flavin-containing cysteine decarboxylase (HFCD) catalyses oxidative decarboxylation of the C-terminal cysteine of mescacidin pro-peptide. Introduction of amino acids to mersacidin rings exhibits a loss of activity.

Sublancin 168 (Fig. 2E) contains two disulphide bridges and a β-methyllananthionine bridge. A hybridization probe based on the peptide sequence was used to clone the pre-sublancin gene, which encoded a 56-residue polypeptide consisting of a 19-residue leader segment and a 37-residue mature segment. The mature segment contained one serine, one threonine, and five cysteine residues. The sublancin leader was similar to the known type AII lantibiotics, containing a double-glycine motif that is typically recognized by dual-function transporters. A protein encoded immediately downstream from the sublancin gene possessed features of a dual-function ABC transporter with a proteolytic domain and an ATP-binding domain. The antimicrobial activity spectrums of sublancin were like other lantibiotics, inhibiting Gram-positive bacteria but not Gram-negative bacteria; and like the lantibiotics, nisin and subtilin, are able to inhibit both bacterial spore outgrowth and vegetative

growth. Sublancin is an extraordinarily stable lantibiotic, showing no degradation or inactivation after being stored in an aqueous solution at room temperature for two years (Paik et al., 1998).

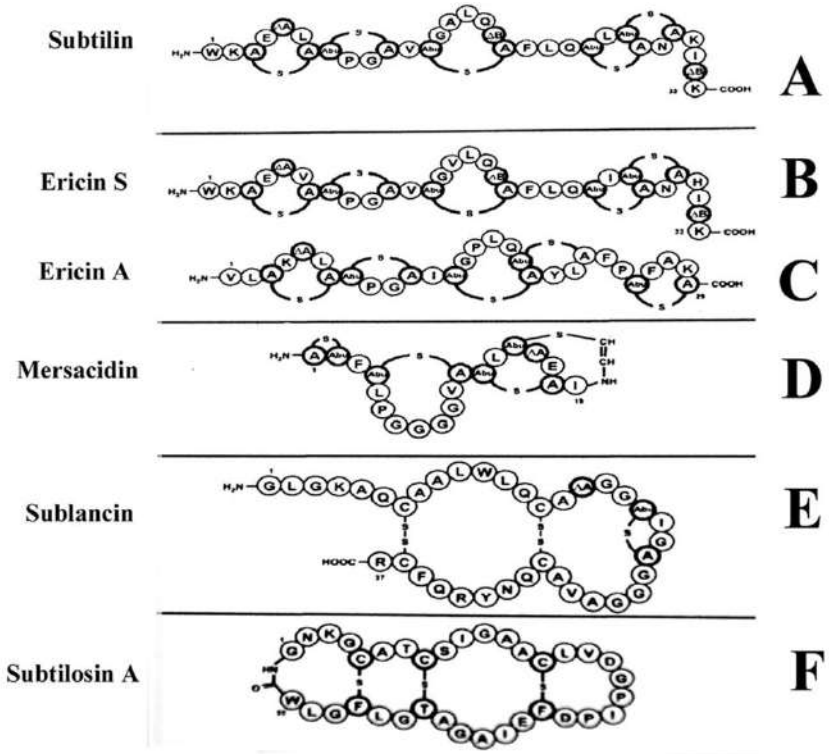

FIG.2. PENTACYCLIC LANTIBIOTICS -SUBTILIN (A); ERICIN S (B); ERICIN A (C). UNUSUAL LANTIBIOTICS WITH MACROCYCLIC STRUCTURE AND WITH ONE MERSACIDIN (D); TWO–SUBLANCIN (E) ; AND THREE INTER-RESIDUAL LINKAGES SUBTILOSIN A (F).

Subtilolisin A (Fig. 2F) has a macrocyclic structure with three inter-residual linkages (Marx et al., 2001) and is produced by B. subtilis (Zheng et al., 1999; Stein et al., 2004). In the processing of subtilolisin AlbF (YwhN) protein and immunity proteins AlbB-D (YwhQPO) are included (Zheng et al., 2000). It has been shown that inter-residual connection is mediated by the thioester bond between cysteine sulphur and alfa amino acid carbons (Kawulka et al., 2004). Subtilolisin is active against Gram-positive bacteria including Listeria (Zheng et al., 1999). The Antilisterial bacteriocin cluster encodes AlbA (YwiA) protein which is probably involved in post-translational modification of pre-subtilosin. Expression of the anti-listerial bacteriocin (sbo-alb) is under AbrB control (Zheng et al., 1999) and under stress conditions (Nakano et al., 2000).

From municipal solid waste a strain of Brevibacillus borstelensis RH 102 was isolated a component with good activity against G+ bacteria (M. flavus, S .aureus, B. subtilis and Difzia K44). Antibiotics produced at 60 °C that are soluble in methanol and water suggests a polar nature of their active components (Venugopalan et al., 2013).

III. TWO COMPONENT LANTIBIOTICS

Lacticin 3147 (Fig. 3A) contains two melan and two lan rings D-alanine, and two Dhb residues (Ryan et al., 1996). Lacticin 3147 was identified in a supernatant solution of Lactococcus lactis (DPC3147). This bacteriocin is very active against Listeria monocytogenes and resistant strains of Staphylococcus aureus, vancomycin resistant Enterococci, penicillin resistant Pneumococcus and Streptococcus mutant strains (McAuliffe et al., 1999). Lacticin 3147 is an effective protective agent in the production of cheese. Solid phase peptide synthesis was used in examination of the role of lan and melan residues in lactin 3147. Three ring analogues were synthesized. When thioester of lan or melan is oxidized, the peptide loses its antibacterial activity. Lactococcus lactis also produces lactin 481 containing one melan, andthe two lan rings with one Dhb residue. Each ring can exist as lan or melan, and the peptide remains active. When the ring was opened the peptide lost activity (Rince, 1994).

Haloduracin β (Fig. 3B) is a two-component lantibiotic comprising α-globular peptide and elongated β–peptide. This peptide was identified in *Bacillus halodurans*. Haloduracin α consists of one lan, one cysteine, two melan rings and three Dhbs.

Haloduracin β contains one lan, three melan groups and three Dhbs. Haloduracin is more stable at pH 7 than nisin. Ring A has a small effect on activity in contrast to rings C and D that are important for activity. N-terminal cysteine of peptide is not essential for activity. Haloduracin synthesis is accompanied by sporulation and stationary cultures and spores containing haloduracin peptides were collected. Two products with 2.332 Da and 3.046 Da were identified (McClerren et al., 2006).

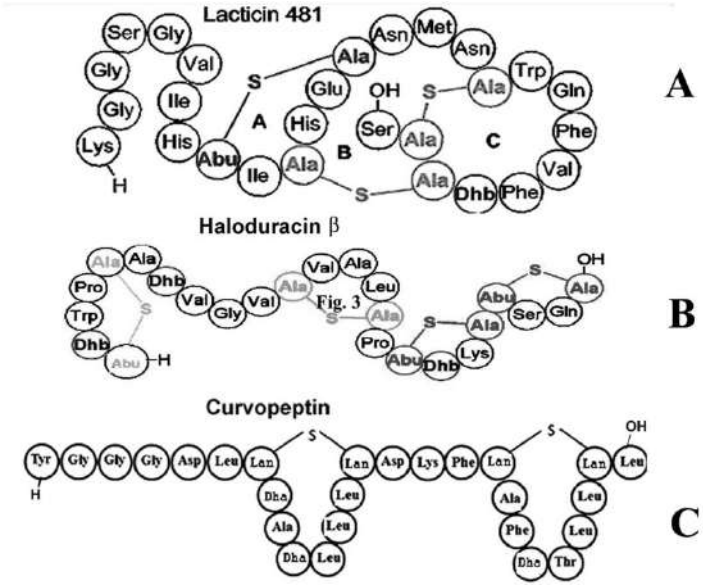

FIG.3. THE TWO-PEPTIDE LANTIBIOTICS DESCRIBED AMONG BACILLI HALODURACIN (FIG. 3B) AND LICHENICIDIN ARE CLOSELY RELATED TO TWO-PEPTIDE LANTIBIOTICS PRODUCED IN OTHER BACTERIA SUCH AS LACTICIN (FIG. 3A) PRODUCED BY *L. LACTIS* DPC3147. CURVOPEPTIN (FIG. 3C) FROM THERMOMONOSPORA CURVATA IS THE FIRST CLASS III LANTIBIOTIC OF THERMOPHILIC ORIGIN.

Thermomonospora curvata synthetizes Curvopeptins (Fig. 3C), that is labionin-carbocyclic variant of lantione (Krawczyk et al., 2012). Enzymatic studies with a precursor peptide mutant allowed the assignment of all dehydration sites. Curvopeptin biosynthesis of nine intermediates was studied by high-resolution mass spectrometry combined with deuterium-labeling. This approach makes it possible to create a model of three post-translational modification reactions: phosphorylation, elimination, and cyclization. These data support the characterizetion of the modifying enzyme CurKC, and in particular its specificity toward phosphorylation co-substrates. The enzyme accepted NTPs and dNTPs although the purine nucleotides ATP/dATP and GTP/dGTP were the preferred co-substrates. These data give important mechanistic insights into the processing and directionality of the multifunctional class III modifying enzymes (Jungmann et al., 2014).

Bacillus thermoleovorans S-II and *B. thermoleovorans NR-9* produce bacteriocins: thermoleovorin-S2 and thermoleovorin-N9, respectively. The bacteriocins are stable at pH from 3 to 10 and at temperatures 70-80°C. Thermoleovorins are produced during log-phase growth and are inhibitory to actively growing cells, they are effective against *Salmonella typhimurium, Branhamella catarrhalis, Streptococcus faecalis, and Thermus aquaticus.* The bacteriocins are digested by protease type XI and pepsin. Thermoleovorin-S2 was more thermostable than thermoleovorin-N9 at 70 and 80 °C. Thermoleovorins-S2 and -N9 apparently act by binding to susceptible organisms, resulting in lysis of the cell. Thermoleovorins-S2 has an estimated M(r) of 42,000, while thermoleovorin-N9 has M(r) of 36,000. (Novotny and Perry, 1992). The ability of thermoleovorins to inhibit *Salmonella typhimu*num, *Branhamella catarrhalis*, and *Streptococcus faecalis* was an unexpected finding. The antimicrobial effect on *Salmonella typhimurium* permits further investigation and may provide a use for these bacteriocins either in the food industry or as a feed additive for poultry. From composts thermophilic bacteria sensitive to penicillin G were isolated. Facultative autotrophic strains isolated from hot composts were Gram-variable rods with terminal endospores. Optimum temperature for growth was between 65-70 °C. These cells can growt either autotrophically or heterotrophically with hydrogen, or can oxidize thiosulfate. Under mixotrophic conditions they can utilize pyruvate or hydrogen with thiosulfate. DNA content and DNA: DNA homology of these strains had more than 75% with a reference strain of *Bacillus schlegelii.* Strains with inhibitory effects against pathogenic bacteria were isolated from cow manure compost. These bacteriocin-like components were thermal unstable (Abdel-Mohsein et al., 2003). Supernatant solutions of *Bacillus licheniformis* H1 inhibit growth of various Gram negative bacteria, e.g. *Listeria monocytogenes* ATCC 19111, but with the exception of *Pseudomonas fluorescents* ATCC11251, bacteriocin(s) are inactivated by proteolytic enzymes (chymotrypsin,

trypsin and papain) and are stable under pH from 3 to 9 and temperatures up to 75 °C. Using SDS-polyacrylamide gel electrophoresis of partially purified supernatant an active protein with M_r approximately 3.5 kDa was identified. *Streptococcus thermophilus* producing bacteriocin that lost antibacterial activity after incubation 1h at 60 °C was isolated from raw milk. When co-cultured with *Lactobacillus delbruecki* susp. *Lactis*, the production of bacteriocin was enhanced. The isolated bacteriocin termophilin T (Aktypis et al., 1998) from *S.thermophilus* ACA-DC 0040 inhibits both lactic acid bacteria and clostridia. The inhibition of clostridia was also described for acidocin B (tenBring et al., 1994) and pedocins (Daeschel, 1989; Ray et al., 1989). Thermophilin T regulates population dynamics in the yogurt production and hard cheeses. Since proteolytic enzymes and α-amylase inactivate thermophilin T, this indicates that bacteriocin is glycoprotein.

Paracin 1.7 is peptide produced by *Lactobacillus paracasei* HD1-7 from sauerkraut juice. The molecular mass of Parecin 1.7 was about 10 kDa. The N-terminal structure was similar to that of an ABC-oligopeptide transport system. Paracin 1.7 was sensitive to protease K, had antimicrobial activities at a broad pH range (3.0-8.0), and was heat resistant (121 °C for 20 min). Paracin 1.7 from *Lactobacillus paracasei* HD1-7 is a novel bacteriocin that has potential applications in food preservation. Paracin 1.7 shows a broad spectrum of activities against various strains in the genera of Proteus, Bacillus, Enterobacter, Staphylococcus, Escherichia, Lactobacillus, Micrococus, Pseudomonas, Salmonella and Saccharomyces, some of which belong to food borne pathogenic bacteria (Ge et al., 2016)

Amylocyclin is a circular bacteriocin produced by *Bacillus amyloliquefaciens* FZB 42 (Scholz et al., 2014) which is released into cultivation medium. Amylocyclin with molecular mass of 6. 381 Da is synthetized on ribosomes. Self-protections against drug produced is directed by small cationic peptides AcnC, AcnO, AcnE and AcnF. The drug inhibits Gram-positive cells only. Amylocyclicin is released into the culture medium by wild-type strain *B. amyloliquefaciens* FZB42 and *sfp* mutants derived from there. It can be obtained from ammonium sulfate precipitation of the supernatants, followed by extraction of the pellet with methanol. In addition, the bacteriocin is attached in an appreciable amount to the outer surface of the bacterial cells, from where it can be extracted with a 50% aqueous acetonitrile–0.1% trifluoroacetic acid. Such surface extracts are the source of choice for further purification and characterization of the bacteriocin.

IV. NON-RIBOSOMAL SYNTHESIS OF PEPTIDE ANTIBIOTICS

Large multienzymes non-ribosomal peptide synthetases (NRPSs) contain domains that catalyse ordered selections and polymeration of amino acid residues (Sieber and Marahiel 2003; Finking and Marahiel, 2004). Elongation steps in peptide biosynthesis need three core domains: i) The 350 amino acid residues of adenylation domain, are required for recognition of cognate amino acid, which resembles the acylation of tRNA synthetases during ribosomal peptide synthesis. ii). The peptidyl carrier domain containing 4'phosphopantheine group accepting adenylated amino acid under thioesterification and release of AMP. The 4'phosphopantheine cofactor serves as a transporter of intermediates between various catalytic domains. Peptidyl carrier proteins are posttranslationally modified from inactive apoforms to holoforms by 4´phosphopantheine-transferases (Lambalot et al., 1996). iii) Condensation domains (450 aa), which are located between pair of adenylation and peptidyl carrier domains catalysing formation of peptide bonds (Herbst et al., 2013). Biosynthesis is terminated by cyclization of the peptide (Kohli and Walsh, 2003) and such reactions are catalysed by thioesters-part of C-terminus. Lipopeptide antibiotics with β-hydroxyl or β amino fatty acids are synthetized in *Bacillus subtilis*.The branching and length of the chains of amino and fatty acids participate in microheterogeneity (Kowall et al., 1998). The most-well known lipopeptide surfactin (20nM) causes a decrease in tension of water from 72 to 27 $mMm,^{-1}$and it is an efficient detergent on cell membranes (Carrillo et al., 2003). PCR screening for the presence of nonribosomal synthetase and polyketide synthetase show a role of antibiotic lipopeptides as a potential resource of novel therapeutic drugs (Palomo et al., 2013).

Rhizovital is a lipopeptide antibiotic produced by *B. amyloliquefaciens* FZB42 (Sylla, et al., 2013) and the product requires sfp-dependent 4´phosphopanteinyl transferase to transmit 4´phosphopanteinyle from coenzyme A onto peptidyl carrier protein. RhizoVital 42 fl. suppresses *Botrytis cinerea* infections.

Surfactin (Fig. 4A) catalyse the three peptide synthetases Srf A-C. The thioesterase/acyltransferase enzyme SrtD initiates the process (Steller et al., 2004). The excretion of surfactin by passive diffusion across the cytoplasmic membrane is anticipated. Resistance to surfactin is acquired by the YerP multidrug efflux pump (Tsuge et al., 2001a). Production of surfactin is regulated by the 4´phosphopantheine transferase Sfp that transmit inactive apoform of surfactin and fengycin synthetase to active holoform (Lambalot et al., 1996; Mootz et al., 2001). The transfer of native *stp* allel into *Bacillus subtilis* induces the production of surfactin (Nakano et al., 1992) and fengycin (Tosato et al., 1997). Biosurfactant from certain strains of Bacillus and Pseudomonas are mixtures of different lipopeptides or isoforms (Naruse et al., 1990; Abalos et al., 2001; Vater et al.,

2002; Mukherjee and Das 2005). Surface tension or antimicrobial properties of lipopeptides are dependent on its molecular structure. Branching and length of the chains of amino and fatty acids participate in microheterogeneity (Kowall et al., 1998). The antimicrobial part of the biosurfactant is formed by lipopeptides. The biosurfactant and surfactin showed overlapping patterns in IR spektra, characteristic of lipopeptides (Lin et al., 1994). The iturin family includes cyclic lipopeptides mycosubtilin (Fig. 4B), iturins (Fig.4C), and bacillomycins (Fig. 4D). These compounds are antifungal and haemolytic, but their antibacterial activity is low (Thimon et al., 1995). The synthesis of these peptides catalyses similar nonribosomal peptide synthetases: mycosubtilin (Duitman et al., 1999), iturin (Tsuge et al., 2001b) and bacillomycin synthetases (Moyne et al., 2004). Fengycin (plipastatin) (Fig. 4E) inhibits growth of filamentous fungi (Vanittanakom et al., 1986) and contains β-hydroxy fatty acids ligated to the N-terminus of a decapeptide including four D-amino acids. C terminal residue of the peptide part is connected to the tyrosine residue, forming branching points of acylpeptide and cyclic lactone. Fengycin is synthesized by a complex of fengycin synthetases (Fen1-Fen5) (Steller et al.,1999) that are regulated with *fen* operon, catalysing different properties as cyclization, branching and unusual constituents. For fenglycin biosynthesis, the UP element between -55 and -39 position in *feng* DNA of *B. subtilis* is important. Other factors than UP may regulated the transcription of fengycin. More detailed analysis must be conducted as to how these factors operate in biosynthesis of fengycin.

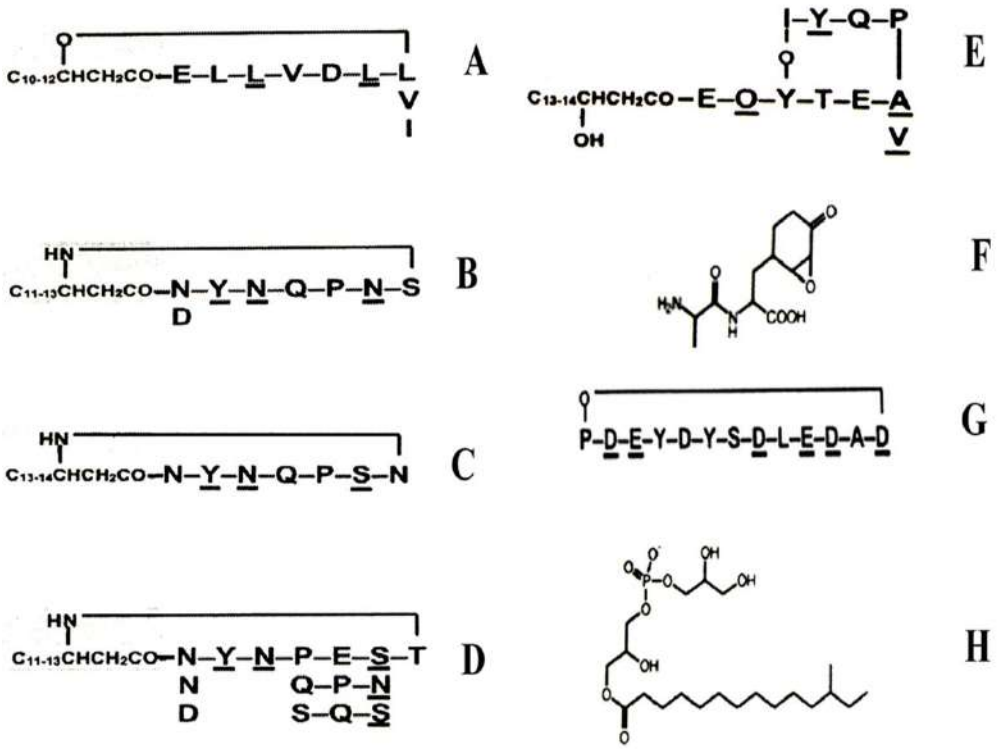

FIG.4. NON-RIBOSOMALLY GENERATED PEPTIDE ANTIBIOTICS. SURFACTIN (FIG.4A); ITURIN (FIG. 4B); MYCOSUBTILIN (FIG.4C); BACILOMYCIN (FIG.4D), FENGYCIN (FIG.4E); BACILYSIN (FIG. 4F); MYCOBACILLIN (FIG.4G) AND RHIZOCTICIN (FIG. 4H).

Taromycin A is a lipopeptide antibiotic produced by marine actinomycete *Saccharomonospora* CNQ-490. Taromycin gene *tar* is similar to the antibiotic daptomycin from *Streptomyces raseosporus*, but there are differences in the three amino acids and a lipid side chain (Yamanaka et al., 2014). *Streptomyces roseosporus* produced an acidic lipodepsipeptide antibiotic Daptomycin by a nonribosomal peptide synthetase (NRPS) mechanism *(*Walsh and Fischbach, 2010). Daptomycin is composed of a 13-member peptide, cyclized to form a 10-member ring and a 3-member exocyclic tail, to which is attached a decanoic acid side chain to the N terminus of l-Trp_1. In the biosynthesis of daptomycin by *S. roseosporus* three nonribosomal peptide synthetases: DptA, DptBC, and DptD are involved.

Fusaricidins are a group of lipopeptide antibiotics produced by *Paenibacillus polymyxa* (formerly *Bacillus polymyxa*) and consist of a guanidinylated β-hydroxy fatty acid linked to a cyclic hexapeptide containing four amino acid residues in the d-configuration (Kajimura and Kaneda, 1996, Kajimura and Kaneda, 1997). In most peptides epimerization of l-amino acids requires a specialized domnain. An l-amino acid is activated, and the epimerization (E) domain then catalyzes l-to-d

racemization of the thioester-bound amino acid. In the lipopeptide arthrofactin, there are no E domains detected in any of the 3 arthrofactin synthetases, although 7 of the 11 amino acids are in the d-configuration. Additional analyses demonstrated that A domains in modules corresponding to d-amino acids were specific for activation of l-isomers, and epimerase activity was supported by a new type of C domain with dual epimerization and condensation functions. A third strategy for incorporation of d-amino acids involves the direct activation of d-isomers by the A domains.

Bacilysin (Fig. 4F) the epoxy-modified amino acid anti-capsin (l-alanine [2.3-epoxycyclohexane-4] l-alanine), depend on the *ywfBCDEFGH* cluster (Inaoka et. al., 2003) Nonribosomal synthesis of dipeptide is synthesized by *Bacillus amyloliquefaciens* FZB42 and is independent of Sfp. The genes *basDE*(*ywfEF)* encode the function of amino acid ligation as well as bacilysin self-protection (Steinborn et al., 2005). Bacilysin is negatively regulated by GTP via the transcription regulation *AbrB* and *Cod Y*. Positive regulation is directed by guanosine-5-diphosphate-3-diphosphate (Inaoka et al., 2003) and a quorum sensing mechanism utilizing peptide PhrC (Yazgan et al., 2003). Bacilysin- has anticyanobacterial activity and thus could be used to moderate the detrimental algal effects (Wu et al., 2014). Bacilysin caused apparent changes in the algal cell wall and cell organelle membranes, and this resulted in cell lysis. Meanwhile, there was downregulated expression of *glmS*, *psbA1*, *mcyB*, and *ftsZ*—genes involved in peptidoglycan synthesis, photosynthesis, microcystin synthesis, and cell division, respectively.

Mycobacillin (Fig. 4G) is produced by *Bacillus subtilis* B_3. The molecule is formed with cyclic peptide composed of 13 residues of 7 different amino acids (Majumdar and Bose, 1960; 1996), and it is an exclusively antifungal antibiotic. Enzyme complex mycobacillin synthetase was created by the hydroxyapatite column chromatography and sucrose-density-gradient centrifugation; each of the fractions contained migrates as a single component in SDS/polyacrylamide-gel electrophoresis and gel electrofocusing. The Mr of the enzyme fractions A, B and C by gel filtration is 260 000, 190 000 and 105 000 and this, by SDS/polyacrylamide-gel electrophoresis, is 252 000, 198 000 and 108 000, respectively. None of the enzyme fractions appears to possess a subunit structure.

Kocurin: Despite the broad distribution of *Micrococcaceae* in sponges, very little is known about the occurrence of the natural products biosynthetic pathways and the production of bioactive compounds, especially by species of the sponge-associated genera *Kocuria* and *Micrococcus*. The production conditions of kocurin by the *Kocuria* strain F-276,345 were analyzed with a time course study monitoring the growth and kocurin production over 4 days. Kocurin is closely related to two known thiazolyl peptide antibiotics with a similar mode of action, produced by a soil strain of *Streptomyces* and *Planobispora rosea*. The strains were PCR screened for the presence of secondary metabolite genes encoding nonribosomal synthetase and polyketide synthases (Palomo et al., 2013), a new member of the thiazolyl peptide family of antibiotics, as a resource for novel drugs.

Rhizocticin (Fig. 4H): Rhizocticins are dipeptide or tripeptide antibiotics and commonly possess l-arginyl-l-2-amino-5-phosphono-3-cis-pentenoic acid. Rhizocticins are produced by the Gram-positive bacterium *B. subtilis* ATCC6633. Rhizocticin A is l-arginyl-l-2-amino-5-phosphono-3-cis-pentenoic acid (Arg-APPA); rhizocticin B is-valyl l-arginyl-l-2-amino-5-phosphono-3-cis-pentenoic acid (Val-Arg-APPA); and rhizocticin C and D are the same as rhizocticin B but Val is substituted with l-isoleucine (Ile) and l-leucine (Leu), respectively. Rhizocticins enter the target fungal cell through the oligopeptide transport system (Kugler et al., 1990) and then are cleaved by host peptidases to release(Z)-l -2-amino-5-phosphono-3-panteonic acid (APPA), which inhibits threonine synthase, catalyzing the pyridoxal 5′-phosphate (PLP)-dependent conversion of phosphohomoserine to l-threonine (Laber et al., 1994). APPA interferes with the biosynthesis of threonine and related metabolic pathways, initially affecting protein synthesis and leading to growth inhibition. The antifungal effect of rhizocticin A was neutralized by the presence of oligopeptides and amino acids. Phosphinothricin (PT) is the only known phosphinic acid natural product, a non-proteinogenic amino acid found in a number of peptide antibiotics. In *Streptomyces viridochromogenes* were discovered the compound as a component of a tripeptide antibiotic (PT-Ala-Ala) produced by (phosphinothricin-tripeptide, PTT) or *Streptomyces hygroscopicus* (bialaphos PT), later it was found as a component of phosalacine, a PT-Ala-Leu tripeptide produced by *Kitasatospora phosalacina* and trialaphos (PT-Ala-Ala-Ala), which is a tetrapeptide produced by *Streptomyces hygroscopicus* KSB-1285 (Higgins et al., 2005; Omura et al., 1984). PT is a structural analog of glutamate and a potent inhibitor of glutamin synthetase. As a free amino acid, PT has relatively poor antibiotic activity, probably due to ineffective transport. Many organisms utilize the peptide versions that are hydrolyzed by cytoplasmic peptidases, releasing the active component. Because glutamine synthetase plays an essential role in pH homeostasis in plants, PT is an outstanding herbicide and both the tripeptide and synthetic versions of the monomer are widely used in agriculture (Thompson and Seto 1995).

Thermotolerant actinobacteria, e.g. *Streptomyces tauricus, S.lanatus, S.coeruleorubidis,* were isolated from the desert of Kuwait during the hot season. These cells were found to inhibit the rhizosphere of many plants and exhibit antimicrobial activity, leading to the protection of plants against phytopathogens (Xue et al., 2013). Thermotolerant streptomycetes isolated from the Himalayan Mountains *(Streptomyces phaeoviridis, S.griseoloalbus, S. viridogens*) inhibit methicillin resistant and vancomycin resistant strains of *Staphylococcus aureus.* Strains of *Streptomyces viridogens* and *S. rimosus* inhibit growth of pathogenic fungi (*Fusarium solani, Rhizoctoconia solani, Colletotricum falcatum* and *Halminthosporium oryzae*) (Radhakrishnan et al., 2007), furthermore, many actinobacteria secreted chelating molecules, retaining a solube form of iron in the rhizosphere of plants grown in iron deficient soil.

The zeamines are peptide antibiotics produced by *Serratia plymuthica* RVH1 (Masschelein et al., 2015). They exhibit activity affecting the integrity of cell membranes of a broad range of bacteria, including multidrug-resistant pathogens. The zeamines irritate rapid release of carboxyfluorescein from unilamellar vesicles with various phospholipid compositions, allowing them to interact directly with the lipid bilayer. The zeamine also facilitated the uptake of small molecules, such as 1-N-phenylnaphtylamine, making it possible to permeabilize the Gram-negative outer membrane. Zeamine at concentrations required for growth inhibition, causes lysis of membrane as indicated by microscopy. It is probable that the bactericidal activity of the zeamines derived from permeabilization membranes caused electrostatict interactions with the negatively charged part of the membrane components.

Pyrrolamides (e.g. congocidine, distamycin, kikumycins, pyrronamycins, noformycin), constitute a family of natural products produced by *Streptomyces* or related actinobacteria. They exhibit a variety of therapeutic applications, against viral, bacterial, tumor and parasitic activities (Juguet et al., 2009). Heat-stable antifungal factor (HSAF) is a secondary metabolite produced by the bacterium *Lysobacter enzymogenes* strain C3. The chemical structure of HSAF suggests that the biosynthesis of this molecule could involve both polyketide and nonribosomal peptide mechanisms, as seen in bleomycins and other natural products. HSAF appears to target a group of sphingolipids that are required for polarized growth of filamentous fungi and appears to be absent from mammals and plants (Yu et al., 2007).

Congocidine (netropsin) consists of peptides that bind to the minor groove of DNA and is a pyrrole-amide antibiotic produced by *Streptomyces ambofaciens.* Congocidine does not bind single stranded DNA or double stranded RNA; it protects such regions from DNase I and other endonucleases, and also inhibits topoisomerases. This peptide disrupts the cell cycle, prolonging G and arresting in G. Congocidine is assembled by a nonribosomal peptide synthetase with unusual features (Juguet et al., 2009). Its single adenylation domain acts applicable, and one of its condensation domains preferably uses CoA- as a substrate.A free standing module and the proposed enzyme mechanism may be used to the synthesis of many oligo-pyrrole molecules, and especially distamycin, which comprises three 4-aminopyrrole-2-carbonyl groups.

V. CONCLUSION

The post-genomic era will provide much new information on target sites and interactions of protein-protein and protein nucleic acids interactions. One of ultimate goals is to adopt order structures of molecules that can past through cell membranes and interact with specific targets. Peptide antibiotics from thermophiles are suitable for the handling of the structure and are more resistant to proteolytic degradation. Peptides can be safer and more selective than small molecular drugs. There is no need for chemical purification and subsequent separation of isomers. There are several hundred of polypeptides that are in various steps of clinical development. There is need for new antimicrobial peptides with hydrophobicity and α-helicity for their activity against mycobacteria in the fight against drug resistant tuberculosis. Natural peptides can be used as food preservatives, chemotherapeutics, and efficient detergents.

REFERENCES

[1] Abdel-Mohsein, H.S., Sasaki T., Tada, C., Nakai, Y (2003**)** Characterization and partial purification of a bacteriocin-like substance produced by thermophilic Bacillus licheniformis H1 isolated from cow manure compost. J Dairy Sci. 86:3068-3074.

[2] Abalos, A., Pinazo, A., Infante, M.R., Casals, M., Garcia, F. Manresa, A *(2001)* Physicochemical and antimicrobial properties of new rhamnolipids produced by *Pseudomonas aeruginosa* AT10 from soybean oil refinery wastes. Langmuir 17*:* 1367–1371.

[3] Abed, R.M., Dobretsov, S., Al-Fori, M., Gunasekera, S.P., Sudesh, K., Paul, V.J (2013) Quorum-sensing inhibitory compounds from extremophilic microorganisms isolated from a hypersaline cyanobacterial mat. J IndMicrobiol Biotechnol 40:759-772.

[4] Aktypis, A., Kalantyopoulos, G., Huis, H. J., tenBrink, B (1998) Purification and characterization of thermophilin T, a novel bacteriocin produced by Streptococcus thermophilus ACA-DC 0040. J Appl Microbiol 84:568-576.

[5] Breukink, E, deKruijff B (2006) Lipid II as a target for antibiotics. Nat Rev Drug Discov 5: 321-332.

[6] Carrillo, C., Teruel, J.A., Aranda, F.J., Ortiz, A (2003) Molecular mechanism of membrane permeabilization by the peptide antibiotic surfactin. Biochim Biophys Acta 1611: 91–97.

[7] Corvey, C., Stein, T., Düsterhus, S., Karas, M., Entian, K.-D (2003) Activation of subtilin precursors by Bacillus subtilis extracellular serine proteases subtilisin (AprE), WprA, and Vpr. Biochem Biophys Res Commun 304: 48–54.

[8] Daeschel, M.A. (1989) antimicrobial substances from lactic acid bacteria. Food Technology 43: 164-167.

[9] Duitman, E.H., Hamoen, L.W., Rembold, M., Venema, G., Seitz, H., Saenger, W (1999) The mycosubtilin synthetase of Bacillus subtilis ATCC 6633: a multifunctional hybrid between a peptide synthetase, an amino transferase, and a fatty acid synthase. Proc Natl Acad Sci USA 96: 13294–13299.

[10] Fawcett, P., Eichenberger, P., Losick, R., Youngman, P (2000) The transcriptional profile of early to middle sporulation in Bacillus subtilis. Proc Natl Acad Sci USA 97: 8063–8068.

[11] Finking, R, Marahiel, M.A (2004) Biosynthesis of nonribosomal peptides. Annu Rev Microbiol 58: 453–488.

[12] Fontana, G., Savona G., Rodríguez, B (2006) Clerodane diterpenoids from Salvia splendens. J Nat Prod 69:1734-1738.

[13] Garg N., Tang W., Goto Y., Nair S.K., van der Donk W.A (2012) Lantibiotics from Geobacillus thermodenitrificans. Proc Natl Acad Sci USA 109: 5241-5246.

[14] Ge J, Sun Y, Xin X, Wang Y, Ping W (2016) Purification and Partial Characterization of a Novel Bacteriocin Synthesized by Lactobacillus paracasei HD1-7 Isolated from Chinese Sauerkraut Juice. Sci Rep 14:19366.

[15] Guder, A., Schmitter, T., Wiedemann, I., Sahl, H.G., Bierbaum, G (2002) Role of the single regulator MrsR1 and the two-component system MrsR2/K2 in the regulation of mersacidin production and immunity. Appl Environ Microbiol 68: 106–113.

[16] Hamoen, L.W., Venema, G., Kuipers,O.P (2003) Controlling competence in Bacillus subtilis: shared use of regulators. Microbiology 149: 9–17.

[17] Hasper, H.E., DeKruijff, B., Breukink, E (2004) Assembly and stability of Nisin–Lipid II pores. Biochemistry 43: 11567–11575.

[18] Herbst,D.A., Boll, B., Zocher, G., Stehle,T., Heide, L (2013) Structural Basis of the Interaction of MbtH-like Proteins, Putative Regulators of Nonribosomal Peptide Biosynthesis, with Adenylating Enzymes J Biol Chem 288: 1991–2003.

[19] Higgins, L.J., Yan, F., Liu, P., Liu, H.W., Drennan, C.L (2005) Structural insight into antibiotic fosfomycin biosynthesis by a mononuclear iron enzyme.Structures illuminating the mechanism of dehydrogenative epoxide formation. Nature 437:838–844.

[20] Inaoka, T., Takahashi, K., Ohnishi-Kameyama, M., Yoshida, M., Ochi, K (2003) Guanine nucleotides guanosine 5′-diphosphate 3′-diphosphate and GTP co-operatively regulate the production of an antibiotic bacilysin in Bacillus subtilis. J Biol Chem 278: 2169–2176.

[21] Jungmann, N,A., Krawczyk, B., Tietzmann ,M., Ensle, P., Süssmuth, R.D (2014). Dissecting reactions of nonlinear precursor peptide processing of the class III lanthipeptide curvopeptin.J Am Chem Soc 136:15222-15228.

[22] Juguet, M, Lautru,S., Francou F.X., Nezbedová, S., Leblond, P., Gondry, M., Pernodet, J.L (2009) An iterative nonribosomal peptide synthetase assembles the pyrrole-amide antibiotic congocidine in Streptomyces ambofaciens. Chem Biol 16:421-431.

[23] Kajimura Y[1], Kaneda M (1996) Fusaricidin A, a new depsipeptide antibiotic produced by Bacillus polymyxa KT-8. Taxonomy, fermentation, isolation, structure elucidation and biological activity. J Antibiot 49:129-135.

[24] Kajimura, Y., Kaneda, M (1997)Fusaricidins B, C and D, new depsipeptide antibiotics produced by Bacillus polymyxa KT-8: isolation, structure elucidation and biological activity

[25] J Antibiot 50:220-228.

[26] Kawulka, K.E., Sprules, T., Diaper, C.M., Whittal, R.M., McKay, R.T., Mercier, P (2004) Structure of subtilosin A, a cyclic antimicrobial peptide from Bacillus subtilis with unusual sulfur to alpha-carbon cross-links: formation and reduction of alpha-thio-alpha-amino acid derivatives. Biochemistry 43: 3385–3395.

[27] Khalil, A., Sivakumar, N., Qarawi, S (2015) Genome Sequence of Anoxybacillus flavithermus Strain AK1, a Thermophile Isolated from a Hot Spring in Saudi Arabia. Genome Announc Jun 4: 3.

[28] Kleerebezem, M. (2004) Quorum sensing controls of lantibiotic production; nisin and subtilis autoregulate their own biosynthesis. Peptides 25: 1405–1414.

[29] Klein, C., Entian, K-D (1994) Genes involved in self-protection against the lantibiotic subtilin produced by Bacillus subtilis ATCC 6633. Appl Environ Microbiol 60: 2793–2801.

[30] Kohli, R.M., Walsh, C.T (2003) Enzymology and acyl chain macrocyclization in natural product biosynthesis. Chem Commun (Camb) 7: 297–307.

[31] Koponen, O., Takala, T.M., Saarela, U., Qiao, M., Saris, P.E (2004) Distribution of the NisI immunity protein and enhancement of nisin activity by the lipid-free NisI. FEMS Microbiol Lett 231: 85–90.

[32] Kowall, M., Vater, J., Kluge, B., Stein, T., Franke, P., Ziessow, D (1998) Separation and characterization of surfactin isoforms produced by Bacillus subtilis OKB 105. J Colloid Interface Sci 204: 1–8.

[33] Krawczyk, B., Völler, G.H., Völler, J., Ensle, P., Süssmuth, R.D (2012) Curvopeptin: a new lanthionine-containing class III lantibiotic and its co-substrate promiscuous synthetase. Chembiochem 13: 2065-2071.

[34] Kugler, M., Loeffler, W., Rapp, C., Kern, A., Jung, G (1990) Rhizocticin A, an antifungal phosphono-oligopeptide of *Bacillus subtilis* ATCC6633: biological properties. Arch. Microbiol 153:276–280

[35] Kunst, F., Ogasawara, N., Moszer, I., Albertini, A.M., Alloni, G., Azevedo, V (1997) The complete genome sequence of the gram-positive bacterium Bacillus subtilis. Nature 390: 249–256.

[36] Laber, B., Lindell, S.D., Pohlenz, H.D (1994) Inactivation of *Escherichia coli* threonine synthase by dl-*Z*-2-amino-5-phosphono-3-pentenoic acid. Arch. Microbiol 161: 400–403.

[37] Lambalot, R.H., Gehring, A.M., Flugel, R.S., Zuber, P., LaCelle, M., Marahiel, M.A (1996)

[38] A new enzyme superfamily–the phosphopantetheinyl transferases. Chem Biol 3: 923–936.

[39] Lin, S.C., Minton, M.A., Sharma, M.M. Georgiou, G. *(*1994*)* Structural and immunological characterization of a biosurfactant produced by *Bacillus licheniformis* JF-2. Appl Environ Microbiol 60*:* 31–38.

[40] Majumar, S.K., Bose, S.K. (1996) Mycobacillin, a new antifungal antibiotic produced by B.subtilis. Nature 181: 134-135.

[41] Majumar, S.K., Bose, S.K. (1960) Amino acid sequence in mycobacillin. Biochem J 74: 596-599.

[42] Masschelein J., Clauwers, C., Stalmans, K., Nuyts, K., De Borggraeve, W., Briers, Y., Aertsen, A., Michiels, C.W., Lavigne, R (2015) The zeamine antibiotics affect the integrity of bacterial membranes. Appl Environ Microbiol 81:1139-1146.

[43] McAuliffe, O., Hill, C., Ross, R.P. (1999) Inhibition of Listeria monocytogenes in Cottage cheese manufactured with a lasticin3147-producing starter culture J.Appl. Microbiol 8: 251-256.

[44] McAuliffe, O., Ross, R.P., Hill, C. (2001) Lantibiotics: structure, biosynthesis and mode of action. FEMS Microbiol Rev 25: 285–308.

[45] McClerren, A.L., Cooper, L.E., Chao Quan Neil. T., Kelleher, N.L., van der Donk, W.A (2006) Discovery and in vitro biosynthesis of haloduracin, a two-component lantibiotic. Proc.Natl.Acad.Sci USA 103: 17242-17248.

[46] Marx, R., Stein, T., Entian, K-D., Glaser, S. J (2001) Structure of the Bacillus subtilis peptide antibiotic subtilosin A determined by 1H-NMR and matrix assisted laser desorption/ionization time-of-flight mass spectrometry. J Protein Chem 20: 501–506.

[47] Mendo, S., Faustino N.A., Sarmento A.C., Amado F., Moir A.J (2004) .Purification and characterization of a new peptide antibiotic produced by a thermotolerant Bacillus licheniformis strain. Biotechnol Lett 26:115-119.

[48] Mikulík, K., Chuan-Ling Qiao., Petřík, T., Puscheva, M., Zavarzin, G.A (1988) Elongation factor Tu of the extreme thermophilic hydrogen oxidizing bacterium Calerobacterium hydrogenophilum Biochem.Biophys. Res.Commun 155: 384-391.

[49] Mikulík, K., Jiránová,A., Manas,J., Spižek, J., Anděra, L., Savelyeva, N.D (1990) Peptide synthesis on ribosimes of an extreme thermophilic hydrogen bacterium Calerobacterium hydrogenophilum.Arch.Microbiol 153:248-253.

[50] Mikulík, K., Anděrová, M (1994) Role of polyamines in the binding of initiator tRNA to the 70S ribosomes of extreme thermophilic bacterium Calerobacterium hydrogenophilum. Arch.Microbiol 161: 508-513.

[51] Mootz, H.D., Finking, R., Marahiel, M.A (2001) 4′-phosphopantetheine transfer in primary and secondary metabolism of Bacillus subtilis. J Biol Chem 276: 37289–37298.

[52] Moyne, A.L., Cleveland, T.E., Tuzun, S (2004) Molecular characterization and analysis of the operon encoding the antifungal lipopeptide bacillomycin D. FEMS Microbiol Lett 234: 43–49.

[53] Muhammad, S.A., Ahmad S., Hameed, A (2009) Report: antibiotic production by thermophilic Bacillus specie SAT-4. Pak J Pharm Sci. 22:339-345.

[54] Mukherjee, A.K. Das, K. *(*2005*)* Correlation between diverse cyclic lipopeptides production and regulation of growth and substrate utilization by *Bacillus subtilis* strains in a particular habitat. FEMS Microbiol Ecol 54*:* 479–489.

[55] Nakano, M.M., Corbell, N., Besson, J., Zuber, P (1992) Isolation and characterization of sfp: a gene that functions in the production of the lipopeptide biosurfactant, surfactin, in Bacillus subtilis. Mol Gen Genet 232: 313–321.

[56] Nakano, M.M., Zheng, G., and Zuber, P (2000) Dual control of sbo-alb operon expression by the Spo0 and ResDE systems of signal transduction under anaerobic conditions in Bacillus subtilis. J Bacteriol 182: 3274–3277.

[57] Naruse, N., Tenmyo, O., Kobaru, S., Kamei, H., Miyaki, T., Konishi, M., Oki, T *(*1990*)* Pumilacidin, a complex of new antiviral antibiotics – production, isolation, chemical properties, structure and biological activity. J Antibiot 43*:* 267–280.

[58] Novotny, J.F.Jr, Perry, J.J (1992) Characterization of bacteriocins from two strains of Bacillus thermoleovorans, a thermophilic hydrocarbon-utilizing species. Appl Environ Microbiol. 58: 2393-2396.

[59] Oman, T.J,. van der Donk, W.A (2010) Follow the leader: the use of leader peptides to guide natural product biosynthesis. Nat Chem Biol 6: 9-18.

[60] Omura, S., Murata, M., Hanaki, H., Hinotozawa, K., Oiwa, R., Tanaka, H (1984) Phosalacine, a new herbicidal antibiotic containing phosphinothricin. Fermentation, isolation, biological activity and mechanism of action. J Antibiot 37:829–835

[61] Paik, S.H., Chakicherla, A., Hansen, J.N (1998)Identification and characterization of the structural and transporter genes for, and the chemical and biological properties of, sublancin 168, a novel lantibiotic produced by Bacillus subtilis 168. J Biol Chem 273: 23134-23142.

[62] Palomo, S., González, I., de la Cruz,M., Martín,J., Tormo,J.R., Anderson,M., . Hill, R.T., Vicente, F., Reyes, F., Genilloud, O (2013) Sponge-Derived *Kocuria* and *Micrococcus* spp. as Sources of the New Thiazolyl Peptide Antibiotic Kocurin. Mar Drugs 11: 1071–1086.

[63] Radhakrishnan, M., Balaji, S., Balagurunathan, R (2007) Thermotolerant actinomycetes from Himalayan Mountain-antagonistic potential, characterization and identification of selected strains. Malaysian Appl.Biol 36: 59-65.

[64] Ray, S.S., Johnson, M.C., Ray, B (1989) Bacteriocin plasmids of Pediococcus acidilactis. J. Indian Microbiology 4: 163-171.

[65] Rea, MC., Dobson, A., O'Sullivan, O., Crispie, F., Fouhy, F., Cotter, P.D., Shanahan F., Kiely, B., Hill, C., Ross, R.P (2011) Effect of broad- and narrow-spectrum antimicrobials on Clostridium difficile and microbial diversity in a model of the distal colon. Proc Natl Acad Sci U S A 108: 4639-4644.

[66] Ren, G., Strobel, J., Sears, M. Park, A (2010) Geobacillus sp., a thermophilic soil bacterium producing volatile antibiotics. Microb.Ecol 60: 130-136.

[67] Ryan, M., Rea, M.C., Hill, C., Ross, R.P (1996). An application of cheddar cheese manufacture for a strain of Lactococcus lactis producing a novel broad spectrum bacteriocin lacticin 3147. Appl. Environ. Microbiol **62**, 612-619.

[68] Rince, A (1994) Cloning, expression and nucleotide sequence of the of genes involved in production of lactoccin DR a bacteriocin from Lactococcus lactis susp.lactis Appl Environ. Microbiol 60 1652-1657.

[69] Rollema, H.S., Metzger, J.W., Both, P., Kuipers, O.P., Siezen, R.J (1996) Structure and biological activity of chemically modified nisinA species. Eur.J.Biochem.241, 716-722.

[70] Ross, R.P., Morgan, S., Hill, C. (2002) Preservation and fermentation: past, present and future. Int J Food Microbiol 79: 3–16.

[71] Scholz, R., Vater, J., Buchharjo, A., Wang, Z., He, Y., Dietel, K., Schwecke, T., Herfort, S., Lasch, P., Borris, R (2014) Amylocyclin a novel circular bacteriocin produced by Bacillus amyloliquefaciens FZB42. J.Bacteriol 196: 1842-1852.

[72] Schneider, T., Sahl, H.G. (2010) Lipid II and other bactoprenol-bound cell wall precursors as drug targets. Curr Opin Investig Drugs 11, 157-164.

[73] Schnell, N., Entian, K.D., Schneider, U., Götz, F., Zahner, H., Kellner, R., Jung, G (1988) Prepeptide sequence of epidermin, a ribosomally synthesized antibiotic with four sulphide-rings. Nature 333: 276–278.

[74] Severina, E., Severin, A., Tomasz, A. J (1998) Antibacterial efficacy of nisin against multidrug-resistant Gram-positive pathogens. Antiot.Chemother 41: 341-347.

[75] Sieber, S.A., Marahiel, M.A (2003) Learning from nature's drug factories: nonribosomal synthesis of macrocyclic peptides. J Bacteriol 185: 7036–7043.

[76] Sylla, J., Alsanius, B. W., Krüger, E., Reineke, A., Strohmeier, S., Wohanka, W (2013) Leaf microbiota of strawberries as affected by bio-logical control agents. Phytopathology 103:1001-1011.

[77] Stein, T., Borchert, S., Kiesau, P., Heinzmann, S., Klöss, S., Klein, C (2002a) Dual control of subtilin biosynthesis and immunity in Bacillus subtilis. Mol Microbiol 44: 403–416.

[78] Stein, T., Borchert, S., Conrad, B., Feesche, J., Hofemeister, B., Hofemeister, J., Entian, K-D (2002b) Two different lantibiotic-like peptides originate from the ericin gene cluster of Bacillus subtilis A1/3. J Bacteriol 184: 1703–1711.

[79] Stein, T., Heinzmann, S., Solovieva, I., Entian, K.D (2003a) Function of Lactococcus lactis nisin immunity genes nisI and nisFEG after coordinated expression in the surrogate host Bacillus subtilis. J Biol Chem 278: 89–94.

[80] Stein, T., Heinzmann, S., Kiesau, P., Himmel, B., Entian, K.D (2003b). The spa-box for transcriptional activation of subtilin biosynthesis and immunity in Bacillus subtilis. Mol Microbiol 47: 1627–1636.

[81] Stein, T., Düsterhus, S., Stroh, A., Entian, K.D (2004) Subtilosin production by two Bacillus subtilis subspecies and variance of the sbo-alb cluster. Appl Environ Microbiol 70: 2349–2353.

[82] Stein, T., Heinzmann, S., Düsterhus, S., Borchert, S., Entian, K.D (2005) Expression and functional analysis of subtilin immunity genes spaIFEG in the subtilin-sensitive host Bacillus subtilis MO1099. J Bacteriol 187: 822–828.

[83] Steinborn, G., Hajirezaei, M.R., Hofemeister, J (2005) Bac genes for recombinant bacilysin and anticapsin production in Bacillus host strains. Arch Microbiol 183: 71–79.

[84] Steller, S., Vollenbroich, D., Leenders, F., Stein, T., Conrad, B., Hofemeister, J (1999) Structural and functional organization of the fengycin synthetase multienzyme system from Bacillus subtilis b213 and A1/3. Chem Biol 6: 31–41.

[85] Steller, S., Sokoll, A., Wilde, C., Bernhard, F., Franke, P., Vater, J (2004) Initiation of surfactin biosynthesis and the role of the SrfD-thioesterase protein. Biochemistry 43: 11331–11343.

[86] tenBrink B., Minekus M., van der Vossen J.M., Leer R.J., Huis in't Veld J.H (1994) Antimicrobial activity of lactobacilli: preliminary characterization and optimization of production of acidocin B, a novel bacteriocin produced by Lactobacillus acidophilus M46. J Appl Bacteriol 77:140-148.

[87] Thimon, L., Peypoux, F., Wallach, J., Michel, G (1995) Effect of the lipopeptide antibiotic, iturin A, on morphology and membrane ultrastructure of yeast cells. FEMS Microbiol Lett 128: 101–106.

[88] Thompson, C.J., Seto, H (1995) Bialaphos. Biotechnology 28:197–222.

[89] Tosato, V., Albertini, A,M., Zotti, M., Sonda, S., Bruschi, C.V (1997) Sequence completion, identification and definition of the fengycin operon in Bacillus subtilis 168.Microbiology 143 :3443-3450.

[90] Tsuge, K., Ohata, Y., Shoda, M (2001a) Gene yerP, involved in surfactin self-resistance in Bacillus subtilis. Antimicrob Agents Chemother 45: 3566–3573.

[91] Tsuge, K., Akiyama, T., Shoda, M (2001b) Cloning, sequencing, and characterization of the iturin A operon J Bacteriol 183: 6265–6273.

[92] Vater, J., Kablitz, B., Wilde, C., Franke, P., Mehta, N., Cameotra, S.S *(*2002*)* Matrix-assisted laser desorption ionization-time of flight mass spectrometry of lipopeptide biosurfactants in whole cells and culture filtrates of *Bacillus subtilis* C-1 isolated from petroleum sludge. Appl Environ Microbiol 68*:* 6210–6219.

[93] Vanittanakom, N., Loeffler, W., Koch, U., Jung, G (1986) Fengycin – a novel antifungal lipopeptide antibiotic produced by Bacillus subtilis F-29-3 J Antibiot (Tokyo) 39: 888–901.

[94] Venugopalan V., Tripathi S.K., Nahar, P., Saradhi, P.P., Das, R.H., Gautam, H.K (2013) Characterization of canthaxanthin isomers isolated from a new soil Dietzia sp. and their antioxidant activities. J Microbiol Biotechnol 23:237-245.

[95] Walsh, C.T., Fischbach, M.A (2010) Natural products version 2.0: connecting genes to molecules J Am Chem Soc 132:2469-2493.

[96] Wu L, Wu H, Chen L, Xie S, Zang H, Borriss, R, Gao X (2014) Bacilysin from Bacillus amyloliquefaciens FZB42 has specific bactericidal activity against harmful algal bloom species. Appl Environ Microbiol ;80:7512-20

[97] Xie**,** L., Miller, L.M ., Chatterjee, C., Averin, O., Kelleher, N.L., van der Donk, W.A (2004) Lacticin 481: in vitro reconstitution of lantibiotic synthetase activity. Science 303:679-681.

[98] Xue, Q.H., Shen, G.H., Wang, D.S (2013) Effects of actinomycetes agent on ginseng growth and rhizosphere soil microflora. Ying Yong Sheng Tai Xue Bao 24: 2287-2293.

[99] Yamanaka K, Reynolds KA, Kersten RD, Ryan KS, Gonzalez DJ, Nizet V, Dorrestein PC, Moore BS (2014) Direct cloning and refactoring of a silent lipopeptide biosynthetic gene cluster yields the antibiotic taromycin A. Proc Natl Acad Sci U S A 111:1957-1962.

[100] Yazgan, A., Cetin, S., Ozcengiz, G (2003) The effects of insertional mutations in comQ, comP, srfA, spo0H, spo0A and abrB genes on bacilysin biosynthesis in Bacillus subtilis Biochim Biophys Acta 1626: 51–56.

[101] Yu, F., Zaleta-Rivera, K., Zhu,X., Huffman ,J., Millet, J.C., Harris, S.D., Yuen, G., Li, X.C., Du, L (2007) Structure and Biosynthesis of Heat-Stable Antifungal Factor (HSAF), a Broad-Spectrum Antimycotic with a Novel Mode of Action Antimicrob Agents Chemother 51: 64–72.

[102] Zheng, G., Yan, L.Z., Vederas, J.C., Zuber, P (1999) Genes of the sbo-alb locus of Bacillus subtilis are required for production of the antilisterial bacteriocin subtilosin. J Bacteriol 181: 7346–7355.

[103] Zheng, G., Hehn, R., Zuber, P (2000) Mutational analysis of the sbo-alb locus of Bacillus subtilis: identification of genes required for subtilosin production and immunity. J Bacteriol 182: 3266–3273.

Effect of Twisted Tape Insert On Heat Transfer During Flow Through A Pipe Using CFD

R V Manikanta[1], D V N Prabhakar[2], N V S Shankar[3]

[1]M.Tech Student, Department of Mechanical Engineering, Swarnandhra Institute of Engineering and Technology, Narsapur - 534280

[2]Department of Mechanical Engineering, Swarnandhra Institute of Engineering and Technology, Narsapur – 534280

[3]Department of Mechanical Engineering, Swarnandhra College of Engineering and Technology, Narsapur – 534280

Abstract— *The effect of nanoparticles on the performance of nanofluids during flow through pipes with dual twisted tape inserts. A detailed literature survey on the use of twisted tape inserts and computation thermal properties of nanofluids is presented. Expressions for nanofluid thermal properties computation are discussed. Properties for Al_2O_3 and TiO_2 nanofluid with volume fraction of 0.1 are computed. CFD simulations to study the behaviour of fluid during heat transfer when flowing through pipes with dual twisted tape inserts. Results of these simulations are discussed in the paper.*

Keywords— nanofluid, CFD, Twisted Tape Inserts, Al_2O_3 nanofluid, TiO_2 nanofluid.

I. INTRODUCTION

Augmenting heat transfer during flow through pipes has always been interest for various researchers. There are three ways of augmenting heat transfer in fluids [1]. They are:

i. Active (use of mechanical aids, magnetic fields etc)

ii. Passive (using swirl generators like twisted tape etc which do no use external energy)

iii. Compound

1.1 Passive Augmenting Techniques

A lot of investigation happened regarding the passive techniques i.e using swirl generators. A review of literature in this area has been presented in [2] & [3]. Sawarkar and Pramod [4] experimentally investigated into the effect of semi-circular cut twisted inserts into augmentation of heat transfer in horizontal pipes. Theoretical calculations that can be used for heat transfer coefficients are also detailed in their work. Tabatabaeikia, et al [5] investigated into the use of lovered tapes and modified twisted inserts for heat transfer augmentation during flow through pipes. Ebenezar Paul, et al [6] investigated to augmentation of heat transfer in Cu2O by the use of twisted tape inserts with alternate axis. These kinds of inserts are shown in Fig 2.3. Shrirao, et al [7], [8] performed experimental study on the mean Nusselt number, friction factor and thermal enhancement factor characteristics in a circular plain tube and internally threaded tube under uniform wall heat flux boundary conditions for pure water and Al2O3 nanofluid as working fluid. Shivaji Munde [9] performed experimental investigation of heat transfer of circular tube fitted with helical wire and twisted tape, have been studied under uniform heat flux conditions with Air as working fluid. Prakash and Karuppasamy [10] using experimental investigations showed that using twisted tapes with wires and rectangular cuts there is a 207% increase in heat transfer coefficient. As stated in [11], Nusselt number and friction factor obtained for louvered strip (with forward backward arrangement) > Nusselt number and friction factor for louvered strip (with semi-forward semi-backward arrangement)> Nusselt number and friction factor for louvered strip (with forward arrangement). A 3-D numerical model was developed to study the performance of (i) bare tube-in-tube heat exchanger, (ii) tube in tube with twisted tape insert and (iii) helical insert at annulus and twisted tape insert inside the inner tube of the heat exchanger in [12]. The use of vortex generator for heat transfer enhancement was discussed in [13]. Patil, et al [14] showed that the use of wire coil and screw tape insert enhances heat transfer coefficient by 150 times. Matini and Swapnil [15] experimentally investigated the influences of twisted tapes and wire coil on pressure drop, friction factor (f), heat transfer and thermal enhancement index (η). Johar & Hrshda [16] studied the effect of reduced twisted tape inserts with baffles and holes on heat transfer during flow through a pipe. Sarada, et al [17] investigated to the use of mesh for augmentation of heat transfer during flow through a pipe. Tamna, et al [18] investigated the use of dual twisted inserts in increasing the heat transfer during flow. Expressions given in this article are used to predict the Nusselt number and thus heat transfer coefficient in the current work.

1.2 Thermal Properties of Nano Fluids

Kumar & Chakrabarti [19] reviewed literature pertaining to numerical modelling and experimental results relating to heat transfer using nanofluid. Heat transfer enhancement characteristics and approaches by various investigators are summarized in the same article. Corcione [20] & Sivashanmugam [21] listed the empirical relations for predicting the thermal properties of nanofluid.

Mohan Kumar & Rajan [22] invested experimentally into the heat transfer characteristics of CuO nanofluid with three different concentrations and compared the results with available correlations. Iqbal and Rehman [23] summarized the work relating to heat transfer enhancement in nanofluids using twisted tapes. Bunker and Vishwakarma [24] investigated into enhancement of heat transfer for CuO nanofluid using swirl generator. Emprical relations pertaining to this process are also discussed. Kulakarni and Oak [25] investigated experimentally into heat transfer augmentation of CuO nanofluid using helical coil wire inserts. Empirical relations that can be used were summarized in this article. Robertis, et al [26] used Modulated Temperature Differential Scanning Calorimetry technique to measure the heat capacity of nanofluids prepared by one-step method, using sodium hypophosphite as reducing agent in ethylene glycol base fluid. Polyvinyl Pyrrolidone (PVP) was used as stabilizing agent for copper particles obtained from two different precursor salts, copper nitrate and copper sulphate.

ÖZERİNÇ [27] numerically, using CFD simulations, investigated into heat transfer characteristics of Al_2O_3-H_2O nanofluid using thermal dispersion model for hydrodynamically fully developed, thermally developing laminar flow. These results were then compared with experimental results presented in the literature surveyed by the same author. Aghaei, et al [28] numerically simulated the heat transfer through Al_2O_3-H_2O nanofluid for various volume fractions and with Reynold's numbers 10000, 20000 and 30000 and summarized that variations of the average Nusselt number relative to volume fractions are not uniform. Also for all of the considered volume fractions, by increasing the Reynolds number the skin friction factor decreases and with increasing volume fractions and Reynolds number the pressure drop increases. Sisodiya & Geete [29] investigated, using CFD techniques, into the use of Al_2O_3-Water nanofluid in helical coil heat exchangers. Various volume fractions are considered during the analysis.

Subramaniyan & Ilangovan [30] investigated into thermal conductivity of metallic and oxide nanofluids. Thermal conductivity of Cu_2O-TiO_2 nanocomposites with water as base fluid using Maxwell model for different volume fractions of nanophase is investigated. Highest thermal conductivity was observed for Cu2O-TiO2 (1:9) with water as base fluid. Bianco, et al [31] used two phase particle simulation model to numerically simulate and determine the thermal properties of nanofluid. These findings are validated using correlations available.

II. NANOFLUID CORRELATIONS

Use of nanofluids in heat exchangers is being widely investigated. When simulating the flow of nanofluids, due to limitations of CFD software and computational capability of the systems, equivalent properties of nanofluids are computed and are then used in simulation. The equations that are used for computing properties are as given in [29]. These equations are given below:

2.1 Nanofluid Density

$$\rho_{nf} = \varphi . \rho_s + (1+\varphi) . \rho_f \quad (1)$$

Where ρ stands for density, subscript *nf* denotes nanofluid, *f* denotes base fluid, *s* denotes solid particle material, φ stands for volume fraction

2.2 Base fluid molecular diameter

$$d_f = 0.1 \cdot \left(\frac{6 \cdot M_f}{N_A \cdot \pi \cdot \rho_f} \right)^{\frac{1}{3}} \quad (2)$$

Where M_f is the molecular weight, N_A is Avogadro number.

2.3 Nanofluid Specific heat

$$C_{pnf} = \frac{1}{\rho_{nf}} \cdot \left(\varphi \cdot \rho_s \cdot C_{ps} + (1-\varphi) \cdot \rho_f \cdot C_{pf}\right) \tag{3}$$

Where C_p stands for specific heat of respective substance

2.4 Prandtl Number

$$Pr = \frac{C_{pf} \cdot \mu_f}{K_f} \tag{4}$$

Where K is the thermal conductivity and μ stands for dynamic viscosity

2.5 Nanofluid Thermal Conductivity

$$K_{nf} = \left(1 + 4.4\, Re^{0.4} \cdot Pr^{0.66} \cdot \left(\frac{T_c}{T_{ff}}\right)^{10} \cdot \left(\frac{K_p}{K_f}\right)^{0.03} \cdot \varphi^{0.66}\right) \cdot K_f \tag{5}$$

Nanofluid Dynamic Viscosity

$$\mu_{nf} = \frac{\mu_f}{1 - 34.87 \cdot \left(\frac{d_p}{d_f}\right)^{-0.3} \cdot \varphi^{1.03}} \tag{6}$$

In the current work, water is taken as the base fluid and nanoparticles are TiO_2 and Al_2O_3. Table 1 summarizes the properties of the components of nanofluid. Mathcad has been used to compute the material properties using the above expressions. Based on equation (5), it can be observed that the thermal conductivity is a function of Reynold's number. This variation for Al_2O_3-water, TiO_2-Water nanofluids is shown in Fig 1. The dynamic viscosity, based on equation (6) is dependent only on nanoparticle size. The dynamic viscosity is thus same for both the nanofluids as the particles is taken as 33nm and in this case the dynamic viscosity is calculated to be 0.0008313PaS. These computed values are then used in simulation.

TABLE 1
PROPERTIES OF COMPONENTS OF NANOFLUID

	Density (ρ) (kg/m^3)	k (W/mK)	cp (J/ kgK)	dp (nm)	Molicular Wt (gm/mole)
Water	997.1	0.613	4179	**	18.01528
Al_2O_3	3970	40	765	33	**
TiO_2	4000	11.7	697	33	**

(Data not required in the calculations are not listed in the table)

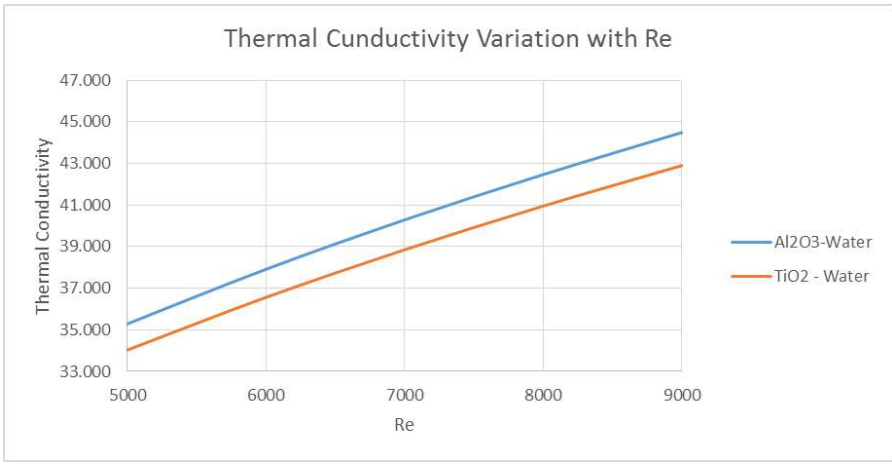

FIG 1: VARIATION OF THERMAL CONDUCTIVITY OF NANOFLUID WITH Re

III. CFD SIMULATION

Initially, CFD simulations are executed to study the effect of double twisted tapes. For this, the experimental conditions stated in [18] are simulated. The simulated model is shown in Figs 2 & 3. Flow through 3m length pipe is simulated. Fist 1m is considered as leading length and is taken so that flow completely stabilizes. For the next 1m length, a constant wall temperature of 150°C is simulated. This is the test section. Two swirl generators are simulated in this length. The next 1m is the trailing length. Average temperature at 11 points along the test section where taken as output. Average heat flux along the test section is also taken as output. Natural convection is simulated along the trailing end.

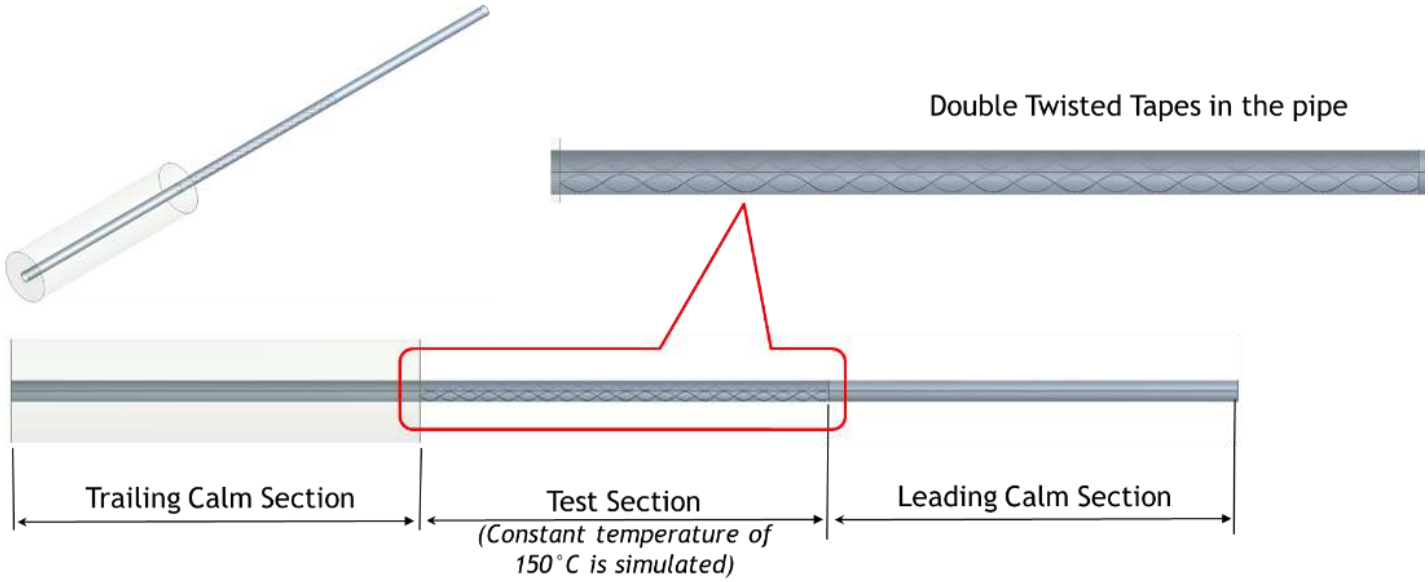

FIG 2: GEOMETRY DESCRIPTION USED FOR SIMULATING THE FLOW

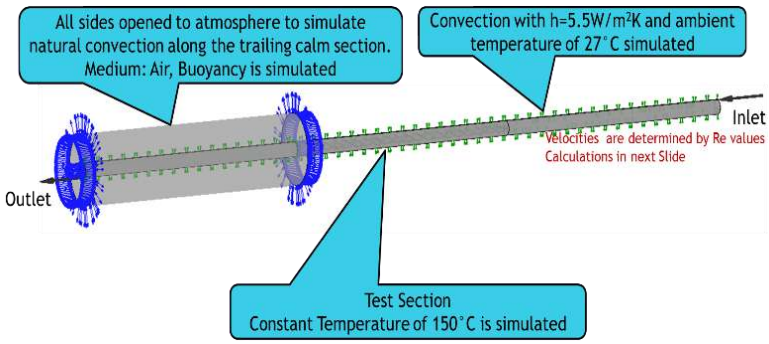

FIG 3: BOUNDARY CONDITIONS

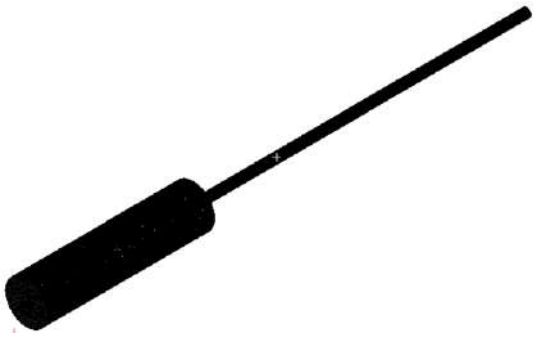

FIG 4: MESHED MODEL

IV. MESHING & GRID ANALYSIS

3 different cases (each with 5 different Re values) are studied during this project execution. The grid analysis was performed until the variation in target parameter (heat flux) is less than 1%. Grid with max element size of 1.5mm is chosen. The results of the simulations are presented in the next section. Fig 4 shows the grid generated.

V. CFD SIMULATION RESULT

Based on the thermal conductivities of the fluids, as shown in Fig 1, it can be observed that with low volume fractions like 0.01, there is little variation in thermal conductivity of the nanofluid and thus there is not much difference in thermal conductivities. Thus similar temperature rise is shown by both nanofluids simulated for a give Re. This variation for Re=5000 is shown in Fig 9. It can be observed that Nanofluids are receiving more heat than compared with that of plain water.

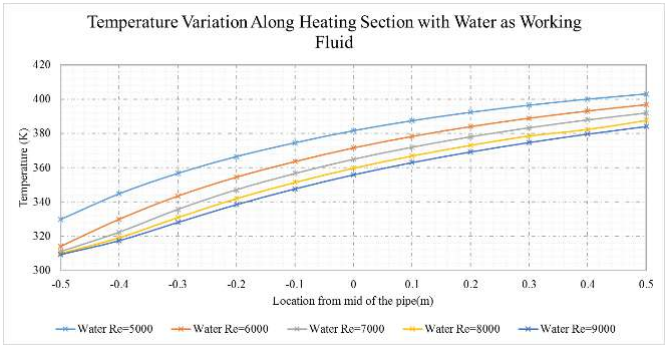

FIG 5: TEMPERATURE VARIATION WITH WATER AS WORKING FLUID

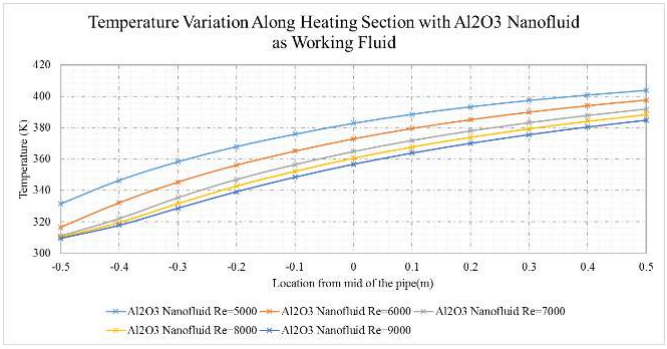

FIG 6: TEMPERATURE VARIATION WITH AL2O3 –WATER NANOFLUID AS WORKING FLUID

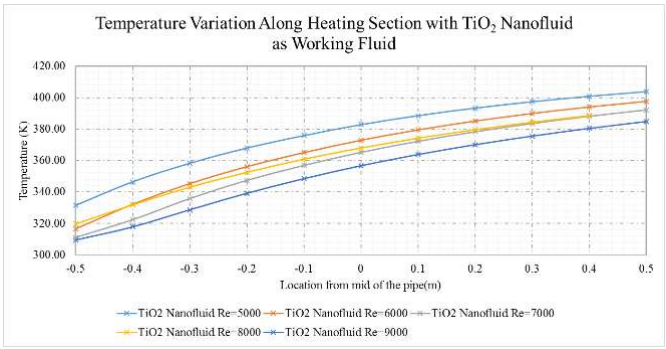

FIG 7: TEMPERATURE VARIATION WITH TIO2 –WATER NANOFLUID AS WORKING FLUID

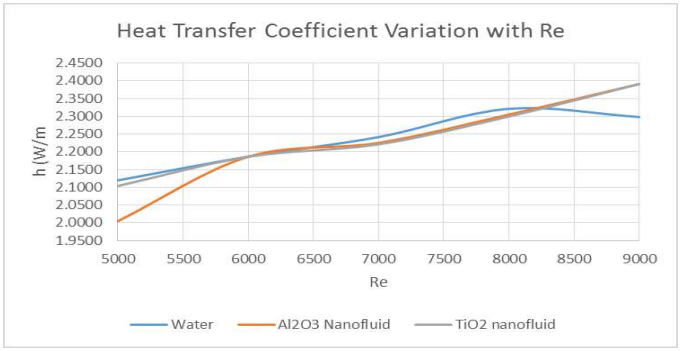

FIG 8: HEAT FLUX VARIATION

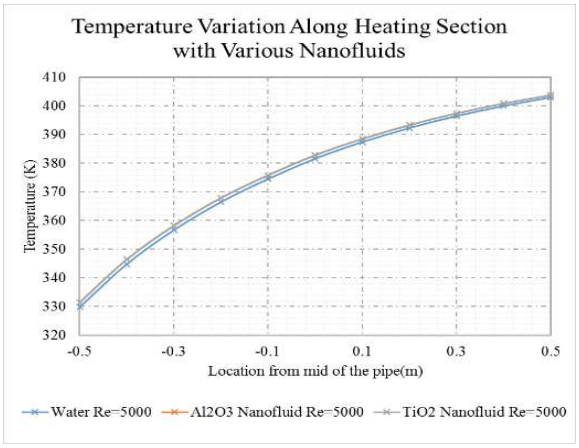

FIG 9: TEMPERATURE VARIATION DUE TO VARIOUS NANOFLUIDS

VI. CONCLUSION

Nanofluids are currently being used for better heat transfer. In the current work, the effectiveness of nanofluid during heat when flowing through a tube with dual twisted tape inserts was investigated. Literature survey pertaining to use of swirl generators and evaluating nanofluid thermal properties is presented. Numerical relations for calculating thermal properties are listed. CFD simulations are executed to compute the heat flux with various nanofluids is executed and the results were discussed. The results indicated that nanofluids show greater increase in temperature but low volume fractions, both Al_2O_3 and TiO_2 showed similar performance.

REFERENCES

[1] N. C. Kanojiya, V. M. Kriplani, and P. V. Walke, "Heat Transfer Enhancement in Heat Exchangers With Inserts: A Review," *Int. J. Eng. Res. Technol.*, vol. 3, no. 10, pp. 494–500, 2014.

[2] N. Nagayach and A. B. Agrawal, "Review Of Heat Transfer Augmentation In Circular And Non- Circular Tube," *Int. J. Eng. Res. Appl.*, vol. 2, no. 5, pp. 796–802, 2012.

[3] S. V Patil and P. V. V. Babu, "Heat Transfer Augmentation in a Circular tube and Square duct Fitted with Swirl Flow Generators : A Review," *Int. J. Chem. Eng. Appl.*, vol. 2, no. 5, pp. 326–331, 2011.

[4] P. A. Sawarkar and P. R. Pachghare, "Experimental Analysis of Augmentation in Heat Transfer Coefficient Using Twisted Tape with Semi- Circular Cut Insert," *Int. J. Sci. Res.*, vol. 4, no. 4, pp. 1174–1179, 2015.

[5] S. Tabatabaeikia, H. A. Mohammed, N. Nik-Ghazali, and B. Shahizare1, "Heat Transfer Enhancement By Using Inserts," *Adv. Mech. Eng.*, vol. 6, p. 250354, 2014.

[6] E. Paul, S. K. Yadav, and S. Kumar, "Numerical Simulation And Enhancement Of Heat Transfer Using Cuo/Water Nano-Fluid And Twisted Tape With Alternate Axis," *Int. J. Mech. Eng. Technol.*, vol. 5, no. 9, pp. 323–335, 2014.

[7] P. N. Shrirao, S. S. Gaddamwar, and P. R. Ingole, "Convective Heat Transfer and Friction Factor Characteristics in Internally Threaded Tube with Constant Heat Flux for Al 2 O 3 / Water Nanofluid," *Int. J. Sci. Res.*, vol. 5, no. 2, pp. 1407–1411, 2016.

[8] P. N. Shrirao, R. U. Sambhe, and P. R. Bodade, "Experimental Investigation on Turbulent Flow Heat Transfer Enhancement in a Horizontal Circular Pipe using internal threads of varying depth," *IOSR J. Mech. Civ. Eng.*, vol. 5, no. 3, pp. 23–28, 2013.

[9] S. V Mundhe and P. W. Deshmukh, "Experimental Analysis of Heat Transfer for Turbulent Flow through Circular Pipe," *Int. J. Innov. Res. Adv. Eng.*, vol. 1, no. 3, pp. 70–75, 2014.

[10] P. Prakash and K. Karuppasamy, "Influences of Combined Inserts on Heat Transfer Enhancement In Circular Tube Equipped With Inserts," in *International Conference On Recent Advancement In Mechanical Engineering &Technology (ICRAMET' 15)*, 2015, no. 9, pp. 388–394.

[11] K. R. Raut and H. S. Farkade, "Convective Heat Transfer Enhancements in Tube Using Louvered Strip Insert," *Int. J. Tech. Res. Appl.*, vol. 2, no. 4, pp. 1–4, 2014.

[12] P. S. Rao and K. K. Kumar, "Numerical and experimental investigation of heat transfer augmentation in double pipe heat exchanger with helical and twisted tape inserts," *Int. J. Emerg. Technol. Adv. Eng.*, vol. 4, no. 9, pp. 180–192, 2014.

[13] Mohamad Asmidzam Ahamat, M. F. Beludtu, and R. Abidin, "Heat transfer enhancement in a rectangular channel using vortex generator," *J. Sci. Eng. Technol.*, vol. 2, no. 2, 2012.

[14] S. V Patil, G. U. Dongare, S. S. Haval, and L. Ambekar, "Heat Transfer Enhancement through a Circular Tube Fitted with Swirl Flow Generator," in *National Conference On "Changing Technology and Rural Development" CTRD 2k16*, 2016, pp. 18–23.

[15] A. G. Matani and S. A. Dahake, "Experimental Study on Heat Transfer Enhancement in a Circular Tube Fitted," *Int. J. Appl. or Innov. Eng. Manag.*, vol. 2, no. 3, pp. 100–105, 2013.

[16] G. Johar and V. Hasda, "Experimental Studies On Heat Transfer Augmenatation Using Modified Reduced Width Twisted Tapes (RWTT) As Inserts For Tube Side Flow Of Liquids," Department of Chemical Engineering, 2010.

[17] S. N. Sarada, A. S. R. Raju, K. K. Radha, V. Atanasiu, I. Doroftei, and C. Rozmarin, "Experimental Numerical Analysis Enhancement of Heat Transfer in a Horizontal Circular Tube using Mesh Inserts in Turbulent Region," *Eur. J. Mech. Environ. Eng. 2010*, vol. 2010, no. 2, pp. 3–18, 2010.

[18] S. Tamna, Y. Kaewkohkiat, S. Skullong, and P. Promvonge, "Heat transfer enhancement in tubular heat exchanger with double V-ribbed twisted-tapes," *Case Stud. Therm. Eng.*, vol. 7, pp. 14–24, 2016.

[19] S. Kumar and S. Chakrabarti, "A Review: Enhancement of Heat Transfer with Nanofluids," *Int. J. Eng. Res. Technol.*, vol. 3, no. 4, pp. 549–557, 2014.

[20] M. Corcione, "Empirical correlating equations for predicting the effective thermal conductivity and dynamic viscosity of nanofluids," *Energy Convers. Manag.*, vol. 52, no. 1, pp. 789–793, 2011.

[21] P. Sivashanmugam, "Application of Nanofluids in Heat Transfer," in *An Overview of Heat Transfer Phenomena*, S. N. Kazi, Ed. InTechOpen, 2012, pp. 411–441.

[22] T. Mohan and K. Rajan, "Investigation of Heat Transfer and Friction Factor Characteristics of Two Phase Nano Fluids by Inserting Twisted Tape and Helical Inserts in the Tube," *IOSR J. Mech. Civ. Eng.*, vol. 13, no. 5, pp. 9–16, 2016.

[23] M. I. A. R. Sheikh and V. P. Ate, "Heat transfer enhancement using CuO / water nanofluid and twisted tape insert in circular tube- A Review .," *Int. J. Recent Innov. Trends Comput. Commun.*, vol. 3, no. 2, pp. 1–3, 2015.

[24] R. Bunker and R. Vishwakarma, "Analysis of Heat Transfer in Semifluid Tube Heat Exchanger Equipped with Spiral Coiled Insert Using CuO-H2O Based Nanofluids," *Int. J. New Technol. Res.*, vol. 2, no. 2, pp. 117–121, 2016.

[25] S. P. Kulkarni and S. M. Oak, "Heat TransferEnhancement in Tube in Tube Heat Exchanger with Helical Wire Coil Inserts and CuO Nanofluid," *IPASJ Int. J. Mech. Eng.*, vol. 3, no. 5, pp. 54–60, 2015.

[26] E. De Robertis *et al.*, "Measurement of the Specific Heat Capacity of Copper Nanofluids By Modulated Temperature Differential Scanning Calorimetry," in *Proceedings of ENCIT 2010, 13th Brazilian Congress of Thermal Sciences and Engineering*, 2010.

[27] S. ÖZERİNÇ, "Heat Transfer Enhancement With Nanofluids," Middle East Technical University, 2010.

[28] A. Aghaei, G. A. Sheikhzadeh, M. Dastmalchi, and H. Forozande, "Numerical investigation of turbulent forced-convective heat transfer of Al2O3-water nanofluid with variable properties in tube," *Ain Shams Eng. J.*, vol. 6, no. 2, pp. 577–585, 2015.

[29] V. Sisodiya and A. Geete, "Heat Transfer Analysis of Helical Coil Heat Exchanger With Al2O3 Nano Fluid," *Int. Res. J. Eng. Technol.*, vol. 3, no. 12, pp. 366–370, 2016.

[30] A. Subramaniyan and R. Ilangovan, "Thermal Conductivity of Cu2 O-TiO2 Composite -Nanofluid Based on Maxwell model A.," *Int. J. Nanosci. Nanotechnol.*, vol. 11, no. 1, pp. 59–62, 2015.

[31] V. Bianco, O. Manca, and S. Nardini, "Numerical simulation of water/ Al2O3 nanofluid turbulent convection," *Adv. Mech. Eng.*, vol. 2010, no. October 2016, 2010.

Design, Sizing and Implementation of a PV System for Powering a Living Room

Marwa Sayed Salem Basyoni[1], Mona Sayed Salem Basyoni[2], Kawther Al-Dhlan[3]

[1,2,3]Computer Science and Engineering College,[1]University of Hail, Kingdom of Saudi Arabia
[1]Modern Science and Arts University (MSA), Cairo, Egypt

Abstract— *This paper aims to design size and implement a Photo Voltaic system (PV system) for powering a living room. The required load to be powered by the PV system is completely determined. A comparison between using normal and power saving loads is carried out. The power saving loads is chosen to reduce the overall cost of the required system. The proposed PV system for powering the predetermined load is introduced. Each part of the system is designed and sized based on the load requirement. Finally, the practical implementation for the overall PV system for powering the required load is done. The implemented system works in an efficient way.*

Keywords— Design, Sizing, Implementation, PV system.

I. INTRODUCTION

Recent researches focus on renewable energy recourses [1, 2]. This is because the already existed energy sources, which mainly based on fuel, are going to run out [3, 4]. There are many types of renewable energy resources [1]. Solar energy is considered the most attractive renewable energy source. This is because it is mainly the source of all other energy sources. In addition it gives higher output power comparing with other renewable energy sources [5, 6]. The main objective of this paper is to use the Photo – Voltaic (PV) system as a renewable energy source instead of the existed energy sources which based on fuel for powering a certain load. The system has to be implemented efficiently to satisfy the load requirements. Thus the load has to be firstly determined. A comparison between normal load and power saving loads is carried out. The power saving loads is chosen to reduce the overall cost of the PV system. The design sizing for each part of the required PV system is presented based on the load requirements. Each part of the PV system is tested practically to check its functionality. Finally the overall PV system is implemented to power the required load.

II. NORMAL LOADS AND POWER SAVING LOADS

The main objective of using the PV system is to power home utilities in the case of light goes out. In emergency cases, it is not required to power the whole home utility. The selected load as a case study in this paper is to power a living room, lamps for both of the kitchen and the bathroom. The utilities which are selected to be powered by the PV system are a LCD TV, Laptops with internet, fan and power saving Lamps. Also, the lighting of both the bathroom and the kitchen are taking into consideration. Table (1) shows some appliances and loads with its power consumption [7]. From table 1, it is obvious that the power saving loads consume less power comparing with the normal loads. For example, the laptop consumes 1 KWH when it is used for 60 hours but the desktop computer with monitor consumes 8KWH. Also the LCD TV uses low power comparing to the standard TV. Thus, the power saving loads is used to reduce the overall cost of the PV system.

The daily energy consumption for a certain load, Wattage * Hours used per day, is calculated as follow [8]:

$$\frac{(\textbf{Wattage} * \textbf{Hours used per day})}{1000} = \textbf{Daily kilo watt hour} \quad (1)$$

The contribution in this paper is to use smart (power saving loads) loads instead of normal loads. Normal loads consume much more power comparing to the power saving loads. Thus by using the power saving loads, the required power reduces. As a result, the overall cost of the required PV system reduces. The system design and sizing are based on calculations.

TABLE 1
SOME APPLIANCES AND LOADS WITH ITS POWER CONSUMPTION

APPLIANCE	HOURS IN USE	KWH USED	MONTHS USED	ANNUAL KWH
Computer - Desktop with Monitor	90	8	12	96
Computer - Laptop	60	1	12	12
Fan – Bath	15	1	12	12
Fan - Ceiling (does not incl. lights)	150	12	6	72
Fan - Table / Box / Floor	71	11	3	33
Lighting - Incandescent, 100 watts	100	10	12	120
Lighting - CFL, 25 watts	100	1	12	12
Television - 27 inch, LCD flat screen	150	18	12	216
Television - 15-27 inch, standard	150	18	12	216

Table (2) shows the difference between using power saving loads and normal loads required for a living room, the used case study. Such loads are assumed to be used for 10 hours per day. The power calculations based on equation (1).

TABLE 2
DIFFERENCE BETWEEN POWER SAVING &NORMAL LOADS IN LIVING ROOM

Used Load (Assume each used 10 hours per day)	Power saving loads power		Normal Load power	
	Watt	Watt-hour/day	Watt	Watt-hour/day
Lighting	4	40	36	360
TV 19”	22	220	80	800
Fan	45	450	60	600
Total	71 W	710 W.H/D	176 W	1760 W.H/D

From table 2, it is obvious that the normal loads require power ten times more than the required power for the power saving loads. Thus the overall cost of the PV system using the power saving loads is predicted to be reduced.

III. PV SYSTEM DESIGN AND SIZING

In this section the design of each part of the PV system is presented. Figure 1 shows the required PV system to be implemented for powering any domestic use [9]. In this paper, it is required to power a living room with the lighting of both the kitchen and bathroom.

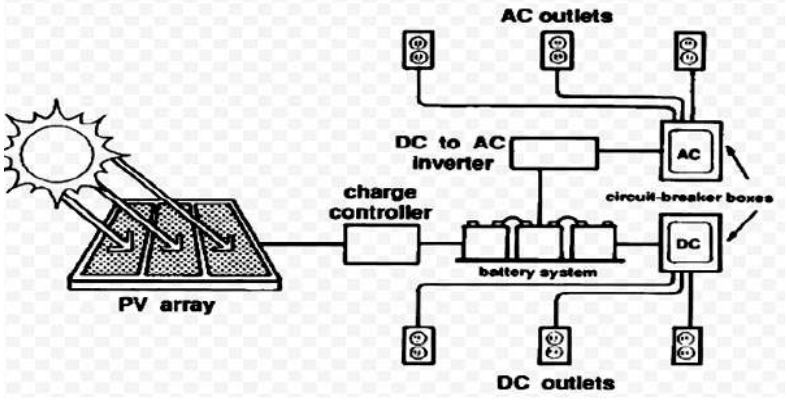

FIGURE 1: THE FUNCTIONAL BLOCK DIAGRAM OF THE REQUIRED PV SYSTEM FOR POWERING BOTH AC AND DC LOADS

3.1 Loads consumption demand

Loads consumption must be determined to be able to determine the specification of PV system components. The loads consumption is determined for the living room utilities. PV system has high power dissipation through its components. Thus a safety margin has to be taking into consideration is the system design [9]. The following calculations show a comparison between the load consumption using normal loads and power saving. This consumption based on powering the main requirements of the living room and the lighting for both the bathroom and the kitchen, one TV, one fan, three light bulbs. The system is designed to power the required loads for 5 hours per day.

3.1.1 Load Consumption using Normal loads:

One 70W LED television 19" used 5 hours per day 70*5 = 350 Wh

One 75W fan used 5 hours per day: 75*5 = 375 Wh

Three-100W light Bulb used 5 hours per day: 3*100*5 = 1500 Wh=1.5KWh

One 100W Desktop with Monitor used 5 hours per day: 100*5=500Wh

TOTAL DAILY LOAD 2725 Wh /day

3.1.2 Load Consumption Power Saving Loads:

One 22W LED television 19" used 5 hours per day 22*5 = 110 Wh

One 20W fan used 5 hours per day: 20*5= 100 Wh

Four -4W light Bulb used 5 hours per day: 4*4*5 = 80Wh

One 60W Lab top used 5 hours per day: 60*5=300Wh

3.1.3 TOTAL DAILY LOAD 590Wh /day

From this calculation, it is obvious that the normal loads consume much more power than the power saving loads. These calculations confirm that using power saving loads reduces the overall cost of the PV system. As it reduces the overall required daily power consumption, it requires less number of solar panel. Also, the requirements of the system components reduce.

Thus the total power consumed by the required loads is 590Wh/day. The system is design to deliver 650 Wh/day as a safety margin for the design.

3.2 Panels' estimation

In this paper, the living room is to be implemented using power saving loads. From loads calculations, the power from the solar panel must be calculated using the following rule [10]:

$$\frac{\textbf{Daily energy loads consumption}}{\textbf{hours of usable sunlight during day}} = \textbf{power of panels power of panels} \quad (2)$$

The number of solar panels used varies based on the load requirements. To size the panels, to determine the required number of panels to be used with its required power, the total peak watt produced must be calculated. The peak watt (W_p) [11] produced depends on size of the PV module and climate of site location. In KSA, it enjoys sunshine all the year. In system design, six hours of sunshine all over the day is assumed. Thus, each watt peak (W_p) of solar panel would therefore deliver 6Wh/day. Thus the required power from the solar panel is calculated using equation 2.

The daily energy loads consumption is 650 Wh. The hours of usable sunlight during day is assumed to be 6 hours. Thus the required output power from the solar panel is 109W. Thus a 120W solar panel is used as a safety margin for the design.

3.3 Charge controller Design and Sizing

The charge controller is used in PV system for controlling charging and discharging operation of battery from solar panels. The main objective of charge controller is to regulate the charge to the batteries and preventing any overcharging. When the battery becomes full the charge controller disconnects it from panels [9].

The input power from panels to charge controller is calculating using equation 3, assuming the worst case efficiency of charge controller equals to 85%:

$$\text{Input Power (from panels)} = \frac{\text{Output power}}{\text{Efficiency } (\eta)} \tag{3}$$

Thus the input power to the controller is 141W.

The charge controller rating is calculated by dividing its input power by the maximum voltage of the used solar panel. The maximum voltage of the solar panel is 18V [12]. Thus the rating of the charge controller to be used for the PV system is 7.88A. It is designed to be 10A, 12V as a safety margin for the design.

3.4 Batteries

The battery is used to store the generated energy from the solar panel and deliver it to the load [9]. There are many types of the battery [13]. The dry battery is the type which is used in this paper. It is most common used because it has a long lifetime and it is good in maintenance.

The capacity of battery is measure in ampere-hours (Ah). It is calculated by using equation 4[13]:

$$\text{Capacity (Ah)} = \frac{\text{Daily energy loads consumption(Wh)}}{\text{max panel volt (V)}} \tag{4}$$

Assume that the battery has efficiency of 85 %. To save its lifetime, it is assumed to discharging to 60 % from its value. So the capacity of the required battery to be used in this system is calculated using equation 5.

$$\text{Capacity (Ah)} = \frac{Total\ Watt{-}hours\ per\ day\ used\ by\ appliances}{(0.85\ x\ 0.6\ x\ nominal\ battery\ voltage)} \tag{5}$$

Assuming the worst case of using 85% battery efficiency and 60% depth of discharge and 12V battery, as the total watt – hours per day is 650W, thus the battery storage energy is calculated using equation 5. It is found to be 106Ah. A 120Ah battery is used for design safety.

3.5 The Inverter

The inverter is used to convert direct current (DC) produced from panel, to alternative current (AC) that needs to power the AC loads in home [9]. The efficiency of inverter is in the range of 90% to 95% because the power loss occurs in the conversion process. The efficiency of inverter can be calculated by using equation 6 [13].

$$\text{Efficiency } (\eta) = \frac{\text{Output power (to loads)}}{\text{Input power (come from charge controller)}} \tag{6}$$

Assuming worst case inverter efficiency to be 90%, so the input power to the inverter coming from the charge controller is calculated using equation 7.

$$\text{Input Power (from charge controller)} = \frac{\text{Output power (to loads)}}{\text{Efficiency } (\eta)} \frac{\text{Output power (to loads)}}{\text{Efficiency } (\eta)} \tag{7}$$

The inverter power must be sufficient to handle the total amount of Watts that required by the system. The inverter size should be 25-30% greater than the required watt for the load [13]. To size the inverter, the total power of the used load must be calculated. It is around 118W. Thus a 150W inverter is required for design safety margin.

Thus the requirement of the PV system required to power a 650Wh/day for a living room with the lighting of a kitchen and a bathroom are:

One solar panel with 120W, Charge controller rated at 10A at 12V, a battery with capacity of 120Ah and 12V, Inverter with size greater than 150W

Figure 2 shows the practical components which are used for implementing the PV system

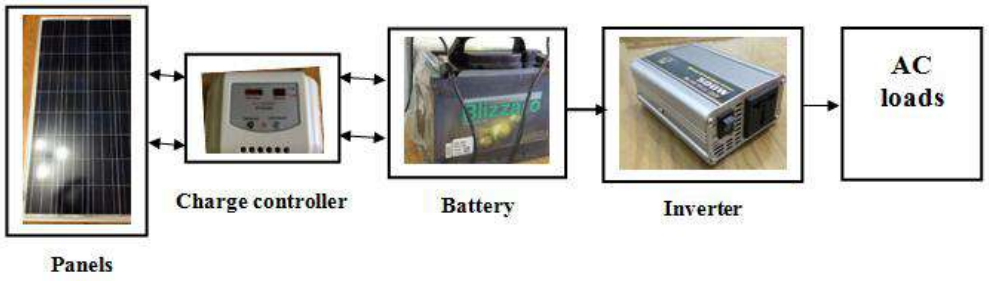

FIGURE 2: THE PRACTICAL COMPONENTS OF THE IMPLEMENTED PV SYSTEM

The PV is implemented and tested. It is working in an efficient way. It powers the loads when the light goes out for 5 continuous hours. There are supporting videos for practical implementation and testing for the PV system.

IV. CONCLUSION

A PV system for powering a living room with the lighting of both the kitchen and the bathroom is implemented. The power saving loads is used instead of the normal loads. It consumes less power. Thus it reduces the overall cost of the PV system. The required load is completely determined. Each part of the PV system is designed and sized. The implemented system is tested. It works effectively. It powers the required load for five continuous hours when light goes out.

REFERENCES

[1] Faruk Yildiz, "Potential Ambient Energy-Harvesting Sources and Techniques", The Journal of Technology Studies, 2009

[2] S. Roundy, P. K. Wright, and J. M. Rabaey, "Energy Scavenging for Wireless Sensor Networks", 1st ed. Boston, Massachusetts: Kluwer Academic Publishers, 2003

[3] V. A. Boichenko, E. Greenbaum, and M. Seibert, Photoconversion of Solar Energy, molecular to global photosynthesis. Imperial College Press London: 2004; p 397-452

[4] S. Bahatyrova, R. N. Frese, C. A. Siebert, J. D. Olsen, K. O. van der Werf, R. van Grondelle, R. A. Niederman, P. A. Bullough, C. Otto, and C. N. Hunter, Nature 430, (7003), 1058-1062 (2004).

[5] Nathan S. Lewis and George Crabtree, Argonne Arthur Nozik, NU Paul Alivisatos, "Basic Research Needs for Solar Energy Utilization", Report of the Basic Energy Sciences Workshop on Solar Energy Utilization , UC-Berkeley, 2005

[6] Z. Fan, J. C. Ho, "Self-assembly of One-dimensional Nanomaterials for Cost-effective Photovoltaics", International Journal of Nanoparticles, 4, 164 (2011)

[7] "Electrical Appliance Typical Energy Consumption Table", http://www.chabotspace.org/assets/BillsClimateLab/Electrical%20Appliance%20Typical%20Energy%20Consumption%20Table.pdf

[8] "How to calculate domestic power consumption?" https://dmohankumar.wordpress.com/2012/08/12/how-to-calculate-domestic-power-consumption-fact-file-24/

[9] Vince Lombardi, ed. "A Practical Guide to Solar Power System Design for Homeowners", Version 08.08.12

[10] http://www.solartechnology.co.uk/support-centre/calculating-your-solar-requirments

[11] Hemakshi Bhoye, Gaurang Sharma, "An Analysis of One MW Photovoltaic Solar Power Plant Design", International Journal of Advanced Research in Electrical, Electronics and Instrumentation Engineering, Vol. 3, Issue 1, January 2014

[12] http://www.centsys.co.za/upload/CENTSYS%20Documentation/0_07_B_0133%20120W%20Solar%20Panel%20Specifications%20sheet-29062015-NG.pdf

[13] B. Westover, "Difference between Dry Cells and Wet Cells". http://www.ehow.com/about_6360799_difference-wet-cell-dry-cell_.html#ixzz2rAxAHcmk.

[14] H. Wade,"Solar PV Design Implementation O& M" ,March 31- April 11, 2008

Compared of Surface Roughness Nitride Layers formed on Carbon and Low Alloy steel

Wayan Sujana[1], Komang Astana Widi[2]

Mechanical Engineering Department, National Institute of Technology of Malang, Karanglo Street Km 2, Malang East Java-Indonesia

Abstract— *A comprehensive study of fluidized bed nitriding was performance on a carbon steel (grade AISI St 41) and low alloy steel (grade AISI 4140) at 550 ^0C in 20 % N^2 and 80 % NH^3 atmosphere at a flow rate gasses of 0.7 m^3/hr. Various surface roughness were used to incorporate nitrogen into these steels. The nitride layer formed at AISI 4140 showed better surface roughness and surface hardness than AISI St 41. With low chromium alloy (grade AISI 4140), nitrogen diffusion is more uniform in the lower surface roughness after nitriding process. It has been found that the surface microhardness of the compound layer increases with decreasing surface roughness and chromium alloy contents. The layer nitride has a decrease surface roughness ranging from 50 % at 0,1 µm to about 17 % at 0,5 µm. On the contrary, the carbon steel without chromium alloy (grade AISI St 41) sample show an enhance surface roughness between 1.3 to 2.5 times after nitriding process, but on 0.5 µm surface roughness sample show a decrease surface roughness of about 10%. All sample show an enhanced surface microhardness after nitriding significantly. Chromium alloy is found to enhanced the nitriding efficiency. Without chromium in the steel, a lower surface roughness provides a supplementary amount of implanted nitrogen available for further diffusion, and the uniform of the surface passive oxide. So, with limited surface roughness, more uniform layers with higher amounts of nitrogen can be achieved by low chromium alloy. However, with limited solubility of nitrogen atom in α-Fe into iron nitride form, the nitrogen becomes supersaturated reaction and nitride layer is more brittle and porosity. It is can be ascribed to the nitrogen solubility in the nitride layer, which at AISI St 41 is higher due to the formation of porosity phase while at AISI 4140 a phase rich in nitrogen (Υand ε phases) is formed.*

Keywords— roughness, fluidized bed, nitride layers, microstructures, SEM.

I. INTRODUCTION

Fluidized bed reactor is more effective dan efficient than conventional reactor [1]. Surface roughness plays an important role in improving the quality of a component at the time of its use, especially in the application of cutting tool and sometimes coated parts, electric hardware, automotive component [1,2]. Increase the surface hardness, alter the surface chemistry and to increase the surface roughness are important things to observe the surface modification in nitriding component. Specific characteristics defined surface roughness mentioned above has a close relationship with nature and durability surface roughness. Thereby to increase the life time of cutting tool components generally utilize surface hardening treatment especially thermochemical treatment the right to apply is nitriding because this treatment has the advantage of precision for most components is better than other thermochemical treatments such as carburising, carbonitriding etc. Investigated of surface roughness effects is already discussed [3,4,5].

However, in the nitriding thermochemical treatment which although in the process will include a nitrogen atom (alter the composition of the material) but will not affect the dimensions of the components, so in this study will focus on changes in surface roughness after gas nitriding treatment by utilizing materials with a chemical composition different . And to better focus the composition of concern in this study is the composition of the chromium contained in the specimens.

II. EXPERIMENTAL PROCEDURE

The material used in this study is a type of carbon steel (AISI St 41) which does not have the elements chromium and type of tool steel (AISI 4140) which has the element chromium. Sectioning, grinding and polishing were used for preparation on the surface specimen for identification of surface roughness. Both specimens will be treated the same nitriiding gas namely the fluidised bed reactors at temperatures of 550^0C with the composition of the gas mixture of 20 % N_2 and 80 % NH_3 gas at a flow rate of 0.7 m3 / hr and a process for 4 hours is further cooled by air cooling. Then, will be given the test specimen

surface roughness before and after nitriding treatment. The surface roughness value changes that occur will be correlated with the morphological observation and characteristics of hard nitride layer is formed utilizing microstructure and SEM examination.

III. RESULTS AND DISCUSSION

Table 1 shows the composition ratio of the second test specimen before nitriding treatment. It appears that the AISI St 41 does not contain chromium while the AISI 4140 has a chromium content of up to 1.07 %. Chemical composition content in material especially chrome, which very important influenced the homogeneity of nitride compound layers [8]. In this investigation we will learn more about it, in which the specimens used with and without chrome alloys.

TABLE 1
COMPOSITION OF AISI 4140 AND AISI St 41

Specimen	Conc. (%)				
	C	Si	Mn	Cr	Mo
AISI 4140	0.41	0.34	0.81	1.07	0.19
AISI St 41	0,12	0,25	0,6	-	-

The surface hardness of AISI 4140 of approximately 872 HV after fluidized bed nitriding, it is show that nitride compound layer is formed on the top of surface [8]. This is supported also from the results of testing of the type AISI steel St 41 which has a varied surface roughness on the condition before and after the nitriding process compared to specimens tool steel AISI 4140 (Figure 1). This can be explained that the phase of forming compound layers, when there is nitrogen activity (an) that have lower, so nitrogen solution to the phase is thoroughly, so that phase γ'Fe4N is formed. With nitrogen and carbon content that increase together with higher alloy nitride form composition, it causes balance of forming phase γ'Fe4N is passed, and it causes phase of εfe2-3N is formed. So, phase γ' generally will be located beneath phase of εFe2N [9].

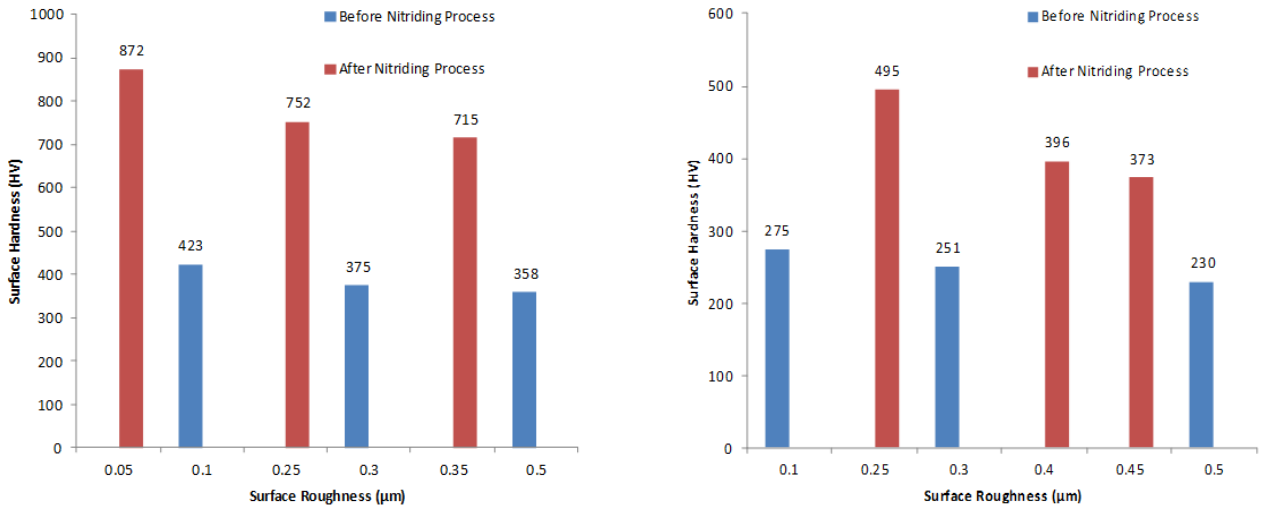

(A) **(B)**

FIGURE 1. COMPARED OF SURFACE ROUGHNESS AND SURFACE HARDNESS ON A) AISI 4140 AND B) AISI ST 41 BEFORE AND AFTER NITRIDING PROCESS

The surface hardness of the different surface zones of a nitrided specimen. The compound layer usually contains pores and britle characteristic have a relatively low surface hardness and poor mechanical properties. If nitrogen atomic content is increased so it passes saturated limit of phase ε formed, so activity of diffused N atoms will supersaturated reactions to form N_2 gas. We can says that the *denitriting* reaction. This reaction product is called porosity, which is showed in figure 2, is effected by saturation with nitrogen element.

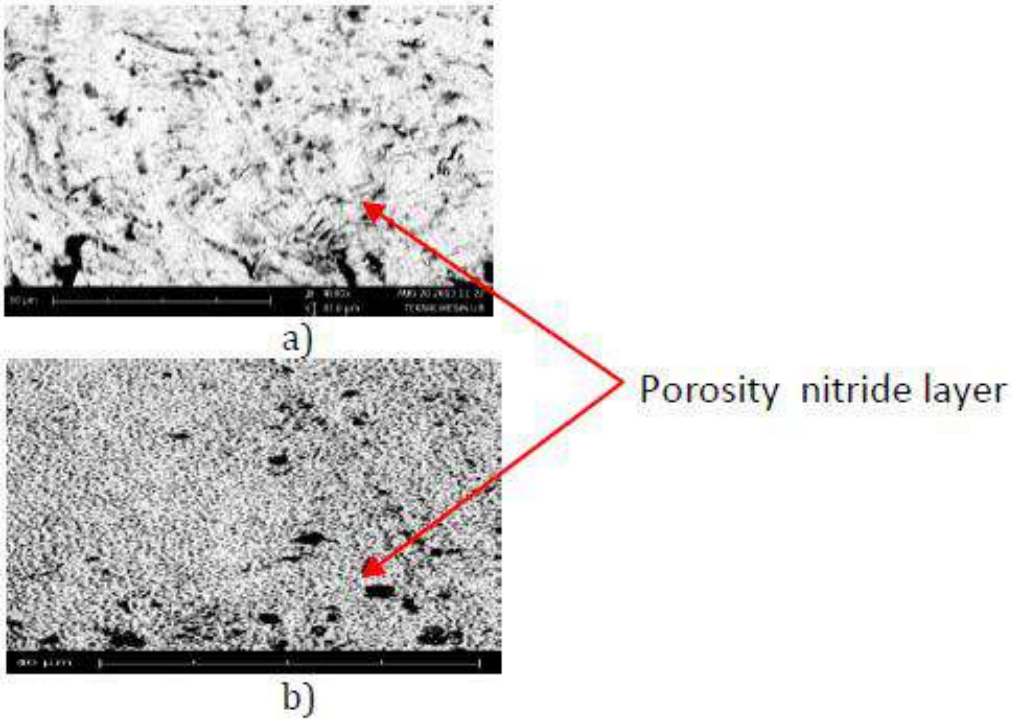

FIGURE 2. SURFACE TOPOGRAPHY A) AISI 4140, B) AISI St 41

Observations on the second specimen after nitriding shows different surface topography where steel AISI St 41 has a surface more uniform micro porosity / homogeneous compared with the type of steel AISI 4140 (Figure 2) . This shows the nitride layer is formed not too loud and very easily detached from the substrate interface as shown in figure 3. The data had a good correlation with the surface hardness and the surface roughness nitride layer, respectively. Brittle surface nitride compound layer depend on nitriding treatment technology [7]. It is shown in this observation in which the compound nitride layer large amount of spalling.

Brittle nitride compound layer formed in this treatment can be mechanically removed conventionally by grinding. It is shows that fluidized bed nitriding treatment can produces only diffusion layer without formation of the compound layer.

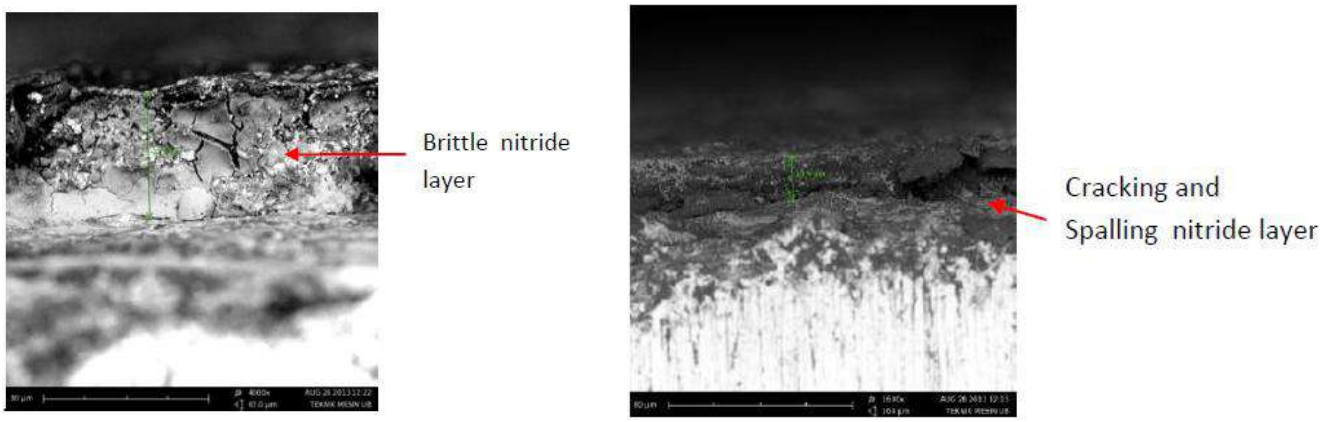

(A) **(B)**

FIGURE 3. NITRIDE LAYER OF AISI St 41 A) BRITLENESS B) SPALLING

Surface hardness will increase with decreasing surface roughness values. An increase in surface roughness as a result of the formation porosity which is nitrogen atom solubility is very high on the surface. It is also supported by solubility limitations of the alloying element especially chrome element.

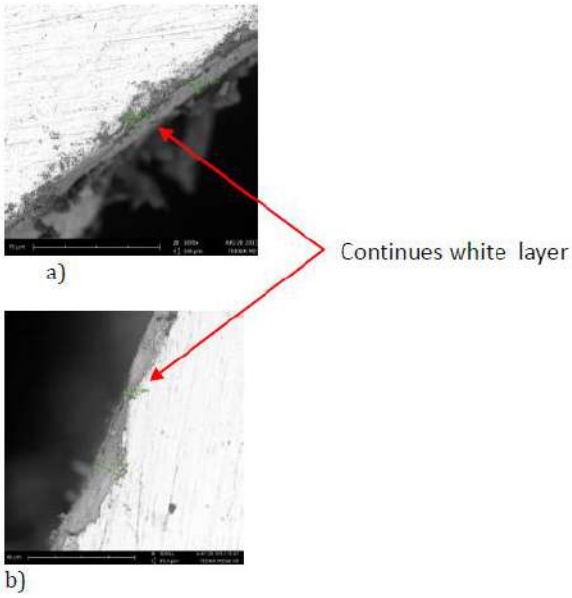

FIGURE 4. SURFACE MORPHOLOGY OF AISI 4140 WITH SURFACE ROUGHNESS a) 0,1 µm AND b) 0,5 µm

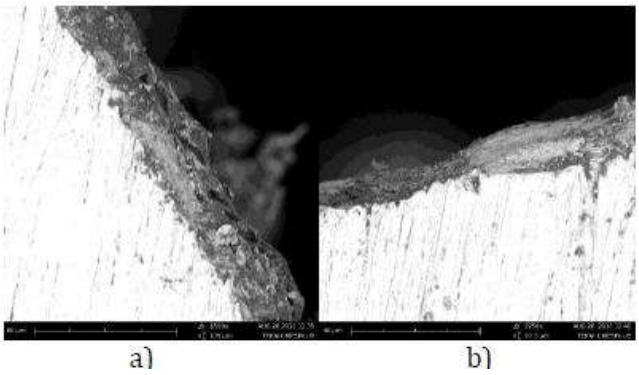

FIGURE 5. SURFACE MORPHOLOGY OF AISI St 41 WITH SURFACE ROUGHNESS a) 0,1 µm and b) 0,5 µm

Figures 4 and 5 show the cross section of the test specimen which shows the homogeneity of the layer formed nitride layer on the tool steels with chromium content of 1.07 % is smooth with the test results an average surface roughness of 0.1 µm while the carbon steel type AISI St 41 in which do not have the element chromium showed a greater surface roughness that is about 0.5 µm. This was evident in the results of the comparison test specimen microstructure is shown in Figure 6. In addition to this, decreasing in the surface roughness by chrome content in low alloy steel will improved surface hardness. But, non-continuity of porosity on low alloy nitride compound layer which occurs by denitriding reaction must be considered.

SURFACE ROUGHNESS (µM)	MATERIALS	
	AISI 4140	AISI ST 41
0,1		
0,3		
0,5		

FIGURE 6. COMPARE OF CROSS SECTION MICROSTRUCTURE ON AISI 4140 AND AISI St 41 AFTER NITRIDING PROCESS

The presence of the element chromium nitriding process is very important in producing nitride layer morphology and characteristics. The formation of chromium and nitrogen reaction will give a better bond to the nitride layer with a lower

level of porosit . Role elements besides chromium forms a bond with the N to form a nitride layer membeantu also reduce the release into the atmosphere of N atoms (reaction supersaturated) so that porosity can be minimized. This shows the ability of chromium is better to increase the wear resistance performance than Fe element in the process nitridisasi.

IV. CONCLUSION

An investigation of the effects of surface roughness on carbon and low alloy steel after nitriding fluidised bed process has been done. We can conclude that the enhanced energetic nitrogen atoms would absorb at the steel surface and then diffuse faster into the matrix. Therefore, then nitriding depth in the diffusion layer is more significant form alloy steel (AISI 4140) with hardness between 715 – 872 HV compared with carbon steel (AISI St 41) with the surface hardness just only about 373 – 495 HV after nitriding fluidized bed process. This result indicated that the diffusion rate of nitrogen atoms in alloys steel was much higher than that in carbon steel. A large amount of continues porosity in nitride compounds layers was when carbon steel was used in fluidized bed nitriding treatment and they caused surface roughness.

ACKNOWLEDGEMENTS

The author thanks the supports given by BPPS foundation from DIKTI and Materials Laboratory, Mechanical Engineering Department at ITN Malang.

REFERENCES

[1] R. W. Reynldson, Case Studies On The Use Of Fluidised Beds For The Heat Treatment of Metals, Heat Treatment in FluidisedBed Furnaces, ASM, 1993.

[2] E. Çelik, O. Çulha, B. Uyulgan, N.F. Ak Azem, I.Özdemir and A. Türk, "Assessment of microstructural and mechanical properties of HVOF sprayed WC-based cermet coatings for a roller cylinder," Surface & Coatings Technology, SCT-11323, 2005.

[3] Gajendra Prasad Singh[a], J. Alphonsa[b,], P.K. Barhai[a], P.A. Rayjada[b], P.M. Raole[b], S. Mukherjee[b], Effect of surface roughness on the properties of the layer formed on AISI 304 stainless steel after plasma nitriding, Surface and Coatings Technology, Volume 200, Issues 20–21, 22 May 2006, Pages 5807–5811.

[4] Khyoupin KhoO, Manabu Takeuchi, Jin Onuki, and Takao Komiyama, Improvement of the Surface Layer of Steel Using Microwave Plasma Nitriding, materials Transactions, Vol. 45, No. 3 (2004) pp. 942 to 946, 2004 The Japan Institute of Metals, Express Regular Article.

[5] Ş. Ekinci1, A. Akdemir and M.T.Demirci, Effect of Surface Roughness of Salt Bath Nitrided AISI 4140 to the Wear Rate, 6th International Advanced Technologies Symposium (IATS'11), 16-18 May 2011, Elazığ, Turkey

[6] K. A. Widi, I.N.G. Wardana, W. Sujana, *The effect of Chemical Compositions of Tool Steel On TheLevel of White Layers Homogeneity and The Surface Hardness*, International Journal of Materials, Mechanics and Manufactureing, May 2013, Vol I No 2.

[7] Insup Lee, Yong-Ho Park and Ikmin Park, The Characteristics of Surface Layers Produced On SKD 61 Steel By Plasma Radical Nitriding Compared With Conventional Plasma Ion Nitriding, Solid State Phenomena Vol. 118 (2006) pp 155-160, Trans Tech Publications, Switzerland, doi:10.4028/www.scientific.net/SSP.118.155.

[8] Widi K.A., Wardana I.N.G., Suprapto W., Irawan Y.S., (2016), The Role of Diffusion Media in Nitriding Process on Surface Layers Characteristics of AISI 4140 with and without Hard Chrome Coatings, *Tribology in Industry*, Vol. 38, No. 3 308-317.

[9] E. Haruman, Y. Sun, H. Malik, AG.E. Sutjipto, K. Widi, *Low Temperatur Nitriding of Austenitc Stainless Steel*, The 3 Asian Conference on Heat Treatment of Materials, Nov. 10-12 Gyeongiu, Korea, 2006

[10] J. Breckling, Ed., *The Analysis of Directional Time Series: Applications to Wind Speed and Direction*, ser. Lecture Notes in Statistics. Berlin, Germany: Springer, 1989, vol. 61.

[11] S. Zhang, C. Zhu, J. K. O. Sin, and P. K. T. Mok, "A novel ultrathin elevated channel low-temperature poly-Si TFT," *IEEE Electron Device Lett.*, vol. 20, pp. 569–571, Nov. 1999.

The influence of impregnating chemicals on the carbonization process of viscose fiber cloths

Bui Van Tai[1], Nguyen Hung Phong[2], Tran Van Chung[3]

Institute of Chemistry and Material, 17 Hoang Sam, Cau Giay, Hanoi

Abstract**—** *The influence of some chemical impregnating such as polyphosphate urea, $ZnCl_2$, $AlCl_3$, $FeCl_3$, H_2NaPO_4, H_3PO_4 on the carbonization process of viscose fiber cloth at the temperature range from 30 to 700 ^0C was studied in detail. By the thermalgravimetric analysis, the obtained results have showed that the presence of these chemical impreganating agents caused lowering the activation energy and increasing the carbonization viscose mass left at 700^0C. The polyphosphate urea was proven to be a good chemical agent for the carbonization process.*

Keywords**— Viscose fiber, TGA, carbonization process.**

I. INTRODUCTION

Activated carbon such as powdered or granular forms is well known owing to its widespread application in many fields as a exellent adsorbent for purification, remediation of wastewater and toxic gas generated in industry [1-4]. In the recent years the activated carbon fiber cloths have receive an increasing concern because they exhibit a comparative advantages over the traditional activated carbon, including their application in high technological inovation as use in cell therapy as a support for stem cell growth [5]. Besides, activated carbon fiber cloths belong to the light stable materials with the higher surface area and pore volume that are easily used in different objectives [5]. The activated carbon fiber cloths are resulting from two main processes including physical or thermal and chemical activation [5]. Physical activation involves two stages such as pyrolysis of the fabric used as a precursor, then followe gasifiction with and oxidizing gas like steam or carbon dioxide [6]. On the other hand, the chemical activation process used for preparation of activated carbon cloths consists of (i) impregnation of the precursor with a Lewis acid such as $ZnCl_2$, $AlCl_3$, H_3PO_4, (ii) pyrolysis of the impregnated precursor, (iii) washing of the obtained product to eliminate the remaining impregnating chemicals before it is allowed to dry. However, in the pyrolysis process there are two steps. The former step is precursor carbon fiber cloth cabonized to remove hydrate and volatile substance, while, the latter is a process of carbonized fiber cloth is activating. The practice has indicated that the role of impregnating agents is essential issues in preparation of carbonization carbon fiber cloths [4]. In this aricle, the influence of impregnating agents such as $FeCl_3$, $AlCl_3$, $ZnCl_2$, Na_2HPO_4, H_3PO_4, polyphosphate urea on the chemical the carbonzation process of viscose fiber cloth was studied in detail. It includs their influence on the main factors about kinetics and thermdynamics of carbonization process. The influence of the impregnating agent on carbonizing process was determined based on the kinetics analysis, using thermogravimetric analysis (TGA) and Kissinger equation.

Kinetics backgroud

Carbonization is a conversion of an organice substance in to carbon or a carbon- containing reidue through pyrolysis [7,8]. The carbonization reaction under thermal decomposition may take play as follows:

$$(C_6H_{10}O_5)_n \text{ (solid)} \xrightarrow{Activatedccomp.} \longrightarrow C_m \text{ (solid)} + n\ H_2O \text{ (gas)}$$

According to the thermal decomposition preocess the conversion reaction rate is generally presented as following:

$$\frac{d\alpha}{dt} = k(T)\, f(\alpha) \tag{1}$$

Here α is the extent of conversion at decomposition time t; k is the reaction rate constant; f (α) is the reaction mechanism function. The $\frac{d(\alpha)}{dt}$ is the conversion rate at a ceatain temperature, therefore the parameter k is obtained from the Arrhenius expression as follows:

$$k(T) = Ae^{-\frac{Ea}{RT}} \tag{2}$$

When the reaction temperature varying with the heating rate of $\beta = dT/dt$, the constant k(T) is given in (3):

$$k(T) = \frac{A}{\beta} e^{-\frac{Ea}{RT}} \quad (3)$$

Where A is the pre-exponenttial factor (mim^{-1}), E_a is the apparent activation energy (kJ. mol^{-1}), R is the gas constant (8.314 kJ. $mol^{-1}.K^{-1}$), T is the absolute temperature (K). Combining exppression (1) and expression (3) resulting in expression (4):

$$\frac{d(\alpha)}{dt} = \frac{A}{\beta} e \frac{-E_a}{RT} f(\alpha) \quad (4)$$

Denoting:

$$\frac{d\alpha}{dt} = \frac{d\alpha}{dT}\frac{dT}{dt} \quad (5)$$

and

$$g(\alpha) = \frac{A}{\beta}\int_0^T e^{-\frac{Ea}{RT}} dT \quad (6)$$

According to Coats-Redferm [9 -11], through intergating the equation (6) we obtained the following expression:

$$\ln\left[\frac{g(\alpha)}{T^2}\right] = \ln\left[\frac{d\alpha}{dt}\right] = \ln\left[\frac{AR}{\beta E}\left(1 - \frac{2R\bar{T}}{E}\right)\right] - \frac{E}{RT} \quad (7)$$

Eq. (2), Eq. (4) and (7) are the fundamental expressions of analytical methods used to calculate kinetic parameters on the basis of TGA data. Here, the activation energy and the pre-exponential factor, reaction constant and entropy would be determined from the slope and the ordinate of theo linear plot of $\ln[\frac{d\alpha}{dt}]$ versus 1/TP at a certain rating rate β (^{0}C/min).

Thay are:

$E_a = -\text{tg}\,\gamma \times R$ with tg γ is slope value of the linear plot,

$$A = \frac{e^b \times \beta \times E_a}{R\left(1 - \frac{2R\bar{T}}{E_a}\right)}, \quad b = \ln\left[\frac{AR}{\beta E_a}\left(1 - \frac{2R\bar{T}}{E_a}\right)\right],$$

$$k = A e^{-\frac{Ea}{RT}}, \qquad A = \left(\frac{k_b T}{h}\right) e^{\frac{\Delta S}{R}}$$

Here k_b is Boltzmann constant, and h is Plank constant. From here other parameters would be calculated by this way:

$$\Delta H = E + (\Delta n - 1)\,RT, \text{ with } \Delta n = -2,$$

$$\Delta H = E - 3RT, \qquad \Delta G = \Delta H - T.\Delta S$$

II. EXPERIMENTAL PROCEDURE

2.1 Chemicals:

- Viscose fiber cloth made in Japan.
- H_3PO_4 (Analytical purity) from China.
- NaH_2PO_4 (Analytical purity) from China.

- Urea (Analytical purity) from China.
- $AlCl_3$ (Analytical purity) from China.
- $FeCl_3$ (Analytical purity) from China.
- $ZnCl_2$ (Analytical purity) from China.

2.2 Apparatus

TA Instruments TGA 2950 Thermogravimetric Analyzer, USA and 409 PC NETSZCH , GERMANY

2.3 Experimental procedure

2.3.1 Cloth samples

The cleaned viscose fiber cloth samples were cut off in small speces in size of 20 x 30 cm. The solutions suitable for impregnation of precursor (cleaned viscose fiber cloth) were prepared by the dissolution of these reagents in distilled water. The viscose fibers were impregnated in each impregnating chemical solution with the certain time, then after dried at ambient temperature to remove water, was taken to analyze by thermogravimetric analysis (TGA).

III. RESULTS AND DISCUSSION

3.1 Thermogravimetric analysis (TGA)

3.1.1 The thermogravimetric analysis (TGA) of precusor material (viscose fiber cloth)

The TGA precursor denoted M(0) was carried out under nitrogen atmosphere and in the temperature range from 30 to 700^{0}C with the hating rate 5^{0}C/min. The TGA of viscose fiber cloth is present in Figure 1.

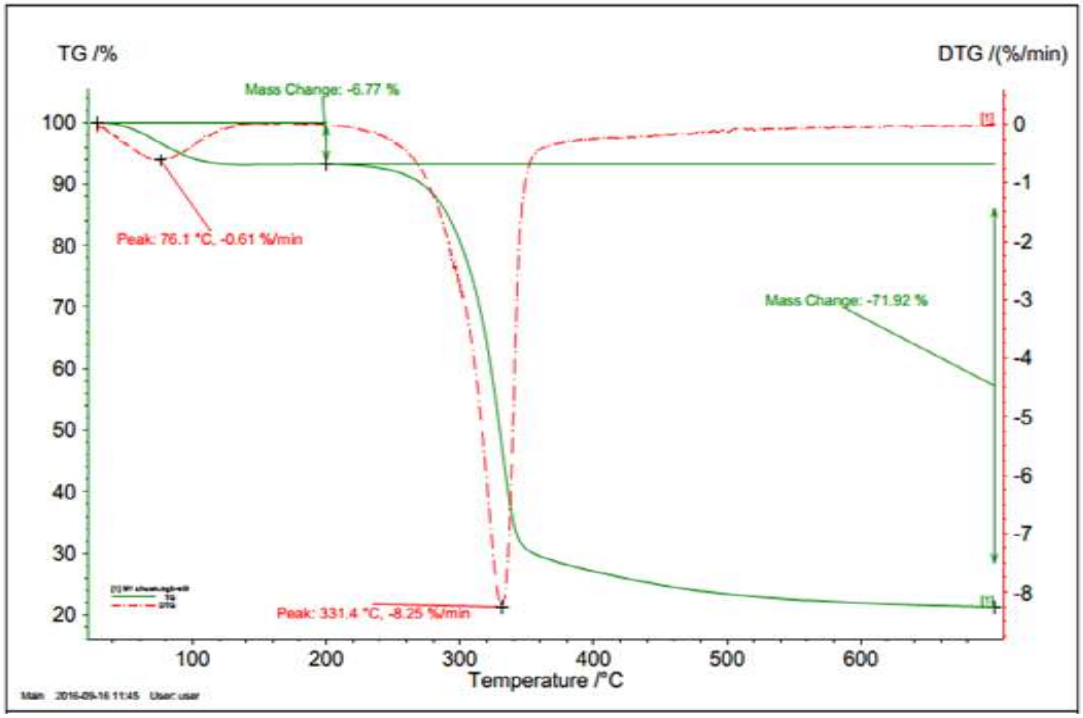

FIGURE 1. TGA CURVE OF THE EXPERIMENT A VISCOSE FIBER CLOTH

The figure 1. shows TGA of viscurse untreated with impregating chemical that when at the temperature < 135^{0}C there was a weight loss of 6.77% due to removing water from fiber surface, from 135 to 300 ^{0}C, the weight loss is due to the removing water within fiber, at 300^{0}C the weight loss reach to 20%. The carbonization of fiber was carried out in the temparature range from 300 to 360^{0}C with the weight loss of about 50%. The carbonization continued to 700^{0}C with the fiber mass remaining in 20 %. According to [8] during carbonization process, thermal decomposition of raw materials eliminates non-carbon elements such as oxygen, hydrogen and nitrogen lead to a carbon skeleton (char) with a rudimentary pore structure.

3.1.2 The thermogravimetric analysiz (TGA) of viscose fiber cloth impregnated by polyphosphate urea solution of 5% (wt/v), M(1)

The before carbonization, the viscose fiber cloth was impregnated in 5% (wt/v) -polyphosphate urea for the certain time at room temperature. The influence of the polyphoshate urea as impregnating chemical on the carbonization process of this sample was determined by TGA curve (figure 2). Process of this carbonization was carried out under the condition with the temperature range from 30 to 700^{0}C and the hating rate of 5^{0}C/min, atmosphere of nitrogen.

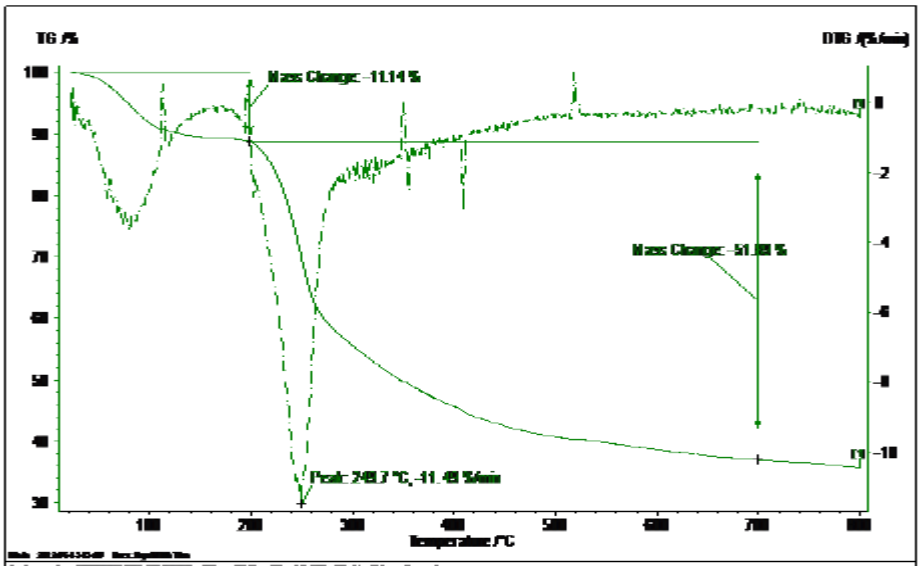

FIGURE 2. TGA CURVE OF THE EXPERIMENTAL VISCOSE FIBER CLOTH CLOTH IMPREGNATED IN 5% SOLUTION POLYPHOSPHATE UREA

The figure 2. shows TGA of viscurse with impregating chemical (polyphosphate urea 5% wt/v) that when at the temperature < 110^{0}C there was a weight loss of 11.14 % due to removing water from fiber surface, from 110 to 200 ^{0}C, the weight loss is due to the removing water within fiber. At the temperature range from 200 to 700^{0}C the weight remaining in 39 %. This value of the pregnating viscose fiber cloth is higher than of those precursor (20%).

An experiment of carbonization of viscose fiber cloth impregnated in 5% $ZnCl_2$, M(2) solution, its TGA was present in figure 3.

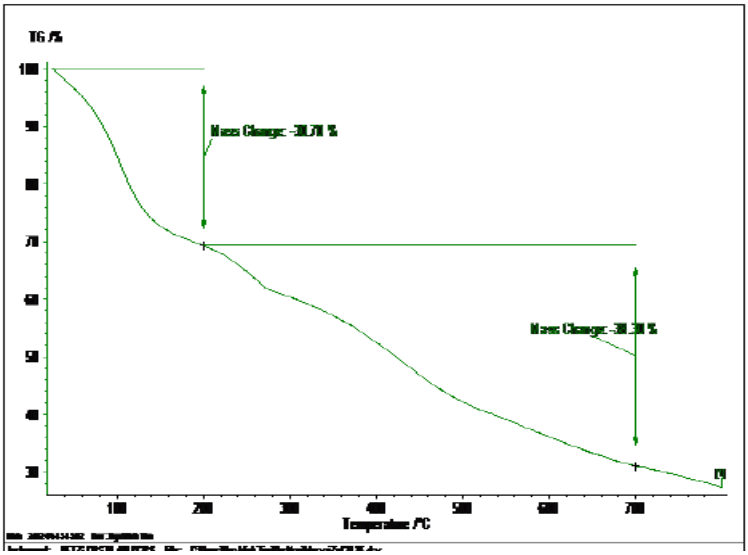

FIGURE 3. TGA CURVE OF THE EXPERIMENTAL VISCOSE FIBER CLOTH IMPREGNATED IN 5% SOLUTION $ZNCL_2$

Here, the weight loss of about 20% at the temperature < 180^{0}C and the viscose fiber cloth left of about 30% at 700^{0}C were

observed.

Other experimants of the viscose fiber cloth were impregnated in the different pregnating solutions such as 5% $FeCl_3$ M(3); 5% Al Cl_3, M(4), 5% Na_2HPO_4 M(5); 5% axit H_3PO_4 M(6) to continue investigating the influence on the carbonization. The TGA curves of these samples were present in figure 4.

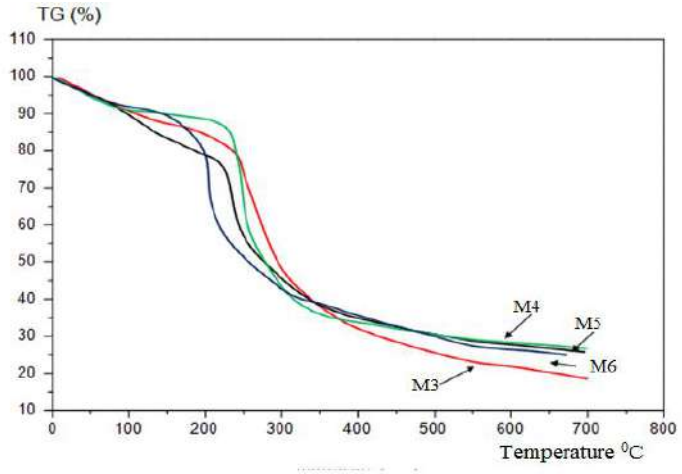

FIGURE 4. TGA CURVES OF THE EXPERIMENTAL VISCOSE FIBER CLOTH IMPREGNATED IN 5% SOLUTIONS OF $FeCl_3$, M(3); $AlCl_3$, M(4); Na_2HPO_4,M(5); H_3PO_4 M(6).

Here, analogy with the M(2) the their weight loss of about 30% at the temperature < 180^{0}C and their viscose fiber cloth mass left of about from 25 to 28 % at 700^{0}C were observed. Studing the imfluence of the impregnating chemcals on the carbonization process of the viscose fiber cloth as suggested above, the carbonizating temrperature of these samples was slower than of the precursor. Besides, the weight mass left at 700^{0}C was higher than of precursor, in which for the polyphosphate urea impregnated sample, the weight mass left was 39%, the highest value comparing with other impregnating agents. The highest weight mass left of viscose fiber cloth at 700^{0}C relating with polyphosphate urea can be illustrated in [9]. According to this author the two negatively charged oxygen atoms in phosphate ion can align themselves adjacent to similar atoms accociated with the cellulose molecule. This occurs most readily with the HPO_4^{2-}ion, explaining why it is so effective as a retardant in this system. A part from that, the attachment of two adjaent HPO_4^{2-}ion on a cellulose molecule enables water to be eliminated between them on thermal treatment, thus providing a protective skin for various part of the internal structure.

3.2 Influence of chemical impregnating agents on carbonization of viscose fiber cloth

3.2.1 The influence of chemical impregnating agents on carbonization temperature

The influence of chemicalc agents on carbonization process of viscose fiber cloth was determined through carbonization temperature: initial T(i) and final T(f), the temperature range T(f) – T(i), the fiber cloth weight m (i) at begining T(i) and m(f) at ending T(f) and $T_{1/2}$ the temperature corresponding the fiber cloth weight left in 50% in carbonizing process. From the obtained TGA curves the influence of chemical agents on carbonizing process of viscose fiber cloth were present in table 1.

TABLE 1
INFLUENCE OF CHEMICAL AGENTS ON CARBONIZATION

Samples	$T_{(i)}$(^{o}C)	$m_{(i)}$ (%)	$T_{(f)}$ (^{o}C)	$m_{(f)}$ (%)	T½ (^{o}C)
M0 (unimpregnated)	300	86	360	20	340
M1(with 5% Polyphosphate urea)	220	89	700	39	270
M2 (with 5% $ZnCl_2$)	200	74	700	25	270
M3(with 5%$FeCl_3$)	250	86	650	25	350
M4 (with 5% $AlCl_3$)	240	85	700	28	280
M5 (with 5% Na_2HPO_4)	230	88	700	26	350
M6 (with 5% H_3PO_4)	210	89	700	25	300

The obtained data from the table 1. indicate that the presence of chemical impregnating agents cause lowering the carbonization beginning temperture (T(i) and elevating the carbonation final temperature comparing with the precursor-unimpregnated viscose fiber cloth. This was explained the interaction betweent chemical agents with cellulose mollecules on their surface.

3.2.2 The influence of chemical impregnating agents on kinetics

Basing on the TGA curves of the viscose fiber cloth unpregated pregnated by chemical agents, the plots of $\ln\frac{d\alpha}{dt}$ vs. $\frac{1}{T}$ were determined present in figure 5.

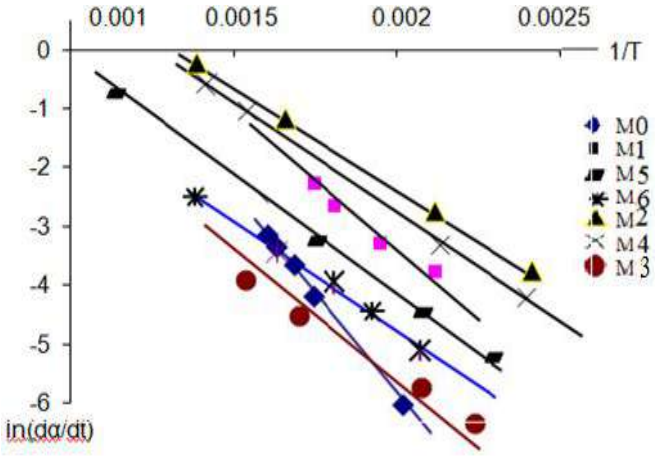

FIGURE 5. THE PLOTS OF $\ln\frac{d\alpha}{dt}$ VS. $\frac{1}{T}$

From the plots of $\ln\frac{d\alpha}{dt}$ vs. $\frac{1}{T}$ the kinetic parameters of the linear equation (7) such as activation energy, pre-exponential factor and rate constant, were determined present in table 2.

TABLE 2
THE KINETIC PARAMETERS OF CARBONIZATION PROCESS

Samples	E_a (kJ/mol)	pre-exponential factor A(s^{-1})	Rate constant
M0	63.8	$1.65x10^{11}$	$k = 1.65x10^{11}.e^{\frac{-63,81}{RT}}$
M1	28.4	$2.38x10^{8}$	$k = 2.38x10^{8}.e^{\frac{-28,4}{RT}}$
M2	20.7	$5.51x10^{7}$	$k = 5.51x10^{7}.e^{\frac{-20,7}{RT}}$
M3	22.7	$3.28x10^{8}$	$k = 31.28x10^{8}.e^{\frac{-22,5}{RT}}$
M4	17.3	$1.57x10^{8}$	$k = 1.57x10^{8}.e^{\frac{-17,3}{RT}}$
M5	25.3	$2.87.10^{8}$	$k = 2.87x10^{8}.e^{\frac{-24,73}{RT}}$
M6	20.2	$7.31x10^{7}$	$k = 7.31x10^{7}.e^{\frac{-19,05}{RT}}$

The obtained data showed that the presence of chemical impregnating agents cause lowering the activation energy of carbonization process. These results were fitted the work [x]

3.2.3 Effect of heating rate on the carbonization process of polyphosphate urea impregnated viscose fiber cloth

The experimental data have indicated the advantages of the polyphosphate urea impregnating on viscose fiber cloth, therefore a study of Influence of heating rate on the carbonization process of polyphosphate urea impregnated viscose fiber cloth was carried out. This effect was present in the figure 6.

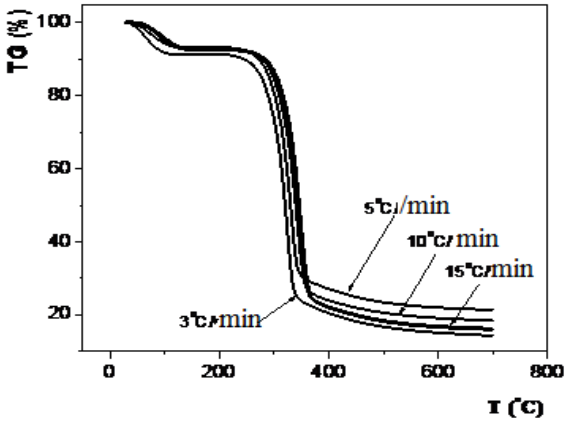

FIGURE 6. THE EFFECT OF HEATING RATE ON CARBONIZATION PROCESS

Basing on the obtained TGA curves, the influence of heating rate on kinetic parmeters of carbonization prcess of polyphosphate urea impregnated viscose fiber cloth were present in table 3.

TABLE 3
INFLUENCE OF THE HEATING RATE ON CARBONIZATION PROCESS

Heating rate β ^{0}C/min	pre-exponential factor A(s^{-1})	E_a (kJ/mol)	Rate constant
3	$2.6.10^7$	28.91	$k = 2.6x10^7.e^{\frac{-28,91}{RT}}$
5	$4.5x10^7$	28.87	$k = 4.5x10^7.e^{\frac{-28,87}{RT}}$
10	$9.1x10^7$	28.78	$k = 9.1x10^7.e^{\frac{-28,78}{RT}}$
15	$1.2x10^8$	28.69	$k = 1.2x10^8.e^{\frac{-28,69}{RT}}$

The obtained results showed that the heating rates increasing cause the pre-exponent coeffients increasing and activation energy decreasing lightly. The pronounced increase of pre - exponential factor can promote the reaction rate increasing like suggested by [4].

3.2.4 The influence of chemical impregnating agents on thermodynamics

Basing on the equation (7) combining with the experimental data, the change in entropy, enthalpy and Gibbs free energy corresponding to the carbonization process were calculated present in table 4.

TABLE 4
THE INFLUENCE OF CHEMICAL IMPREGNATING AGENTS ON THERMODYNAMICS

Samples	ΔS (kJ/mol.K)	ΔH (kJ/mol)	ΔG (kJ/mol)
M0	0.186	58.60	-58.62
M1	0.132	24.20	-45.60
M2	0.122	15.44	-54,60
M3	0.163	17.15	-84.42
M4	0.147	20.21	-72.60
M5	0.109	12.49	-50.23
M6	0.120	16.39	-51.25

The obtained experimental data the carbonization process proceed spontaneously corresponding to $\Delta S > 0$, $\Delta G < 0$. In this case of $\Delta S > 0$ indicating a thermal decomposition reaction of viscose fiber might occur with non structured activated complex comparing with the initial reactants. This can be suggested that the carbonization reaction is classified as fast [8]. The obtained experimental data from table 4 show that the presence of chemical agents such as polyphosphate urea, $ZnCl_2$, $FeCl_3$, $AlCl_3$, Na_2HPO_4 and H_3PO_4 cause a change in ΔS, ΔH and ΔG, however, all thermodynamic parameters indicating the carbonization process is endothermic reaction occurring spontaneously.

IV. CONCLUSION

The study of the influence of chemical impregnating on viscose fiber cloth was carried out in detail. The chemical impregnating agents such as polyphosphate urea, $ZnCl_2$, $FeCl_3$, $AlCl_3$, Na_2HPO_4 and H_3PO_4 have been used as chemical agents for carbonization process of viscose fiber cloth. The presence of these agents might cause the change in the mass of viscose fiber remaining after carbonization at temperature from 30 to 700^0C. The carbonization process of viscose fiber occurred spontaneously and along endothermic reaction. The main effect of chemical agents is to lowering the carbonization temperature of impregnated viscose fiber comparing with precursor. The chemical agent as polyphosphate urea was proven with the most effective advantage in carbonization of viscose fiber with the highest mass left reached to 39%.

REFERENCES

[1] T. J. Bandosz, Activated Carbon Surfaces in Environmental Remediation, Academic Press, 2006.

[2] G.Mezohegyi, et. al Fabregat, "Towards advanced aqueous dye removal processes: a short review on the versatile role of activated carbon, "Journal of Environmental Management, vol.102, pp.148–164, 2012.

[3] J. Rivera-Utrilla et. al "Activated carbon modifications to enhance its water treatment applications. An overview", Journal of Hazardous aterials, vol.187, pp.1–23, 2011.

[4] Ana Lea Cukierman, Development and Environmental Applications of Activated Carbon Cloths. Chemical Engineering Volume 2013, Article ID 261523,31pages

[5] A. Linares-Solano and D. Cazorla-Amor´ os, "Adsorption on activated carbon fibers," in Adsorption By Carbons, E.J. Bottani and J.M.D.Tasc´ on, Eds., Chapter 17, pp.431–449, Elsevier, Oxford, UK, 2008.

[6] F. Rodr´ıguez-Reinoso, "Production and applications of activated carbons," in Handbook of Porous Solids, F.Sch¨ uth, K. S. W.Sing, and J. Weitkamp, Eds., Chapter 4,8,1, pp.1766–1827, Wiley-VCH, Weinheim, Germany, 2002.

[7] Tao Wang, et al. Kinetics of Thermal Degradation of Viscose Fiber and Fire Retardant Viscose Fiber, Journal of Engineered Fibers and Fabrics Volume 9, Issue 2 – 2014.

[8] Sevdalina Turmanova, Kinetics of Nonisothermal Degradation of Some Polymer Composites: Change of Entropy at the Formation of the Activated Complex from the Reagents, Journal of Thermodynamics Volume 2011, Article ID 605712, 10 pages.

[9] P. Budrugeac and E. Segal, "Some methodological problems concerning nonisothermal kinetic analysis of heterogeneous solid-gas reactions," International Journal of Chemical Kinetics, vol. 33, no. 10, pp. 564–573, 2001.

[10] A. Ruvolo-Filho and P. Curti, "Chemical kinetic model and thermodynamic compensation effect of alkaline hydrolysis in waste poly(ethylene terephtalate) in non-aqueous ethylene glycol solution," Industrial and Engineering Chemistry Research, vol. 45, no. 24, pp. 7985–7996, 2006.

[11] D.S.Dias, et al Non-isothermal decomposition kinetics of the interaction of poly(ethylene terephthalate) with alkyd varnish," Journal of Thermal Analysis and Calorimetry, vol. 94, no. 2, pp. 539–543, 2008.

Hand Gesture Recognition from Surveillance Video Using Surf Feature

Dona Merin Joy[1], Dr. M.V Rajesh[2]

[1]M.tech-student, College of Engineering Poonjar, Kerala, India
[2]Department of Electronics & Communication, College of Engineering Poonjar, Kerala, India

Abstract— *The Sign language is very important for people who have hearing and speaking deficiency. It is the only mode of communication for such people to convey their messages. In this paper, a feature detection scheme is introduced called SURF, which stands for Speeded Up Robust Features. The real time images will be captured first and then stored in directory and on recently captured image and feature extraction will take place to identify which sign has been articulated by the user through SURF algorithm. A Text to Speech conversion is also included in this project. An experimental result shows that the proposed approach performs well with low time.*

Keywords— speeded up robust feature, Convolutional neural network, Text to speech, Deep dynamic neural network.

I. INTRODUCTION

In recent years, human action recognition has drawn increasing attention of researchers, primarily due to its potential in areas such as video surveillance, robotics, human computer interaction, user interface design, and multimedia video retrieval.

The works on video based action recognition focused mainly on adapting hand-crafted features [1],[2],[3] .These methods usually have two stages, an optional feature detection stage followed by a feature description stage. Well known feature detection methods are Harris3D[4],Cuboids[5],and Hessian3D[6].For descriptors, popular methods are Cuboids[7] , HOG/HOF[4] , HOG3D[8] and Ex-tended SURF[4] . In the recent work of Wang et al. [9], dense trajectories with improved motion based descriptors and other hand crafted features achieved state of the art results on a variety of datasets. Based on the current trends, challenges and interests with in the action recognition community, it is to be expected that many successes will follow.

However, the very high dimensional and dense trajectory features usually require the use of advanced dimensionality reduction methods to make them computationally feasible. The best performing feature descriptor is dataset dependent and no universal hand engineered feature that outperforming all others exists. This clearly indicates that the ability to learn dataset specific feature extractors can be highly beneficial and further improve the current state of the art. For this reason, even though hand crafted features have dominated image recognition in previous years, there has been a growing interest in learning low level and mid level features, and either in supervised, unsupervised, or semi supervised settings. Since the recent resurgence of neural networks invoked by Hinton et al. [14], deep neural architectures have become an effective approach for extracting high level features from data.

In the last few years deep artificial neural networks have won numerous contests in pattern recognition and representation learning. Schmidhuber [15] compiled a historical survey compactly summarizing relevant works with more than 850 entries of credited papers. From this overview we see that these models have been successfully applied to aplethora of different do-mains, the GPU based cudaconvnet implementation [16], also known as AlexNet, classifies 1.2 million high resolution images into 1,000 different classes. Multi column deep neural networks [17] achieve near human performance on the handwritten digits and traffic signs recognition benchmarks. 3D convolutional neural networks recognize human actions in surveillance videos. Deep belief networks combined with hidden Markov models for acoustic and skeletal joints modeling outperform the decade dominating paradigm of Gaussian mixture models (GMM) in conjunction with hidden Markov models. Multimodal deep learning techniques were also investigated to learn cross modality representation, for instance in the context of audio visual speech recognition. Recently Baidu Research proposed the Deep Speech system that combines a well optimized re-current neural network (RNN) training system, achieving the lowest error rate on a noisy speech dataset. Across the mentioned research fields, deep architectures have shown great capacity to discover and extract higher level relevant features.

Gestures are basically the physical action forms performed by Gestures are basically the physical action form performed by a per-son to convey some meaningful information. Gestures are a powerful means of communication among humans. In fact

gesturing is so deeply rooted in our communication that people often continue gesturing when speaking on the telephone. There are various signs which express complex meanings and recognizing them is a challenging task for people who have no understanding for that language. Sign language is categorized in accordance to regions like Indian, American, Chinese, Arabic and researches on hand gesture recognition, pattern recognitions, image processing have been carried by supposedly countries as well to improve the applications and bring them to the best levels. This Gesture recognition system can be further used in many application like home automation, banking, Robotics like autonomous robot to test its usability in the context of a realistic service task, smart watches. We can control application like Air Conditioner, TV, Mixer, Fan, Lights, etc. through gesture without use of switch. Even by using special image compression method, we can reduce the recognition time and design the specific chip for the same.

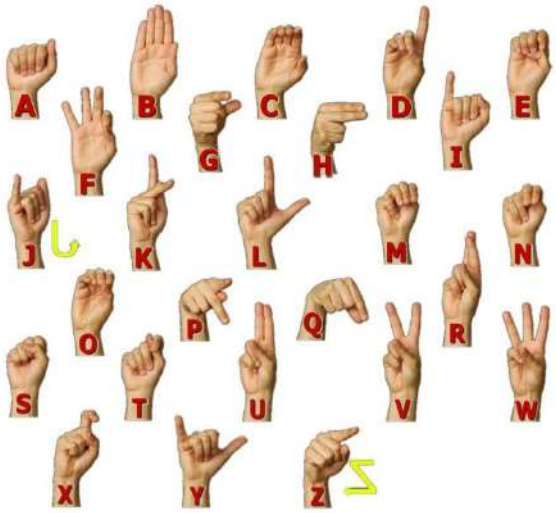

FIGURE 1: THE DIFFERENT SIGN LANGUAGES

In this paper, we have SURF feature that is speeded up robust features which is a patented local feature detector and descriptor. It can be used for tasks such as object recognition, image registration, classification or 3D reconstruction. It is partly inspired by the scale invariant feature transform (SIFT) descriptor.

To detect interest points, SURF uses an integer approximation of the determinant of Hessian blob detector. The standard version of SURF is several times faster than SIFT and claimed by its authors to be more robust against different image transformations than SIFT. We are also converting the detected gesture in to audio using Text To Speech.

II. METHODOLOGY

The Hand Gesture Recognition using surf feature consists of Training and Testing videos. The training videos extracted as training frames and Testing video is extracted as testing frame. After the preprocessing step we are finding the best match of test image with training images. For that we have to identify the interest points or the important points. By using SURF Feature we detect the interest points, by using Hessian Matrix. Here the interesting points are blob like structures. The following block diagram explains the working of the proposed system.

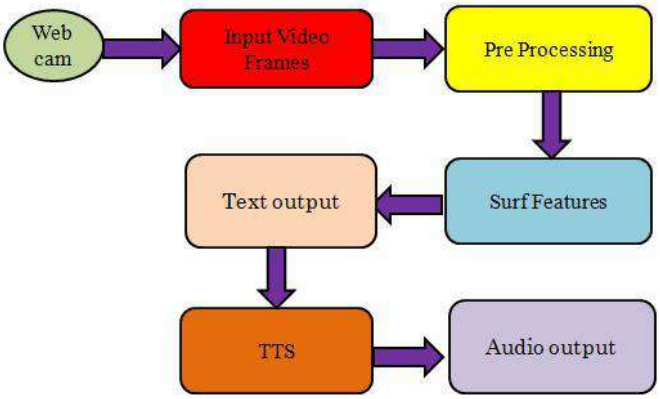

FIGURE 2: THE BLOCK DIAGRAM OF PROPOSED SYSTEM

2.1 Webcam &Input Frames

A webcam is essentially just a camera that is connected to a computer either directly or wirelessly and gathers a series of images. Here the train images are extracted from training video and the test images are extracted from testing video by using snapshot.

FIGURE 3: THE TRAINING VIDEO FRAMES

FIGURE 4: THE TESTING VIDEO FRAME

The above figures represent the training frames and testing frames. We are recognizing the hand gestures here. Therefore we have to crop the particular part of hand in pre-processing.

2.2 Pre-Processing

The aim of preprocessing is an improvement of the image data that enhance some image features important for further processing. We are cropping the input image frame to get the gesture from it, and thereby we reduce the high dimensionality.

2.3 Surf Feature

The main working of the gesture recognition is based on SURF. Speeded up robust features (SURF) is a patented local feature detector and descriptor. It can be used for tasks such as object recognition, image registration, classification or 3D reconstruction. It is partly inspired by the scale-invariant feature transform (SIFT) descriptor. The standard version of SURF is several times faster than SIFT and claimed by its authors to be more robust against different image transformations than SIFT. There are SURF Detector, SURF Descriptor, and SURF Comparator.

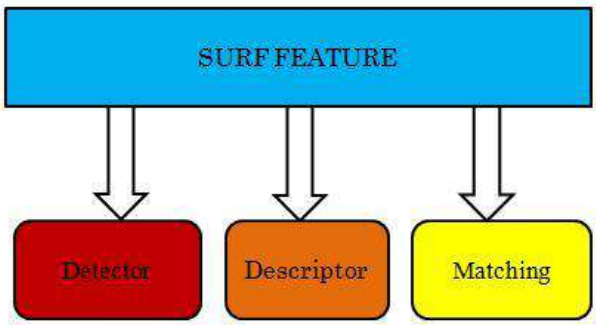

FIGURE 5: SURF DETECTOR, SURF DESCRIPTOR, AND SURF COMPARATOR.

2.3.1 Surf Detector

The SURF detector focuses its attention on blob like structures in the image. These structures can be found at corners of objects, but also at locations where the reflection of light on specular surfaces is maximal blob detection methods are aimed at detecting regions in a digital image that differ in properties, such as brightness or color, compared to surrounding regions. Informally, a blob is a region of an image in which some properties are constant or approximately constant.

Given some property of interest expressed as a function of position on the image, there are two main classes of blob detectors: (i) differential methods, which are based on derivatives of the function with respect to position, and (ii) methods based on local extrema, which are based on finding the local maxima and minima of the function. With the more recent terminology used in the field, these detectors can also be referred to as interest point operators, or alternatively interest region operators.

Gaussian derivative filters could be used to locate features. Specifically, we can detect blobs by convolving the source image with the determinant of the Hessian (DoH) matrix, which contains different 2D Gaussian second order derivatives. This metric is then divided by the Gaussians variance, σ2, to normalize its response.

$$DoH(x,y,\sigma) = \frac{G_{xx}(x,y,\sigma)\cdot G_{yy}(x,y,\sigma) - G(x,y,\sigma)^2}{\sigma^2} \tag{1}$$

$$G_{ij}(x,y,\sigma) = \frac{\partial N(0,\sigma)^2}{\partial i \cdot \partial j} * image(x,y) \tag{2}$$

The local maxima of this filter response occur in regions where both G_{xx} & G_{yy} are strongly positive, and where G_{xy} is strongly negative. Therefore, these extrema occur in regions in the image with large intensity gradient variations in multiple directions, as well as at saddle points. Interest points can be found at different scales, partly because the search for correspondences often requires comparison images where they are seen at different scales. In other feature detection algorithms, the scale space is usually realized as an image pyramid. Images are repeatedly smoothed with a Gaussian filter, and then they are sub-sampled to get the next higher level of the pyramid. Therefore, several floors or stairs with various measures of the masks are calculated:

$$\sigma_{approx} = CurrentFilterSize * \frac{BaseFilterScale}{BaseFilterSize} \tag{3}$$

The scale space is divided into a number of octaves, where an octave refers to a series of response maps of covering a doubling of scale. In SURF, the lowest level of the scale space is obtained from the output of the 9x9 filters. The output of the above 99 filter considered as the initial scale layer at scale s=1.2.The following layers are obtained by filtering the image with gradually bigger masks, taking into account the discrete nature of integral images and the specific filter structure. This results in filters of size 99, 15x15, 21x21, 27x27.Non-maximum suppression in a 3x3x3 neighborhood is applied to localize interest points in the image and over scales. The maxima of the determinant of the Hessian matrix are then interpolated in scale and image space. SURF detector interpolates the coordinates of any local maxima found into the subpixel and subscale range. Finally, SURFs propose to make the distinction between bright blobs found on a dark can be represented by the sign of the Laplacian, as shown below:

$$\operatorname{sgn}\{G_{xx}(x,y,\sigma) + G_{yy}(x,y,\sigma)\} = \begin{cases} +1 \Rightarrow \text{bright blob over dark background} \\ -1 \Rightarrow \text{dark blob over bright background} \end{cases} \tag{4}$$

2.3.2 Surf Descriptor

To describe each feature, SURF summarizes the pixel information within a local neighborhood. The first step is determining an orientation for each feature, by convolving pixels in its neighborhood with the horizontal and the vertical Haar wavelet filters. These filters can be thought of as block based methods to compute directional derivatives of the images intensity. By using intensity changes to characterize orientation, this descriptor is able to describe features in the same manner regardless

of the specific orientation of objects or of the camera. This rotational invariance property allows SURF features to accurately identify objects within images taken from different perspectives.

2.3.3 Surf Comparator

The SURF comparator is nothing but we are finding the matching. Here the matching is done with the help of testing and training images. By comparing the descriptors obtained from different images, matching pairs can be found.

FIGURE 6: THE MATCHED SURF FEATURE

2.4 Text To Speech

TTS stands for Text-to-Speech a form of speech synthesis that converts text into voice output. There are numerous ways you can create audio from text.

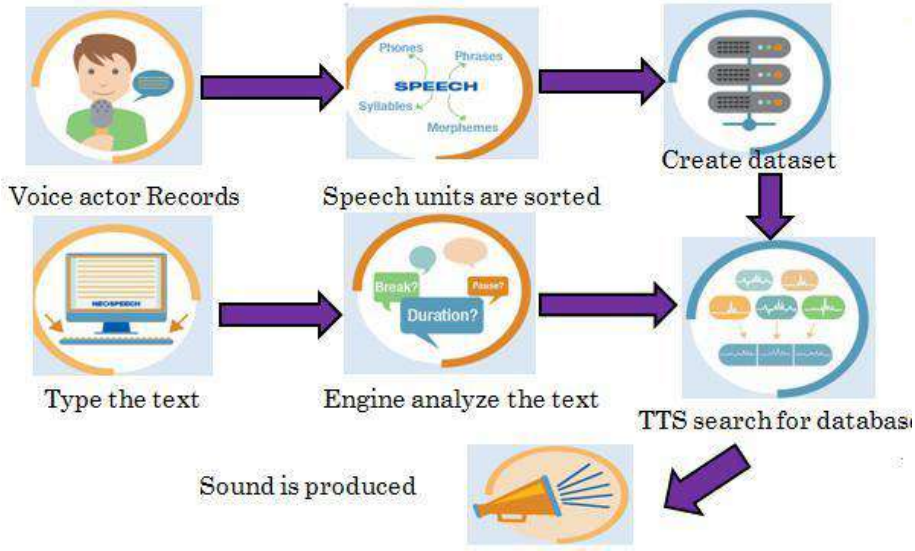

FIGURE 7: WAY TO CREATE AUDIO FROM TEXT

First, choose a voice actor with a great sounding voice who is frequent in any language. Record the voice actor speech units, from whole sentences to syllables. There by we get the natural sound of the actor. Now there are thousands of recorded sound files, we need to sort them and organize them. The speech units are labeled and segmented by phones, words, phrases, and sentences. These speech units are used to build a large voice database.

Type the text that we have to convert to audio. Here the text we consider for the signs are superb, nice, good, etc. The next process is language processing .We are considering these text for audio creation. From the language processing end, the text is normalized and broken down into phonetic sounds before going through a series of analyses to understand the structure of the sentences as well as to determine the context of the word for pronunciation. Through these processes, we are able to establish prosodoy rhythm, stress, and produce natural sounding speech. the Natural Language Processing (NLP) Part and the Voice Database come together to start producing speech.

III. EXPERIMENTAL RESULTS

In order to verify the effectiveness of the proposed method, all the algorithms are implemented in the MatlabR2013a environment on a I3 -3.30GHz PC with 4GB RAM. Our algorithm is mainly based on the concept of SURF. Surf detects the blobs and finding the best matches .First of all we have to take the testing video and training video with the help of webcam.

FIGURE 8: THE TESTING VIDEO AND TRAINING VIDEO WITH THE HELP OF WEBCAM

The testing video is extracted as testing frame and the training video extracts the training frames. We have now 25 frames of training images and one testing image. The figures shows the trained images and test images.

FIGURE 9: THE EXTRACTED TEST IMAGE

FIGURE 10: THE MATCHED TESTING AND TRAINING SURF IMAGES

The next step is to checking the training images with our test image. If the image 1 (trained frame) having best match the output =a. If the image 2 has best match output =b. Here the testing image is 18 then we have to get the output as 'r'. Finally we get the output corresponding to our test image with some blobs. We compared all the train images with our test image. The output is also displayed as the corresponding alphabet.

The figure shows the corresponding letter and matched train image. We are giving each gestures with different names, such as superb, good, nice, etc. it will also displayed in the window corresponds to the letter. Finally, we are converting the text SUPERB to an audio by using a TTS function.

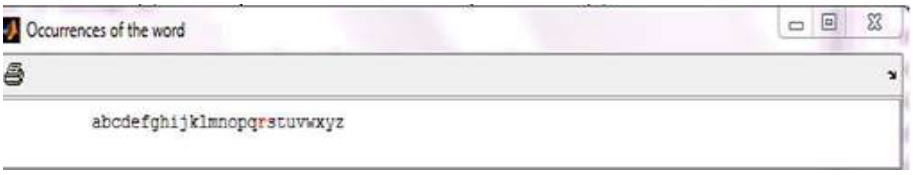

FIGURE 11: THE MATCHED LETTER FOR TEST IMAGE

Therefore using the surf algorithm we get better fast performance compare with other algorithms. Thus we can identify our test image of 18 by the letter 'r'. The text is also converted as audio by using text to speech conversion. Compare with other methods hand gesture recognition using surf feature has good performance. They take less time to recognize a gesture.

IV. PERFORMANCE EVALUATION

The Jaccard index, also known as Intersection over Union and the Jaccard similarity coefficient is a statistic used for comparing the similarity and diversity of sample sets. The Jaccard coefficient measures similarity between finite sample sets, and is defined as the size of the intersection divided by the size of the union of the sample sets.

A is the binary image of train image and B is binary image of test image. And jaccard index value should be in between 0 and 1 (0 J(A; B) 1).It calculates the similarity points in between trained and testing image. And this similarity is taken as jaccard

index. The numerator portion represents similar points between images and the denominator portion represents total points between trained and tested image. The ratio between these values represents jaccard index.

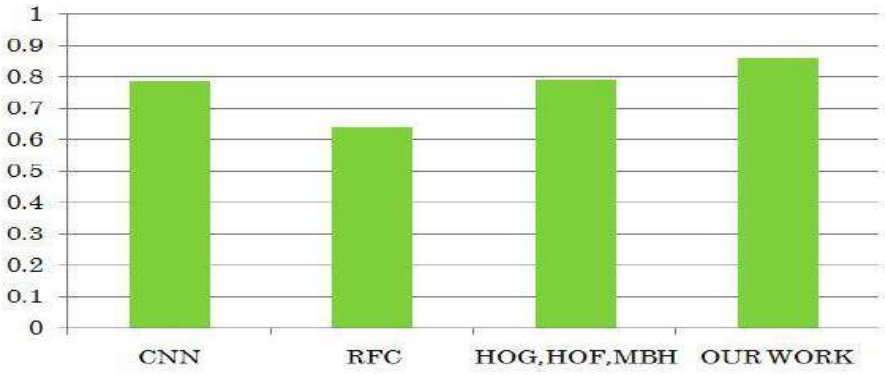

FIGURE 12: COMPARISON OF PREVIOUS WORKS OUR WORK

In the figure 5.1 our method shows jaccard index value greater than 0.8,which is larger than other algorithms.RFC method shows least jaccaed index value.HOG method have second largest jaccard index value. So from the graph we can clearly say that our method have better performance than previous methods. There is another performance evaluation which is done by accuracy index. In jaccard index section the convolutional neural network has the nearest performance with this work. So we consider the accuracy index with CNN. Let X_i is the accuracy index we are consider number of correctly classified samples and total number of samples.

TABLE 1
PERFORMANCE EVALUATION BASED ON ACCURACY INDEX

Methods	Total number of samples	Correctly classified samples	Accuracy (%)
CNN[9]	20	15	78.5
This Work	20	17	80

Thus the performance evaluation in accuracy index shows that this work consists of more accuracy than the CNN method. We considered total number of samples as 20 in both case. The number of correctly classified samples in CNN method is 15 and in this method we have 17 correctly classified samples. Therefore CNN has the accuracy of 78.5 % and we have 80 % of accuracy.

V. CONCLUSION

In this paper, we are finding the best match comparison with our train image and test image using SURF feature. The SURF feature detects the important points or interest point's .With the help of these interest points we can find the matching gestures and thereby we are converting a text to audio. Here we are only considering RGB images. An advantage of the SURF algorithm is that, it takes less time to find matching. By using jaccard index values, we can find that our performance is high compared to other algorithms. As a future work we can find the position of the gesture in the video without fixed position of gesture and also we can perform different mathematical algorithms by replacing surf feature.

REFERENCES

[1] L. Liu, L. Shao, F. Zheng, and X. Li, "Realistic action recognition via sparsely-constructed Gaussian processes," Pattern Recog., vol. 47, pp. 38193827, 2014, Doi: 10.1016/j.patcog. 2014.07.006.

[2] L. Shao, X. Zhen, D. Tao, and X. Li, "Spatio-temporal Laplacianpyra-mid coding for action recognition," IEEE Trans.Cybern., vol. 44, no. 6, pp. 817827, Jun. 2014.

[3] D. Wu and L. Shao, "Silhouette analysis-based action recognitionvia exploit-ing human poses," IEEE Trans. Circuits Syst. Video Technol., vol. 23, no. 2, 236243, Feb. 2013.

[4] I. Laptev, "On space-time interest points,"Int. J. Comput. Vis.,vol. 64, pp. 107123, 2005.

[5] P. Dollar, V. Rabaud, G. Cottrell, and S. Belongie, "Behavior recognition via sparse spatio-temporal features,"in Proc. 2nd Joint IEEE Int. Workshop Vis. Surveillance Perform. Eval. Tracking Surveillance, 2005, pp. 6572.

[6] G. Willems, T. Tuytelaars, and L. V. Gool, "An efficient dense and scale-invariant spatio-temporal interest point detector,"in Proc. 10th Eur. Conf. Comput. Vis., 2008, pp. 650663.

[7] P. Scovanner, S. Ali, and M. Shah, "A 3-dimensional sift descriptor and its application to action recognition," in Proc. 15th Int. Conf. Multimedia, 2007, 357360

[8] A. Klaser, M. Marszalek, and C. Schmid, "A spatio-temporal descriptor based on 3D-gradients," in Proc. Brit. Mach. Vis. Conf., 2008, pp. 2751.

[9] L. Pigou, S. Dieleman, P.-J. Kindermans, and B. Schrauwen, "Sign language recognition using convolutional neural networks,"in Proc. Eur. Conf. Com-put.Vis. Pattern Recog.Workshops, 2014, pp. 16.

[10] H. Wang, M. M. Ullah, A. Klaser, I. Laptev, C. Schmid, et al., "Evaluation of local spatio-temporal features for action recognition," in Proc. Brit. Mach. Vis. Conf., 2009, pp. 111.

[11] G. W. Taylor, R. Fergus, Y. LeCun, and C. Bregler, "Convolutional learning of spatio-temporal features," in Proc. 11th Eur. Conf. Comput. Vis., 2010, PP. 140153

[12] D. Wu and L. Shao, "Deep dynamic neural networks for gesture segmenta-tion and recognition,"in Proc. Eur. Conf. Comput. Vis. Pattern Recog. Work-shops, 2014, pp. 552571.

[13] Q. V. Le, W. Y. Zou, S. Y. Yeung, and A. Y. Ng, "Learning hierarchical invariant spatio-temporal features for action recognition with independent subspace analysis," in Proc. IEEE Conf. Comput. Vis. Pattern Recog., 2011, PP: 33613368

[14] M. Baccouche, F. Mamalet, C. Wolf, C. Garcia, and A. Baskurt, "Spatio-temporal convolutional sparse auto-encoder for sequence classification," in Proc. Brit. Mach. Vis. Conf., 2012, pp. 112.

[15] G. E.Hinton, S. Osindero, and Y.-W. Teh, "A fast learning algorithm for deep belief nets,"NeuralComput., vol. 18, pp. 15271554, 2006.

[16] J. Schmidhuber, "Deep learning in neural networks: An overview," arXiv preprint arXiv:1404.7828, 2014.

[17] A. Krizhevsky, I. Sutskever, and G. E. Hinton, "Imagenet classification with deep convolutional neural networks," in Proc. Neural Inf. Process. Syst., 2012, pp. 11061114.

Optimized Coverage and Efficient Load Balancing Algorithm for WSNs-A Survey

P.Gowtham[1], P.Vivek Karthick[2]

[1]PG Scholar, [2]Assistant Professor
Kathir College of Engineering Coimbatore (T.N.), India.

Abstract— *Major challenge in field of wireless sensor networks (WSN) is to provide full coverage of a sensing field and connectivity of relaying nodes. Many applications—such as object tracking, healthcare, natural environment protection and battlefield intrusion detection —requires the full coverage at any time. Load balancing aims to optimize resource use, maximize throughput, minimize response time, and avoid overload of any single resource. In this paper we are over viewing techniques which are used in WSN for load balancing. The maximum cover tree (MCT) difficulty is to construct several connected cover trees and difficult in Nondeterministic Polynomial (NP)-Complete problem, Ant colony based scheduling Algorithm (ACB-SA) can used to solve the efficient coverage problem but it has time delay as drawback, And Temperature aware Algorithms that seek to save energy but the implementation is complex. In order to mitigate limitations above, Novel maximum connected load-balancing cover tree (MCLCT) algorithm is proposed and it is composed by two sub strategies: a coverage-optimizing recursive (COR) heuristic and a probabilistic load-balancing (PLB) method. This Algorithm provides the better coverage and connectivity among others which is presented as a result of this survey. Simulation results show the output in terms of energy efficiency and connectivity maintenance.*

Keywords— wireless sensor networks, Coverage / connectivity preservation, scheduling, lifetime maximization.

I. INTRODUCTION

Data gathering is a fast growing and demanding field in today's world of computing. Sensors give a cheap and easy solution to these applications particularly in the inhospitable and low-maintenance areas where conservative approaches prove to be very expensive. Sensors are tiny devices that are able of gathering physical data like heat, light or motion of an object or surroundings. Sensors are deploying in an ad-hoc way in the area of interest to monitor events and gather data about the environment. Networking of these unattended sensors is expected to have significant impact on the effectiveness of many military and civil applications, such as combat field observation, security and disaster management. Sensors in such systems are typically disposable and predictable to last until their energy drains. Therefore, power is a very scarce reserve for such sensor systems and has to be managed shrewdly in order to extend the life of the sensors for the duration of a particular assignment. Typically sensor networks follow the model of a base station or command node, where sensors relay streams of data to the control node either periodically or based on events. The command node can be statically located in the vicinity of the sensors or it can be mobile so that it can move around the sensors and gather data. In either case, the command node cannot be reached efficiently by all the sensors in the scheme. The nodes that are positioned far away from the command node will consume more energy to broadcast data then other nodes and therefore will die sooner.

A wireless sensor network is characteristically consisting of a potentially big number of resource forced sensor nodes and few relatively powerful manage nodes. Each sensor node has a battery and a low-end processor, a limited amount of memory, and a low power communication module capable of short range wireless communication. As sensor nodes have very restricted battery power and they are randomly deployed it is not possible to recharge the dead battery. So the battery power in WSN is considered as scarce resource and should be efficiently used. Sensor node consumes battery in sensing data, receiving data, sending data and processing data. Generally a sensor node does not have enough power to send the data or communication directly to the base station. Hence, along with sensing the data the sensor node act as a router to broadcast the data of its neighbour. In large sensor network, the sensor nodes can be split into small clusters. Each cluster has a cluster head to organize the nodes in the cluster. Cluster arrangement can prolong the lifetime of the sensor network by creation the cluster head collective data from the nodes in the cluster and send it to the base station.

The cluster heads should also be chosen. There are two approaches used in this process the leader first and the cluster first approach. In the leader first approach the cluster head is selected first and then cluster is formed. In the cluster first move toward the cluster is formed first and then the cluster head is chosen. The schematic diagram of cluster architecture is shown in fig 1.

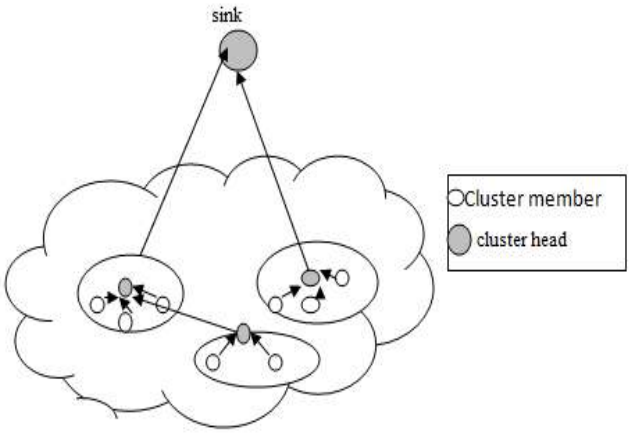

FIG. 1. THE CLUSTER ARCHITECTURE

II. LITERATURE SURVEY

2.1 Ant-colony-based scheduling Algorithm for Energy Efficient coverage of WSNs.

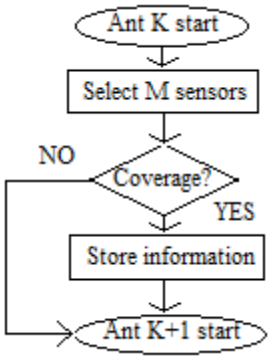

FIG 2. CONSTRUCTION GRAPH OF CONVENTIONAL ACO ALGORITHM

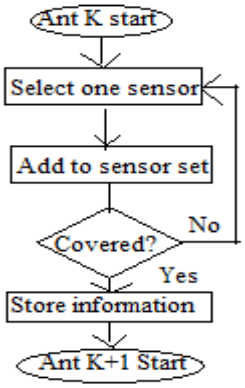

FIG 3.CONSTRUCTION GRAPH OF ACB-SA

The ACO algorithm is based on swarm intelligence, which states that complex collective behavior emerges from the behavior of many simple agents, like ants. The performance of the ACO algorithm is determined by how it initializes a pheromone field and how it makes a construction graph. When most ACO algorithms are applied to different problems, the algorithm is modified to reflect the characteristics of the problem. As a result, the ACO algorithm can get better performance. To improve the performance (which focused on lifetime improvements) of the ACB-SA, we applied a new initialization method, which was unlike the conventional ACO algorithm, for the pheromone field and the modified construction graph.

A novel ACO algorithm is optimized to solve the EEC problem. The ACB-SA has new characteristics that are different from conventional ACO algorithms. The traditional scheduling algorithms that use the ACO algorithm simply follow the lead of the solutions, and they are not optimized to solve the EEC problem. ACB-SA, unlike conventional ACO algorithms, does not consider what values are needed for the user parameters α and ß. The result of the first simulation verifies the effectiveness of the ACB-SA over other algorithms. The limitation is time delay and ACB-SA is the least complex among stochastic algorithms. The simulation was run ten times and the average network lifetime was found to be 58.8 cycles.

2.2 Jenga- inspired optimization algorithm for Energy- Efficient coverage of unstructured WSNs.

A new stochastic optimization algorithm, called the JOA, which overcomes some of the weaknesses of other optimization algorithms for solve the EEC difficulty. The JOA was inspired by Jenga which is a well-known board game. Also introduce the probabilistic sensor detection model, which leads to a more realistic approach to solving the EEC problem. The structure of the JOA is based on a greedy technique for fast meeting and employs a stochastic method for the ability to conduct random exploration. These features of the JOA made a better presentation than that of conventional approaches possible.

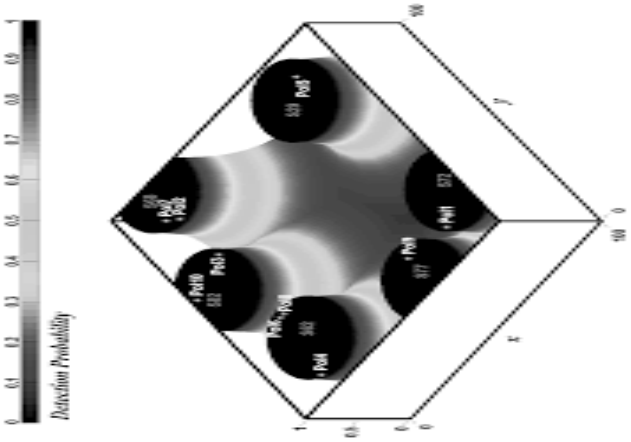

FIG 4. OPTIMAL COVER SET FOUND BY JOA

For the network lifetimes obtained by each algorithm, the case of the ACO and PSO algorithms occasionally is worse performance than the greedy-based approximation algorithm because of the stochastic uncertainty. The TPACO algorithm and JOA, on the other hand, have consistently longer lifetime than the other algorithms. However, in addition to considering the computation time for the solution, the JOA has better performance than the TPACO algorithm because it determines a better solution for prolonging network lifetimes by shortening computation times. The JOA required much more computation than the greedy-based approximation algorithm which was based on the mathematical calculation method. To reduce the computation time, however, is less important than to prolong the network lifetime in solving the EEC problem. The reason is that the EEC problem is not the optimization problem demanding the solution in real time. Therefore, the simulation results demonstrate that the JOA outperforms the other algorithms.

2.3 Efficient Coverage and Connectivity Preservation with Load Balance for Wireless Sensor Networks.

Among the previous algorithms, we investigated a new maximum connected load-balancing cover tree (MCLCT) algorithm to attain full coverage as well as BS-connectivity of each sensing node by dynamically forming load-balanced routing cover trees.

The MCLCT is composed of two sub-ways: a coverage-optimizing recursive heuristic and a probabilistic load-balancing strategy. The COR heuristic aims at detect a most number of disjoint sets of nodes, which can be achieved by one of the sensor nodes (such as the sink node). The PLB approach is used to point out the suitable path from each node to the BS after the disjoint sets are initiated. For each possible broadcast path from a given node to the candidate parent nodes, the PLB strategy will assign different probabilities in order to more equally distribute the load. Maximize the system lifetime while preserving both full coverage and BS-connectivity. The network lifetime of maintaining full coverage can be professionally extended. By increasing the possible links with the neighbor nodes in the same tier, the transmission congestion caused by a relaying node can be avoided. Only essential sensing nodes will be activated during the operation in order to reduce energy waste. The network hot spot and congestion can be avoided, and longer system duration can be assured.

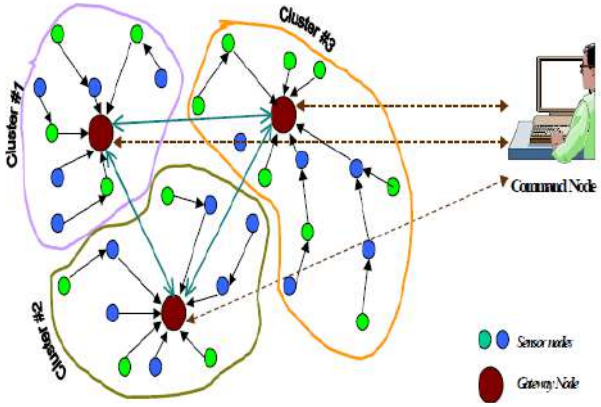

FIG 5.SYSTEM ARCHITECTURE

Maximizes the network lifetime while preserving both full coverage and BS-connectivity. The network lifetime of maintaining full coverage can be efficiently extended. By increasing the possible connections with the neighbor nodes in the same tier, the transmission congestion caused by a relaying node can be avoided. Only necessary sensing nodes will be activated during the operation in order to reduce energy waste. The network hot spot and congestion can be avoided, and a longer network lifetime can be assured.

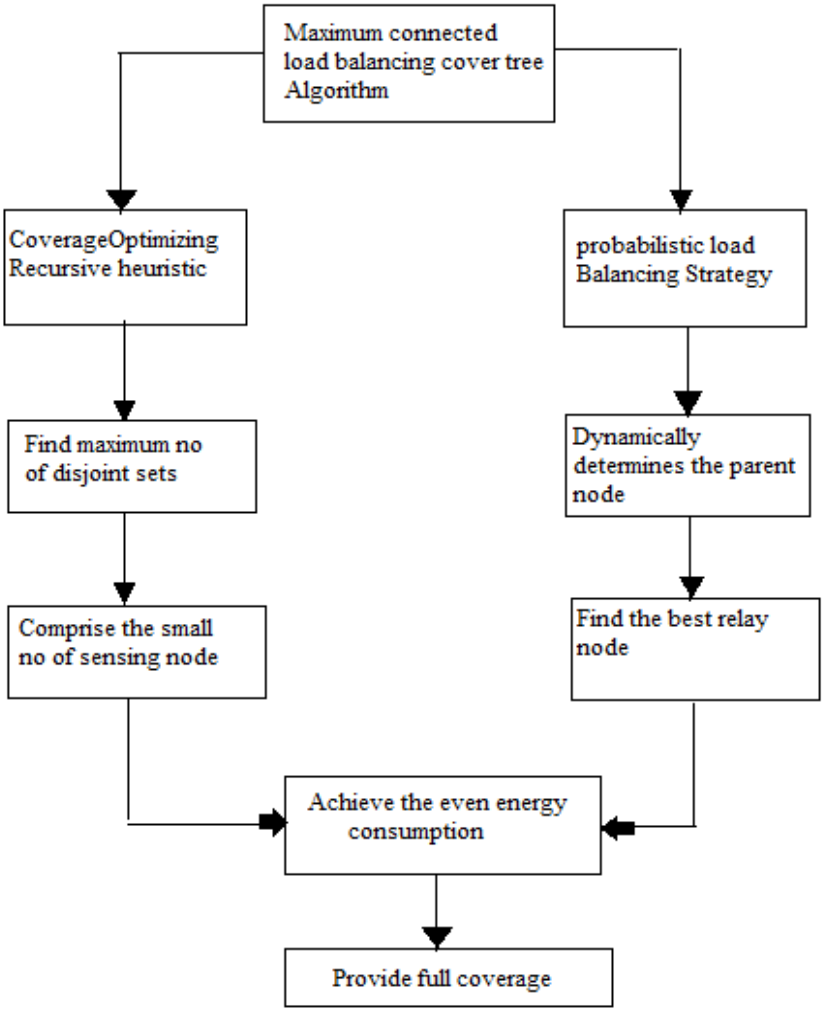

FIG 6: FLOWCHART OF MCLCT ALGORITHM.

The goal of the MCT problem is to construct several connected cover trees. By doing so, a longer network lifetime and full coverage can be acquired. The MCT problem is a complicated NP-Complete problem, so finding a suboptimal solution is a generic approach in order to decrease the time of computation. The proposed MCLCT is composed of two sub strategies: a coverage-optimizing recursive (COR) heuristic and a probabilistic load-balancing (PLB) strategy. The COR heuristic aims at finding a maximum number of disjoint sets of nodes, which can be achieved by one of the sensor nodes (such as the sink node). In each disjoint set, the nodes are able to monitor all the DPOIs together.

That is, the COR heuristic focuses on dealing with the full coverage preservation issue. Moreover, the PLB strategy is used to figure out the appropriate path from each node to the BS after the disjoint sets are initiated. For each possible transmission path from a given node to the candidate parent nodes, the PLB strategy will assign different probabilities in order to more uniformly distribute the load. Figure 6 shows the flowchart of the proposed MCLCT algorithm.

III. RESULT AND COMPARISON

In this section, presented the simulation results regarding the performance of the proposed MCLCT and compare it with previously mentioned algorithms, which include ACBSA [1], JOA [2], and TC&NC [4]. All the simulations are carried out on the MATLAB platform.

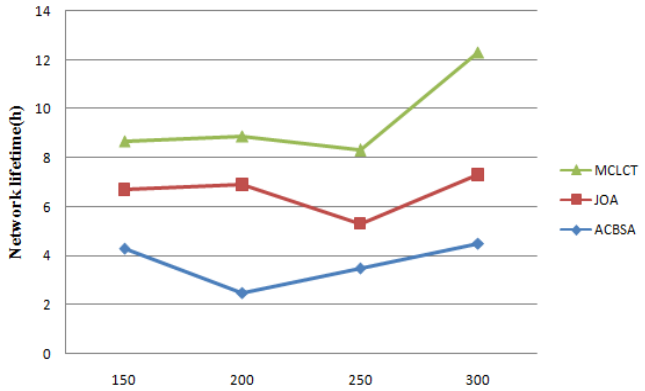

FIG 7. NETWORK LIFETIME WHEN VARIOUS NUMBER OF NODES ARE CONSIDERED.

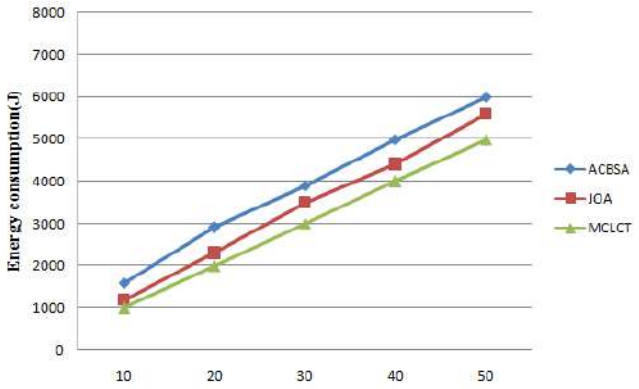

FIG 8.ENERGY CONSUMPTION FOR EVERY NODE

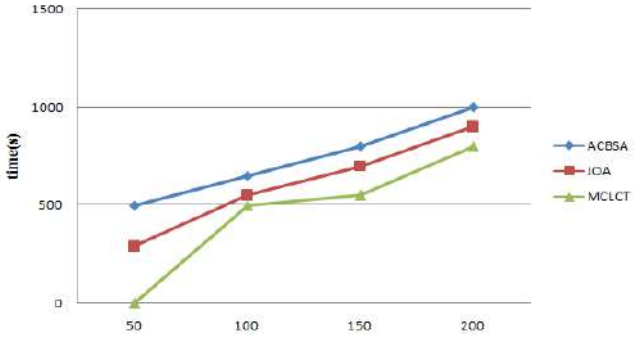

FIG 9.COMPUTATION TIME FOR EVERY NODE

IV. DISCUSSION AND ANALYSIS

The simulation results, it is obvious that network duration is efficiently prolonged since the traffic burden generated by the sensing nodes is dynamically dispatched to various relaying nodes. Furthermore, for power conservation, the analyzed outcomes demonstrate that the future MCLCT surely achieves well-arranged power utilization for nodes through the built dynamic cover tree. Meanwhile, the broadcast hot spots in WSNs bringing a large amount of power uses to nodes are also avoided.

V. CONCLUSION

In this system, an approach for load balancing in the wireless sensor network is proposed. Algorithms for cluster head selection, cluster formation, intra cluster communication and inter cluster communication in wireless sensor network are proposed. Maximum connected load-balancing cover tree (MCLCT) algorithm to attain full coverage as well as BS-connectivity of every sensing node by dynamically forming load-balanced routing cover trees.

REFERENCES

[1] Joon-Woo Lee, and Ju-Jang Lee, "Ant Colony-Based Scheduling Algorithm for Energy-Efficient Coverage of WSN", IEEE sensors journal, vol. 12, no. 10, october 2012.

[2] Joon-Woo Lee, Joon-Yong Lee, Ju-Jang Lee, "Jenga-Inspired Optimization Algorithm for Energy-Efficient Coverage of Unstructured WSNs", IEEE Wireless Communications Letters, Vol. 2, No. 1, February 2013.

[3] Abdelmalik Bachir, Walid Bechkit, Yacine Challal, "Joint Connectivity- overage Temperature-Aware Algorithms for Wireless Sensor Networks" IEEE Transactions On Parallel And Distributed Systems, Vol. 26, No. 7, July 2015.

[4] Zhuofan Liao, Jianxin Wang, Jiannong Cao, Geyong Min, "Minimizing Movement for Target Coverage and Network Connectivity in Mobile Sensor Networks" ,IEEE transactions on parallel and distributed systems, vol. 26, no. 7, July 2015.

[5] Deniz Kilinc, Mustafa Ozger, "On the Maximum Coverage Area of Wireless Networked Control Systems with Maximum Cost-Efficiency under Convergence Constraint", IEEE transactions on automatic control, vol. 60, no. 7, July 2015.

[6] J S Rauthan, S Mishra, "An Improved Approach in Clustering Algorithm for Load Balancing in Wireless Sensor Networks", ISSN: 2278 – 1323, International Journal of Advanced Research in Computer Engineering & Technology, Volume 1, Issue 5, July 2012.

[7] Chia-Pang Chen, Subhas Chandra Mukhopadhyay, Cheng-Long Chuang, Maw-Yang Liu and Joe-Air Jiang, "Efficient Coverage and Connectivity Preservation With Load Balance for Wireless Sensor Networks" IEEE SENSORS JOURNAL, VOL. 15, NO. 1, JANUARY 2015.

AD Publications
Sector-3, MP Nagar, Bikaner,
Rajasthan, India
www.adpublications.org, info@adpublications.org